Critical Contributions of the Ubiquitin-Proteasome System and Phosphorylation to Bromovirus RNA Replication

By

Brandi L. Gancarz

A dissertation submitted in partial fulfillment of

the requirements for the degree of

Doctor of Philosophy

(Cellular and Molecular Biology)

at the

UNIVERSITY OF WISCONSIN-MADISON

2012

Date of final oral examination: 6/6/12

This dissertation is approved by the following members of the Final Oral Committee:

Paul Ahlquist, Professor, Plant Pathology
Mark Craven, Professor, Biostatistics and Medical Informatics
F. Michael Hoffmann, Professor, Oncology
Paul Lambert, Professor, Oncology
William Sugden, Professor, Oncology

To my parents, Libby and Mike, for your endless love, support and encouragement.

I love you and I could not have done this without you.

ACKNOWLEDGEMENTS

I would like to express my sincere gratitude to my advisor, Paul Ahlquist. Your support and encouragement throughout my graduate career ensured a positive outcome. Thank you for constantly challenging me to produce meaningful, quality work and providing guidance while allowing me the freedom to grow independently as a scientist. I thank all members of the Ahlquist lab, past and present, who took the time and energy to teach me, perform "thought experiments" with me, support me and laugh with me along the way. I would especially like to thank Billy Dye, Linhui Hao and Jim Bruce for their incredible mentorship and friendship. I am privileged to know each of you. I thank Priscilla Van Wynsberghe for teaching me (very patiently) how to run my first northern blot and for your endless supportive notes and calls along this journey; Ben Kopek for your love of all things Polish, your festive holiday cheer and for introducing me to your amazing wife Lisa; Ericka Loffredo for so many fun times in and out of the lab; Hernan Garcia-Ruiz for your endless support both while in the lab (especially after my knee surgery) and thereafter; Srikumar Sengupta for your mutual love of Fridays; and Xiaofeng Wang for your lively spirit, love of science and immeasurable help along the way, including your encouraging phone calls and advice on how to eat so I didn't "get fat" while thesis writing – I will be eternally grateful our paths crossed here on the 8th floor of Bock! I thank my very dear friend Arturo Diaz for enriching my life in so many ways, for putting up with my constant invasion of your bench space, for making me laugh until I cried on so MANY occasions and for being so sure this would end positively - I am blessed to know you. A very special thanks to Kathleen Wessels for your amazing friendship, endless support and infinite humor – you have taught me so many life lessons that I will take with me, I have grown from knowing you and I know for certain that I would not have made it through this without you.

I am also privileged to have such a supportive family and a fabulous group of friends. Mom and Dad, thank you for your continuous support of my dreams and reassurance this was

possible. To my extended family - my BFF Libby K, Dr. Carla Fisher and Amy V - you are the three most amazing women I know, you bring me joy each day and I do not know what I would do without your love and support. To the Safferts and the Juckems – you are the best “chosen family” I could’ve ever imagined. Thank you for every family dinner night, hug, wiped tear, wine night on the patio, road trip and nickname – you constantly lift me and I will happily spend my lifetime trying to return what you have given me. To those I walked in the doors of Bock Labs with on day one – my CMB posse – Cabell, Lisa, Nick, Ryan and Karen – you are amazing friends and talented scientists and I will never forget all you have done for me. To the ladies I spend my early mornings with – Vanessa, Elizabeth, Carrie and Sara K. – you give me perspective, keep me healthy and remind me there is life beyond the lab – I adore each of you.

Finally, to the other half of Team G, Mike Gathy. You have been so incredible to me over the past two years that I could never capture it in words. Thank you for every sacrifice you made for us and every act of unconditional love – I could not have a more supportive, patient, generous partner. I am so grateful to have a life with you. I love you.

TABLE OF CONTENTS

Chapter 3

Chapter 4

Chapter 5

APPENDIX A

LIST OF FIGURES

Figure **Page**

Figure **Page**

LIST OF TABLES

ABBREVIATIONS

(+)RNA	positive-strand ribonucleic acid
BMV	brome mosaic virus (*Bromoviridae*, bromovirus)
Co-IP	co-immunoprecipitation
DNA	deoxyribonucleic acid
Dox	doxycycline
dsRNA	double-stranded ribonucleic acid
ER	endoplasmic reticulum
FHV	Flock House virus (*Nodaviridae*, alphanodavirus)
GFP	green fluorescent protein
HCV	hepatitis C virus (*Flaviviridae*, hepacivirus)
hel	helicase
hpi	hours post infection
HIV	human immunodeficiency virus
IP	immunoprecipitation
kDa	kilodalton
mRNA	messenger RNA
NTPase	nucleoside triphosphate
ORF	open reading frame
Pol	polymerase
PCR	polymerase chain reaction
RdRp	RNA-dependent RNA polymerase
PV	poliovirus
RC	replication complex
RHPs	reticulon homology protiens
RNA	ribonucleic acid

rRNA	ribosomal RNA
SARS	severe acute respiratory syndrome
SDS	sodium dodecyl sulfate
TMV	tobacco mosaic virus (*Togaviridae*, tobamovirus)
tRNA	transfer RNA
Ub	ubiquitin
UPS	ubiquitin-proteasome system
wt	wild type

ABSTRACT

Among the six different virus classes, positive-strand RNA viruses encompass over one third of all virus genera and include important human pathogens such as the SARS coronavirus, West Nile virus and hepatitis C virus, which chronically infects an estimated 130-170 million people worldwide. Despite the significance of this virus class and its impact on human health, effective treatments are limited. To understand how positive-strand RNA viruses cause disease, it is critical to identify the host factors and pathways exploited in virus replication and characterize the nature of their contributions and interactions with virus-encoded replication factors. Previously, our laboratory identified ~100 genes whose loss affected RNA replication of a positive-strand RNA virus, brome mosaic virus (BMV). However, classical yeast genetics and other approaches have demonstrated that genes essential for cell growth also modulate BMV. To this end, the work in this thesis focused on identifying additional essential host genes required for BMV RNA replication. Our studies identified 24 novel, essential host genes required for BMV RNA replication and through follow-up studies on these and previous findings, we defined three distinct mechanistic contributions of the ubiquitin-proteasome to BMV RNA replication. Additionally, in independent studies, we investigated the role of phosphorylation in BMV RNA replication and provide the first evidence that the viral RNA-dependent RNA polymerase is phosphorylated *in vivo,* which has possible implications in viral RNA synthesis. Lastly, thorough our phosphorylation studies, we identified Pho80-Pho85 kinase as a novel host factor required for BMV RNA synthesis. Further studies are necessary to define the mechanistic contributions of the ubiquitin-proteasome system and cellular phosphorylation in BMV RNA replication. However, since the implicated cellular pathways are highly conserved and many viruses employ similar replication strategies, these results may extend to other virus classes, presenting potential cellular targets for developing broad-spectrum antivirals.

Chapter 1

GENERAL INTRODUCTION

In 1892, the Russian biologist Dmitri Ivanovsky identified what is known today as tobacco mosaic virus and the field of virology was born (62). Viruses have continued to elude us ever since. The most well known viruses are those that cause devastating disease or death. Such viruses include Ebola virus, smallpox virus, influenza, and human immunodeficiency virus (HIV). Moreover, it is currently estimated that ~15-20% of all human cancers are caused by oncogenic viruses such as human papillomaviruses (HPVs), Epstein-barr virus (EBV), hepatitis B virus (HBV) and hepatitis C virus (HCV), among others (209). Viruses extend beyond human health, to plants and animals where infections, and subsequent loss of agricultural resources, inflict enormous economic damage. The socioeconomic impact of viral infections underscores the importance of controlling viruses. However, the innate dependence of a virus on its host makes the development of effective treatments extremely challenging since antivirals must eliminate the virus while preserving the viability of the host.

Propagation of *all* viruses can be summarized in three unifying principles: (i) viral genomes are packaged within particles that mediate their transmission from one host to another; (ii) the viral genome contains the information required for a complete infectious cycle within a host; and (iii) the viral genome is established in a host population so that virus survival is ensured (62). An infectious cycle includes attachment and entry of the virus particle into a host cell followed by decoding of the genetic material, translation of the viral mRNA by host ribosomes, genome replication and assembly and release of virions.

Viruses can be divided into six different classes based on the genomes they encapsidate. Viruses that contain DNA can package their genetic material as either single-stranded or double-stranded. Similarly, viruses that encapsidate RNA can package single-stranded or double-stranded genomes. Single-stranded RNA viruses are further delineated based on the polarity of their RNA. Positive-strand RNA viruses encapsidate messenger-sense RNA (mRNA), while negative-strand RNA viruses package antisense RNA. Lastly, retroviruses will always initially package RNA forms of their genomes, which may or may not be reverse-transcribed into DNA. Genome replication is a critical step in the life cycle of a virus and the genomic material packaged by a virus determines its replication strategy once inside a host cell. For example, most DNA viruses initiate their replication in the nucleus using cellular machinery, whereas reverse-transcribing viruses package an RNA-dependent DNA polymerase into their virions that transcribes their RNA genome into DNA, which is then replicated in the host nucleus. All RNA viruses encode their own RNA-dependent RNA polymerase (RdRp). dsRNA and negative-strand RNA viruses package an RdRp in their virions which copies the antisense genome into mRNA. Positive-strand RNA viruses, however, encode mRNA genomes that can be immediately translated upon entering a host cell.

1.1 POSITIVE-STRAND RNA VIRUSES

1.1.1 Importance

Positive-strand RNA viruses encompass more than one-third of known virus genera (113) and include many medically and practically relevant human, animal and plant pathogens. Notable positive-strand RNA viruses include poliovirus, Norwalk virus, severe acute respiratory syndrome (SARS) coronavirus, Dengue virus, West Nile virus (WNV) and hepatitis C virus (HCV). Coronaviruses are the etiologic agent for SARS, which is clinically characterized by

fever, acute respiratory and gastrointestinal symptoms and lymphopenia (230). Between November 2002 and July 2003, an outbreak of SARS in Hong Kong and China nearly became a pandemic, with more than 8,000 cases and over 900 deaths reported worldwide (http://www.who.int). Dengue virus is transmitted between people by mosquitoes and is endemic in tropical and subtropical regions. Dengue is responsible for 50 to 100 million infections yearly including 500,000 Dengue hemorrhagic fever cases and 22,000 deaths, mostly among children (http://www.cdc.gov). HCV is estimated to infect ~3-4 million people annually, primarily through exposure to infectious blood via blood transfusions, organ transplants and accidental needle sticks, among others (139). Of the ~170 million people chronically infected with HCV worldwide, ~85% are at risk of developing liver cirrhosis and/or liver cancer, resulting in more than 350, 000 HCV-related deaths per year (http://www.who.int). Additionally, positive-strand RNA viruses encompass the vast majority of plant viruses (113) and are responsible for considerable economic losses in crop productivity on a worldwide scale.

1.1.2 Replication cycle

A general overview of the positive-strand RNA virus lifecycle is depicted in Fig. 1.1. Upon entering a host cell, the messenger-sense genomic RNA of positive-strand RNA viruses is immediately translated in the cytoplasm by host translational machinery to produce viral replication and structural proteins (113). Once replication proteins accumulate they recruit the viral genomic RNA to a host intracellular membrane and induce dramatic membrane rearrangements, often in the form of spherular compartments, to facilitate RNA replication. Within these compartments, the positive-strand RNA serves as a template for synthesizing complementary negative-strand RNA, which then becomes the template for new positive-strand RNA and subgenomic RNA synthesis. The newly synthesized genomes are exported from the replication complex to the cytoplasm where they can be translated to yield additional viral

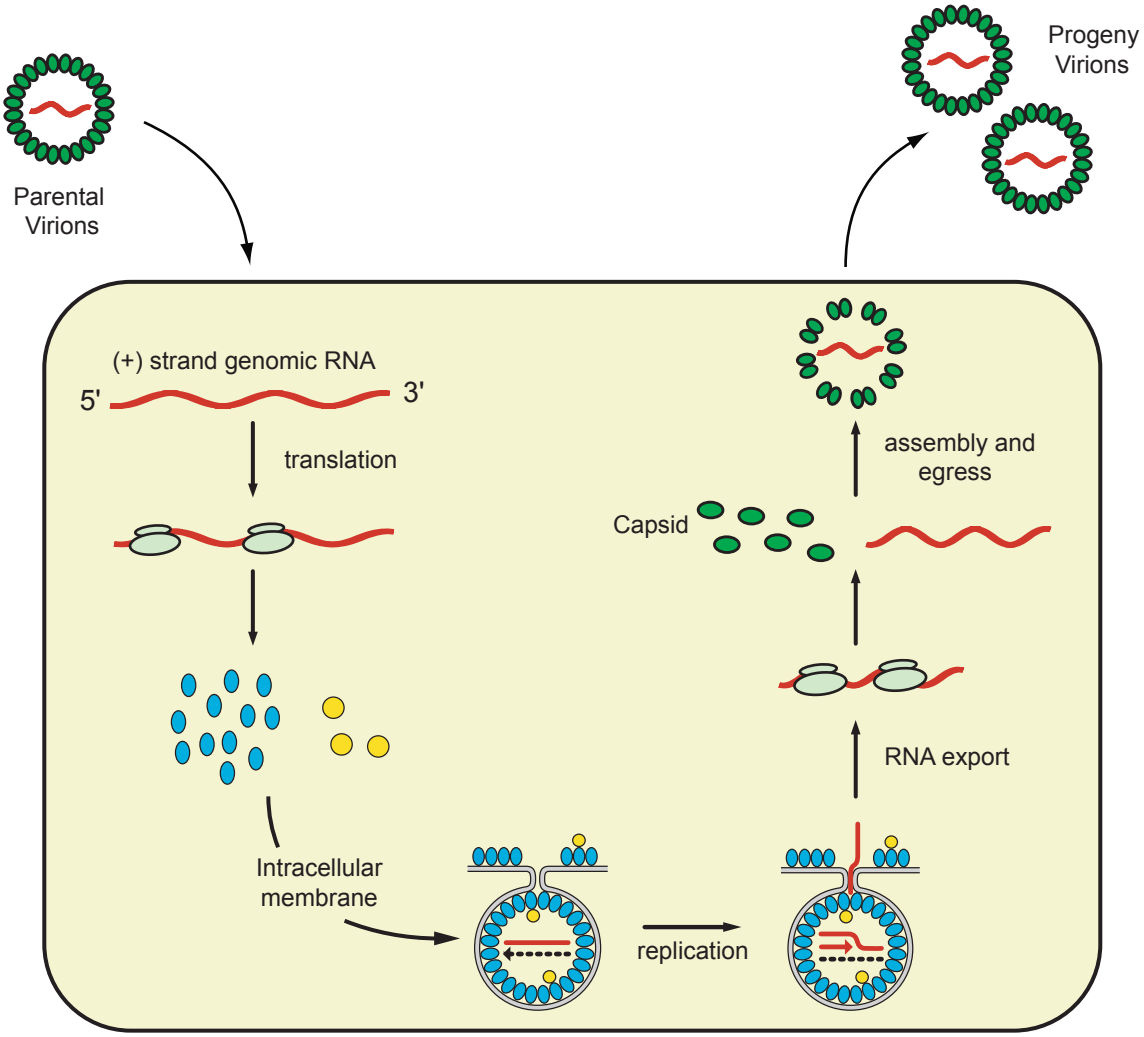

Figure 1.1 Schematic of a positive-strand RNA virus life cycle. After viral entry, virions release the messenger-sense genomic RNA into the cytoplasm for translation of the viral replication (indicated by blue ellipses and yellow circles) and structural proteins. The viral replication proteins then recruit the genomic RNA into a membrane-associated, intracellular replication compartment where viral replication occurs. Negative-strand RNA is produced and used as a template to amplify the positive-strand RNA. The positive-strand RNAs are then used as templates for further rounds of translation or encapsidated into progeny virions.

proteins, recruited to a newly formed replication compartment for additional RNA synthesis or packaged into virions.

The membrane-associated state of genome replication is a universal feature of positive-strand RNA viruses (49, 137, 145, 163, 193). These organelle-like complexes are multifunctional as they concentrate and sequester viral replication factors, genomic templates and host factors (193), provide a scaffold to anchor the replication complex (145), coordinate replication steps (46) and shield double-stranded RNA replication intermediates from the activation of host defense responses (4). Additionally, membrane-associated viral RNA replication is dependent on cellular lipid synthesis and general and localized membrane lipid composition (73, 104, 123, 124, 174, 241), revealing lipids as one of many critical host factors required for efficient genome synthesis.

1.1.3 Host factors in positive-strand RNA virus replication

Although positive-strand RNA viruses have limited genetic material, containing only three to ten genes, these viruses, like all viruses, replicate their genome and survive by interacting with and exploiting host factors at essentially every replication step (3, 7, 21-23, 27, 29, 52, 119, 138, 168, 172, 195, 211). Since there are an estimated ~20,000-30,000 different proteins expressed in a eukaryotic cell, identifying the host factors and pathways exploited in virus replication represents a major challenge. In recent years, however, the use of genome-wide screens and advanced proteomic approaches has significantly aided research efforts focused on identifying and characterizing the nature of positive-strand RNA virus-host interactions (39, 42, 68, 95, 118, 128, 158, 169, 185, 198, 199, 207). Below, a selection of host factors important for positive-strand RNA virus replication are discussed in the context of the replication step for which they are co-opted (Fig. 1.2).

Targeting viral replication proteins to the site of RNA replication. The localization of viral replication proteins to replication complexes is an early step in RNA replication that

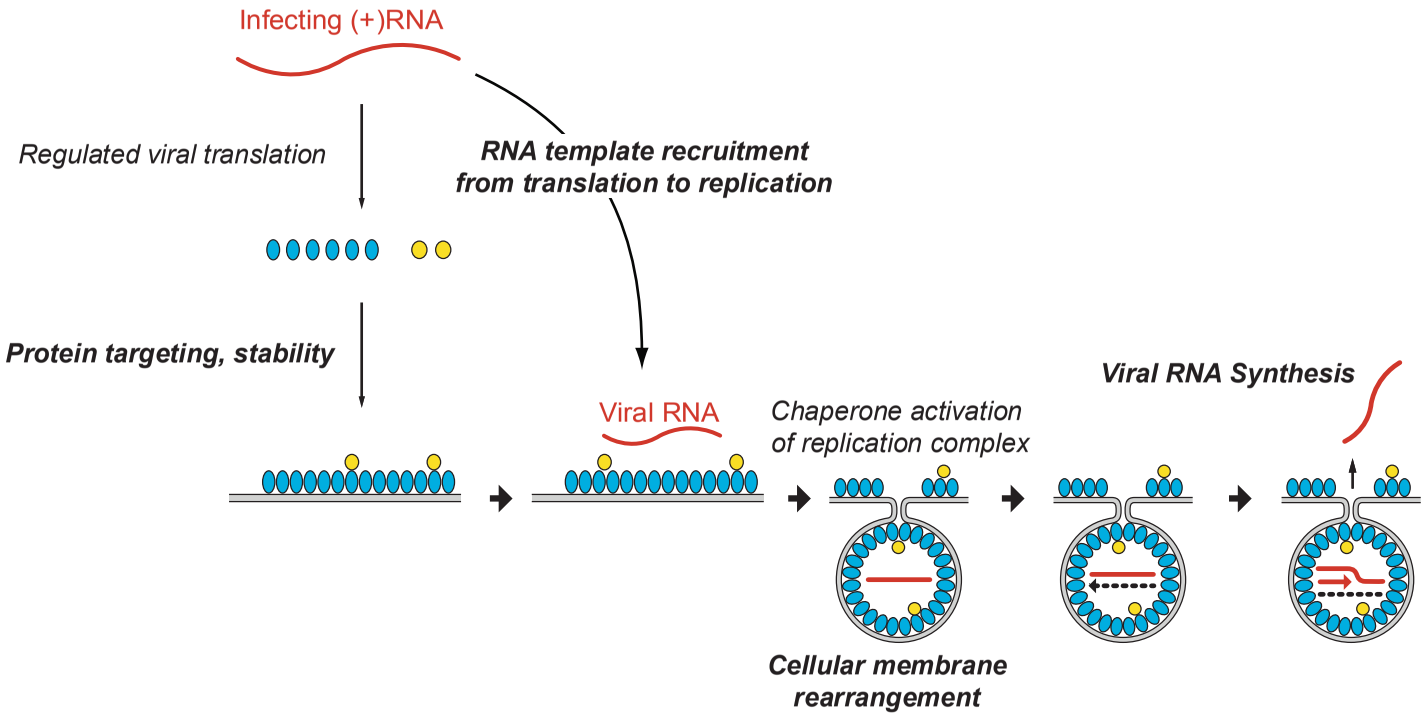

Figure 1.2. Steps in positive-strand RNA virus replication that require host factors. Simplified schematic of the major steps in positive-strand RNA virus genome replication that require host factors, which are represented in italicized text. Host factors required for steps in bold are discussed in the text. It should be noted that although the replication complex depicted here is a spherular compartment, positive-strand RNA viruses induce various types of membrane associated replication compartments.

requires host proteins. For example, HCV NS5A and NS5B replication proteins interact with a host vesicle-associated membrane protein-associated protein of 33 kDa (hVAP-33), which colocalizes with NS5A and NS5B to ER membrane-associated replication complexes and is thought to provide an ideal membrane-docking site for the NS5A and NS5B (215). Similarly, in tomato mosaic virus (ToMV) replication, membrane proteins TOM1 and TOM3 interact with ToMV 130K-180K replication proteins and localize to the ToMV replication complex, where they are proposed to tether ToMV replication proteins to the membranes (238, 239). Additionally, Tomato bushy stunt virus requires the chaperone heat shock protein 70 (HSP70) and the peroxisomal shuttle protein Pex19, which appear to work cooperatively to target viral replication proteins to the peroxisomal membrane (171, 223). The host-mediated targeting of viral components is also necessary for potyvirus, which first forms an ER-derived vesicle containing viral replication factors and then sequentially hijacks the early secretory pathway and the actomyosin trafficking system to shuttle these vesicles to chloroplasts, which are sites of viral RNA replication (229).

RNA template recruitment from translation to replication. Positive-strand RNA virus genomes must fulfill multiple seemingly incompatible functions. Upon entering the cell, genomes are immediately translated to produce viral replication factors, which then recognize the viral RNA and recruit it from translation to a membrane-associated replication compartment. Although viral proteins can selectively bind and recruit viral genomes to subcellular membranes (66, 67, 167, 218, 225), this replication step is aided by host factors. In the case of brome mosaic virus (BMV), in addition to the viral 1a protein, the Lsm1p-7p/Pat1p complex is required. This complex, which is required for cellular mRNA turnover, facilitates two functions of BMV RNAs: translation and 1a-dependent translational repression and recruitment to ER-derived replication complexes (36, 55, 91, 162, 189). For human poliovirus, the role of host poly(rC)-binding protein 2 (PCBP2) has been implicated in RNA recruitment (173). PCBP2 is a multifunctional cellular RNA binding protein involved in mRNA stabilization, transcription and

translation and plays a major role in both the translation and the replication of the PV genome. Through binding of the internal ribosomal entry site (IRES) in PV (+)RNA, PCBP2 promotes cap-independent translation (173). The switch from translation to template recruitment is achieved through interactions between the PV RdRp precursor, PCBP2, and yet another family of host proteins, the poly(A)-binding proteins (PABPs) which induce genome circularization and a subsequent switch to RNA replication (173, 221).

Cellular membrane rearrangement for replication complex formation. Recent results show that host factors are key players in forming replication complexes through inducing membrane curvature (16, 50, 52) and modulating the membrane lipid composition (75, 76, 173, 188, 226, 243). Cellular membrane lipids regulate the fluidity, permeability and integrity of membranes. Since positive-strand RNA viruses replicate their RNA on intracellular membranes, usually in association with invaginations or other dramatic rearrangements (48, 146), it is not surprising that lipids are critical for RNA replication complex formation. For example Dengue virus NS3 protein interacts with and relocalizes fatty acid synthase (FASN), a rate-limiting enzyme in fatty acid metabolism, to the sites of viral replication (75). Additionally, FASN activity is increased in Dengue virus cells, suggesting Dengue infection modulates fatty acid biosynthesis to increase lipid biogenesis to establish or expand its RCs (75). Similarly, fatty acid synthesis is required for poliovirus (73), Semliki Forest virus (31, 174), cowpea mosaic virus (31), BMV (122, 124), HCV (105) and *Drosophilia C* virus (41). Many viruses, including HCV, require cholesterol metabolism require for entry, RNA replication and egress (241).

Other host factors recruited to the replication complex by some positive-strand RNA viruses are involved in membrane bending. Reticulon homology proteins (RHPs), a family of membrane-shaping proteins, are involved in forming nuclear pores, which are topologically equivalent to the necks of BMV's spherular replication compartments. RHPs relocalize to the sites of BMV RNA synthesis through an interaction with viral replication factor 1a, are required for RNA replication and are essential for forming the membrane-bounded replication

compartments in which RNA synthesis occurs (52). Thus, one proposed role for RHPs is maintaining an open channel at the neck to facilitate import of RNA templates and necessary replication factors and export progeny RNA (52).

Despite the progress that has been made in revealing the role of the host in positive-strand RNA virus replication, many aspects of these virus-host interactions remain enigmatic. The continued use of genome-wide and proteomic approaches combined with functional and mechanistic studies should further refine current virus-host interaction models, identify common replication mechanisms employed by positive-strand RNA viruses and aid the development of effective antiviral treatments.

1.2 BROME MOSAIC VIRUS AS A MODEL TO STUDY POSITIVE-STRAND RNA VIRUS REPLICATION

Brome mosaic virus (BMV) is a member of the alphavirus-like superfamily of human, animal and plant positive-strand RNA viruses. First isolated from bromegrass (*Bromus inermis*) in 1942, BMV is a widespread virus infecting grasses and various cereal crops in Europe, Asia, Africa and North America (2, 103), While not considered an economically threatening pathogen, its high virus yield and divided genome, among other features, have established BMV as a useful model system to dissect the features of positive-strand RNA virus gene expression, replication, recombination and virus-host interactions (2, 8). Notably, BMV is one of few viruses with the ability to replicate in the yeast *Saccharomyces cerevisiae*, the advantages of which are discussed further below.

1.2.1 BMV genome organization and replication

BMV has a tripartite genome (Fig. 1.3). The genomic RNAs of BMV have 5' caps, whereas the 3' ends fold into a conserved tRNA-like structure (60, 191). Only the monocistronic

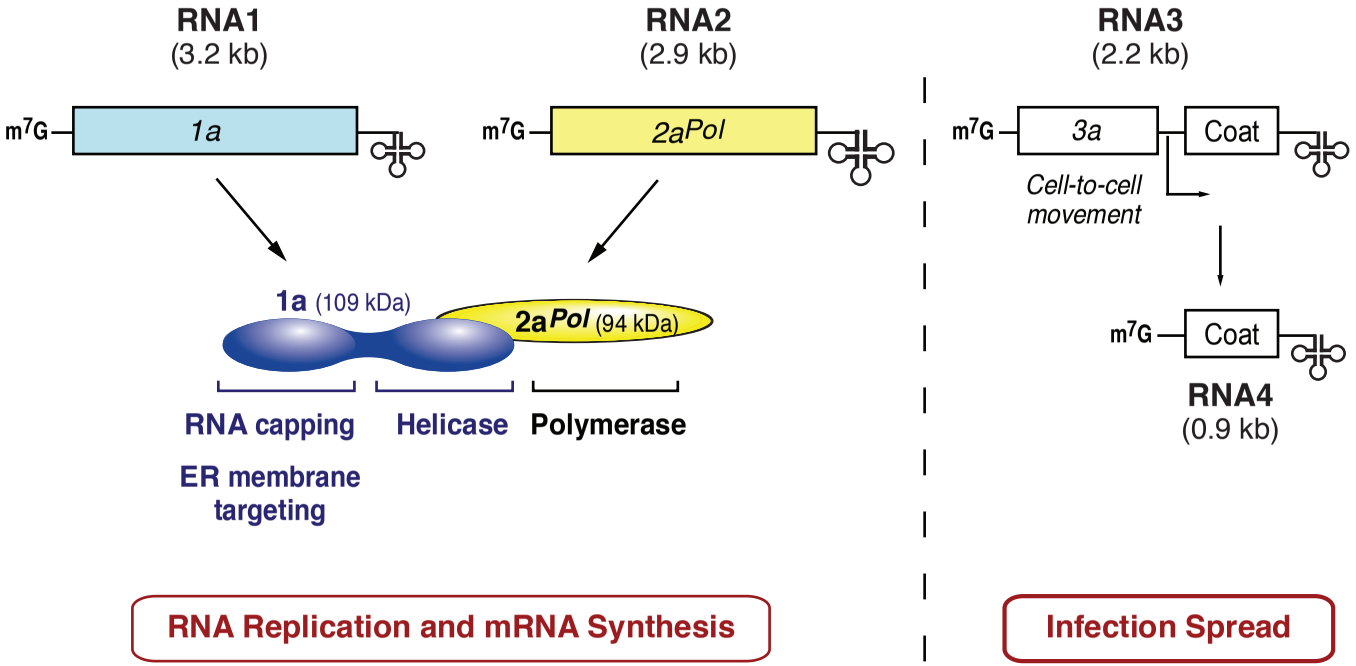

Figure 1.3 BMV genome. RNA1 encodes the multifunctional 1a protein, which has RNA capping and helicase acitivities and is able to target itself and all other viral components to the perinuclear endoplasmic reticulum. RNA2 encodes the $2a^{Pol}$ protein, which is the RNA-dependent RNA polymerase. RNA3 encodes the cell-to-cell movement protein and the coat protein, which is translated from the subgenomic mRNA, RNA4. All RNAs are capped at thr 5' ends while the 3' ends fold into tRNA-like structures that are involved in the initiation of negative-strand synthesis.

RNA1 and RNA2, encoding the viral replication factors 1a and $2a^{Pol}$, respectively, are essential for BMV RNA replication. The dicistronic RNA3 is dispensable for RNA replication *in vivo* (13, 147), but encodes the 3a cell-to-cell movement protein and the coat protein, also required for systemic movement of virus infection (13). The 3' proximal coat gene is not expressed from genomic RNA3, but requires RNA replication to produce a subgenomic mRNA, RNA4, which is initiated internally on negative-strand RNA3. The multifunctional 1a protein (109 kDa) contains an N-proximal domain with m^7G methyltransferase and covalent GTP binding activities required for viral RNA capping *in vivo* (11, 12, 114). The C-proximal helicase domain shares similarity to DEAD box RNA helicases and plays crucial roles in recruiting BMV RNA templates into the replication compartments (12, 222). The $2a^{Pol}$ protein (94 kDa) contains a large central domain conserved with RNA-dependent RNA polymerases and an N-terminal domain that interacts with the C-terminal 1a helicase domain (36, 102). 1a interacts with $2a^{Pol}$ and directs itself, $2a^{Pol}$ and the viral RNAs to the perinuclear ER membranes that become the sites of viral RNA synthesis (189, 190, 196). BMV replication and subgenomic RNA synthesis depend on *cis*-acting signals, which have been extensively characterized. The 3' 135-200 bases of all BMV genomic positive sense RNAs function as promoters directing the synthesis of negative-strand RNAs (33, 56). In turn, the 3' ends of the negative-strand RNAs facilitate the synthesis of positive-strand RNAs. RNA3 negative-strands also contain an intergenic promoter to direct synthesis of subgenomic RNA4 (63). In addition to RNA promoters, regulatory elements on positive-strand genomic RNAs coordinate proper gene expression, selection of genomic viral RNAs for replication and the coregulation of translation to and recruitment from translation to replication. RNA2-specific sequences in the 5' NCR downregulate $2a^{Pol}$ expression relative to other viral proteins (161). Additionally, an element at the 5' terminal ends of RNA1 and RNA2 and the intergenic region of RNA3 functions in proper selection and recruitment of the viral RNAs from translation to the replication complex (19, 37, 206).

1.2.2 Yeast as a model system for virus-host interactions

The yeast *Saccharomyces cerevisiae* is a simple eukaryotic organism with ~6,000 genes, more than 60% of which have been annotated since the complete sequence of *S.cerevisiae* was determined in 1996 (http://www.yeastgenome.org/). One of the most appealing features of using yeast as a model system is the availability of single gene-deletion collections and single gene repression collections, allowing the analysis of viral RNA replication in the presence or absence of nearly every yeast gene. These readily available reagents combined with their rapid growth and ease of manipulation through classical and molecular genetics make yeast a highly advantageous model organism to study virus-host interactions.

To express BMV in yeast, DNA plasmids can be used to transcribe genomic viral RNA with authentic 5' and 3' ends or mRNA encoding the viral proteins (92) and transcripts can be driven from selectable promoters in low or high copy number plasmids (88, 92). Although the initial transcription and export into the cytoplasm of the viral RNA occurs by the cellular machinery, once in the cytoplasm, interactions between the viral proteins and RNA parallel the template selectivity and other characteristics of viral replication in plants (88, 92, 181). BMV RNA replication in yeast recapitulates all known replication features of its natural plant hosts in the yeast. For example, as in plant cells, BMV RNA replication depends on 1a, $2a^{Pol}$ and specific *cis*-acting RNA signals (206); localizes to ER membranes (189, 190); generates a substantial excess of positive- to negative-strand RNA (92); and directs subgenomic mRNA synthesis (92).

Chapter 2[1]

SYSTEMATIC IDENTIFICATION OF NOVEL, ESSENTIAL HOST FACTORS AFFECTING BROMOVIRUS RNA REPLICATION

2.1 INTRODUCTION

Viruses survive with limited genetic material by interacting with and exploiting host factors at essentially every replication step (3, 7, 21-23, 27, 29, 52, 119, 138, 168, 172, 195, 211). Identifying the host factors and pathways exploited in virus replication and the nature of their contributions and interactions with virus-encoded replication factors represent major challenges and opportunities for understanding and controlling viruses.

Positive-strand RNA viruses comprise over one third of all virus genera and include important human pathogens such as hepatitis C virus, dengue virus, chikungunya virus, and West Nile virus (217). Brome mosaic virus (BMV), a member of the alphavirus-like superfamily of human, plant, and animal viruses, has been used as a model system to study gene expression, RNA replication and virus-host interactions of positive-strand RNA viruses (3, 7, 52, 138, 196). BMV has three genomic RNAs and one subgenomic (sg) mRNA. Genomic RNAs 1 and 2 encode the multifunctional replication proteins 1a and 2a polymerase ($2a^{Pol}$), respectively, which are required for RNA replication (12, 36, 133). Genomic RNA3 encodes the 3a movement

---

[1] The work in this chapter was published in PLoS ONE as Gancarz BL, Hao L, He Q, Newton MA, Ahlquist P (2011) Systematic Identification of Novel, Essential Host Genes Affecting Bromovirus RNA Replication. PLoS ONE 6(8): e23988. doi:10.1371/journal.pone.0023988. Author contributions for the paper and this chapter are as follows: Conceived and designed the experiments: BLG LH PA. Performed the experiments: BLG LH. Analyzed the data: BLG LH QH MAN PA. Contributed reagents/materials/analysis tools: BLG LH QH MAN PA. Writing: BLG PA.

protein, required for infection spread in plants. A sg mRNA, RNA4, encodes the viral coat protein and is produced from the (-)RNA3 replication intermediate. BMV RNA replication and encapsidation can be recapitulated in the yeast *Saccharomyces cerevisiae* by expressing the viral replication and/or capsid proteins together with at least one genomic RNA template (88, 92, 116). The ability of BMV to duplicate nearly all major replication features of its natural plant hosts in yeast, combined with yeast genetics, has advanced our understanding of BMV replication and virus-host interactions (3, 7, 119).

Previously, we tested deletions of nearly all non-essential yeast genes (~80% of the yeast genome) and identified 99 genes, that when deleted, altered BMV replication, revealing the involvement of many novel host pathways in viral replication, transcription, and translation (119). However, classical yeast genetics and other approaches have demonstrated that genes essential for cell growth also make major contributions to BMV RNA replication (123, 124, 162, 213). To more globally identify additional essential host factors critical for BMV RNA replication, we assayed a doxycycline (dox)-repressible library of ~900 yeast strains, each of which allows repressing the expression of a selected essential gene by adding dox to growth media (149). Using this genome-wide approach, we identified 24 essential host factors whose repressed expression reproducibly altered BMV RNA replication. These host factors are involved in protein homeostasis, protein trafficking, and translation, among others. The results presented here, in conjunction with previously identified host factors (7, 52, 124, 138, 162), provide a more complete understanding of cellular pathways utilized by BMV. Dissecting the role of these essential host genes in virus replication should significantly advance our understanding of basic virus biology and virus-host interactions. Additionally, these results may lay a foundation for extending such studies to other virus groups, thus potentially identifying common cellular pathways that could be targeted for the development of broad-spectrum antivirals.

2.2 RESULTS

2.2.1 Identification of essential host genes affecting BMV RNA replication

To systematically identify novel, essential host genes affecting BMV RNA replication, we screened a dox-repressible library of essential yeast strains (149). This collection contains ~900 yeast strains, each with a single endogenous essential gene promoter replaced by a tetracycline-repressible promoter (149). Upon the addition of the tetracycline derivative dox to growth media, expression of the essential gene is repressed, and the protein depleted. This library was used to identify changes in BMV RNA replication after repression (dox-treated) relative to continuous expression (untreated) of a specific essential host gene.

To assess the role of essential genes in BMV RNA replication, we co-transformed each of the ~900 strains with BMV expression plasmids pB12VG1 and pB3BG29 (Fig. 2.1). pB12VG1 expresses BMV RNA replication proteins 1a and $2a^{Pol}$ (119). pB3BG29 expresses an Rluc reporter-expressing BMV RNA3 cDNA derivative and, as an expression control, the Fluc reporter gene (Fig. 2.1). DNA-dependent transcription produces an initial (+)RNA3 transcript that serves as a template for 1a- and $2a^{Pol}$-dependent RNA3 replication and sgRNA4 synthesis via a (-)RNA3 intermediate (Fig. 2.1). Because sgRNA4, which encodes the coat protein, is derived from the (-)RNA3 intermediate, its synthesis depends on, and can serve as a reporter for, BMV RNA replication (88). Accordingly, in pB3BG29 we replaced the coat protein ORF with the Rluc reporter gene, so that luciferase assays could be used as a rapid measure of RNA4 production and expression (Fig. 2.1). A similar approach was used for primary screening of the yeast non-essential gene deletion library (119). Of the 892 dox-repressible strains transformed, 151 did not produce colonies after repeated transformation attempts (Table S1 in PLoS ONE 6(8): e23988), suggesting that the transformation process or expression of the viral constructs significantly impacted the fitness of these strains.

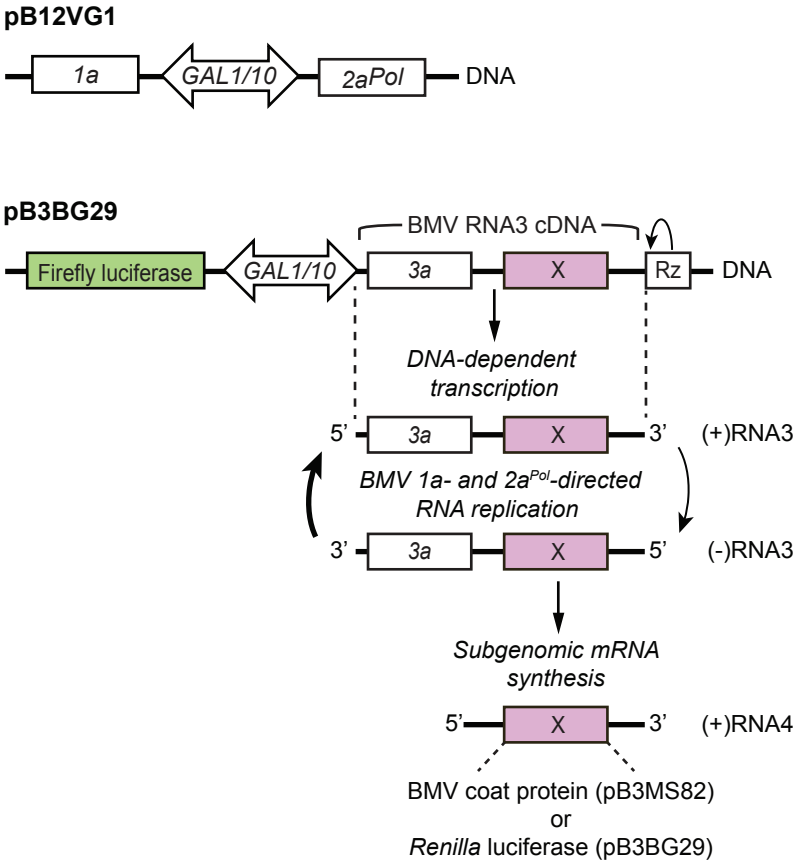

Figure 2.1. BMV expression plasmids. (A) pB12VG1 expresses replication factors 1a and $2a^{Pol}$. (B) pB3BG29 expresses Fluc and RNA3. BMV-specific RNA-dependent RNA replication and subgenomic mRNA synthesis is initiated from a cDNA derivative of RNA3. DNA-dependent transcription produces an initial (+)RNA3 transcript that serves as a template for 1a- and $2a^{Pol}$-dependent RNA3 replication and sgRNA4 synthesis via a (-)RNA3 intermediate. X, the BMV coat protein gene or any gene replacing it, such as Rluc (used here); *GAL1/GAL10*, yeast promoters, Rz, self-cleaving ribozyme.

The remaining 741 transformants were re-formatted on 96-well plates such that duplicates of each strain were present on the same plate (Fig. 2.2), allowing untreated and dox-treated strains to be directly compared for changes in RNA replication. It is important to note for this library that expression levels from the substituted TET promoter are often different than expression levels from the endogenous gene promoter (149). Therefore, to test and to control for possible changes in viral RNA replication and/or gene expression, each treated strain was compared to its untreated counterpart rather than to the parental wild type strain. Strains were grown in raffinose-containing selective medium lacking dox (allowing essential gene expression) or raffinose-containing selective medium containing 10 μg/ml dox (repressing essential gene expression) for 24 hr to allow for initial depletion of the essential gene mRNA and protein turnover in strains treated with dox. After this 24 hr treatment period, strains were sub-cultured into galactose-containing selective medium ±10 μg/ml dox to induce the expression of BMV components and subsequent viral RNA replication in the continued expression (untreated) or repression (dox-treated) of essential host factors. At 24 hr and 48 hr post-virus induction, Rluc expression was measured as a readout of BMV RNA3 replication and sgRNA4 synthesis. Because of expected differences in the kinetics of gene product depletion and their specific and non-specific effects on cell growth and BMV RNA replication, we measured Rluc at 24 hr and 48 hr post-virus induction for every strain. To monitor any potential adverse effects of dox on the viability of these yeast strains and to ensure that *GAL* promoter induction was effective, *GAL* driven Fluc expression, which is independent of BMV RNA replication (Fig. 2.1), was also assayed at 24 hr and 48 hr post-virus induction (Fig. 2.2). Two independent analyses of the entire library were performed.

Since ~70% of the strains in this library exhibit growth defects in the presence of dox (~20% of which exhibit growth defects even in the absence of dox, presumably as a result of endogenous promoter replacement) (149) and because BMV RNA replication levels are often non-specifically enhanced in slow-growing cells, stringent growth requirements were employed

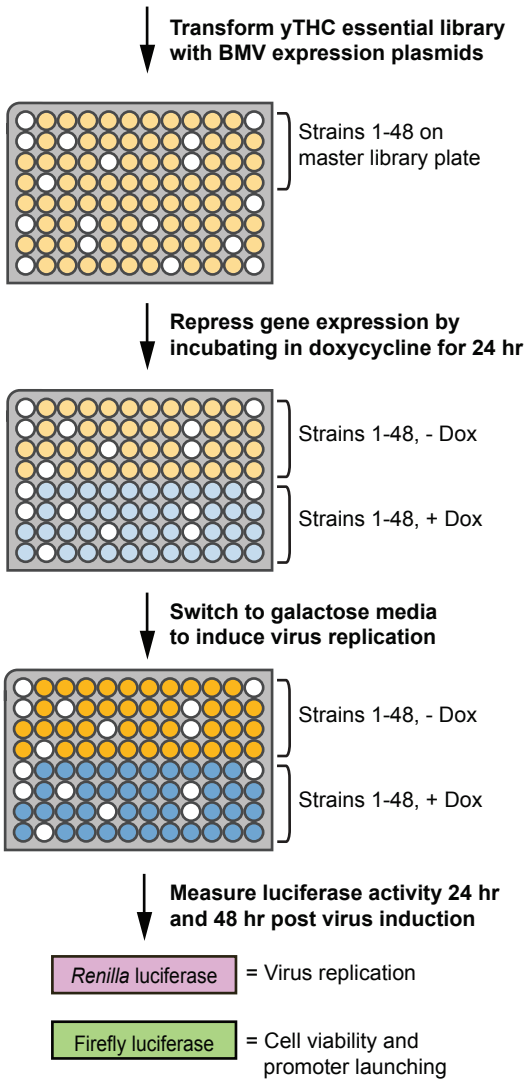

Figure 2.2. Yeast genetic screen used to identify essential host factors affecting BMV RNA replication. 892 yeast strains, each with a single essential gene promoter replaced by a doxycycline (dox)-repressible promoter, were transformed with BMV expression plasmids (Fig. 2.1). White wells indicate strains that did not transform. Transformants were re-formatted on 96-well plates with duplicates of each strain present on the same plate, allowing untreated and dox-treated strains to be directly compared. Strains were grown in raffinose-containing selective medium lacking dox (allowing essential gene expression) or containing 10 μg/ml dox (repressing essential gene expression) for 24 hr to allow for initial depletion of the essential gene mRNA and protein turnover in dox-treated strains. After this 24 hr treatment, strains were sub-cultured into galactose-containing selective medium ±10 μg/ml dox to induce expression of BMV components and subsequent viral RNA replication. Viral RNA replication was quantitated with a chemiluminescent Renilla luciferase assay at 24 hr and 48 hr post-virus induction. Cell viability and promoter launching were monitored with a chemiluminescent firefly luciferase assay at 24 hr and 48 hr post-virus induction. Two independent analyses of the library were performed.

to minimize false positives. Additionally, because we expected some strains to exhibit either immediate dox-induced growth defects and/or transcriptional defects from the *GAL* promoter, Fluc values in untreated vs. dox-treated strains were closely monitored. Accordingly, to be included in the final data analysis for potentially specific effects on BMV replication, each strain was required to: 1) double at least twice between 0-24 hr in galactose-containing media; 2) double at least one additional time between 24-48 hr in galactose-containing media; 3) and have an $Fluc_{dox\text{-}treated}$ value within 20% of its $Fluc_{untreated}$ value. As a reference, wild type strain R1158 doubled 3 times between 0-24 hr and 2 times between 24-48 hr and had comparable $Fluc_{untreated}$ and $Fluc_{dox\text{-}treated}$ values. Strains that did not meet these growth or Fluc value requirements in both passes were excluded from further analysis (Table 2.1). The remaining strains that satisfied these growth and Fluc requirements and were included in analysis (Table S4 in PLoS ONE 6(8): e23988) showed >90% overlap between pass 1 and 2 at the 24 hr time point and >80% overlap between passes at the 48 hr time point, confirming good reproducibility of screen conditions (e.g. growth, dox-treatment, etc.) and assay performance.

From the analyzed strains (Table S4 in PLoS ONE 6(8): e23988), we identified 42 essential yeast genes that, when dox-depleted, altered BMV-directed Rluc expression at least 6-fold in both passes at the same time point (Tables 2.2 and 2.3). A more stringent 6-fold cutoff was used in the primary screen in response to our observation that some strains in this essential gene library showed more luciferase assay variability than in our previous screen of non-essential genes. This increased variability is likely due to the fact that these genes are essential for cell growth. Thus, upon dox-induced repression of these genes, the experiment is a race between specific effects of the relevant gene on virus replication and the nonspecific, general suppression of cell growth and viability that eventually occur with each strain. Therefore, the results are more subject to variations due to small changes in growth conditions or timing of the experiments. Accordingly, a 6-fold cutoff was employed to limit the inclusion of false positives.

Table 2.1. Number of dox-repressible essential yeast strains excluded at each pass and time point due to growth or Fluc values.

	Pass 1, 24 hr	Pass 2, 24 hr	Pass 1, 48 hr	Pass 2, 48 hr
Number of strains excluded due to growth or Fluc[a, b, c]	**226**	**253**	**337**	**286**
Untreated	60	56	173	130
Dox treatment	130	154	137	130
Fluc	36	43	27	26

[a]Numbers are based on the 741 strains that transformed.

[b]Numbers represent strains unique to each filter.

[c]See Table S3 in doi:10.1371/journal.pone.0023988 to identify specific strains.

Table 2.2. Genes whose repression was associated with ≥6-fold enhanced BMV-directed Rluc expression in both primary screen passes.

		Fold increase in Rluc expression	
ORF	**Gene**	**Pass 1**	**Pass 2**
YLR359W	*ADE13*	46	57
YBR070C	*ALG14*	11	14
YDL132W	*CDC53*	8.4	6.3
YOR204W	*DED1*	180	140
YKL078W	*DHR2*	8.3	8.0
YLR129W	*DIP2*	440	160
YMR128W	*ECM16*	12	7.4
YLR274W	*MCM5*	33	19
YGR103W	*NOP7*	46	78
YGR119C	*NUP57*	30	19
YOR122C	*PFY1*	7.9	7.5
YLR196W	*PWP1*	11	28
YOL094C	*RFC4*	21	14
YNL207W	*RIO2*[a]	16	12
YGL044C	*RNA15*	41	12
YOR340C	*RPA43*	17	6.3
YKR008W	*RSC4*	250	310
YPL124W	*SPC29*	13	10
YGR116W	*SPT6*	45	17
YKL018W	*SWD2*	48	9.1
YDR324C	*UTP4*	12	11
YJL069C	*UTP18*	11	50
YGR251W	N/A[b]	33	150

[a] *RIO2* was identified at the 24 hr time point and all other genes were identified at the 48 hr time point.

[b] ORF not annotated in *Saccharomyces* Genome Database.

Table 2.3. Genes whose repression was associated with ≥6-fold inhibited BMV-directed Rluc expression in both primary screen passes.

		Fold decrease in Rluc expression	
ORF	**Gene**	**Pass 1**	**Pass 2**
YKL112W	*ABF1*	15	9.1
YER168C	*CCA1*	7.7	7.6
YFR028C	*CDC14*[a]	12; 9.2	6.0; 7.8
YNR038W	*DBP6*	26	9.9
YPL266W	*DIM1*	36	70
YDR141C	*DOP1*	6.2	46
YJR017C	*ESS1*	22	22
YOL133W	*HRT1*	7.2	6.2
YGL073W	*HSF1*[b]	37	17
YGL018C	*JAC1*	15	45
YAL033W	*POP5*	17	12
YER012W	*PRE1*[a]	21; 8.4	13; 19
YML046W	*PRP39*	9.4	49
YGL048C	*RPT6*	15	52
YKL125W	*RRN3*	13	76
YGR245C	*SDA1*	22	14
YDR472W	*TRS31*	7.5	22
YDR327W	N/A[c]	460	160
YOR262W	N/A[b, c]	9.8	13

[a]*CDC14* and *PRE1* were identified at both the 24 hr and 48 hr time points and data for both time points is listed as "24 hr; 48 hr".

[b]*HSF1* and YOR262W were identified at the 24 hr time point and all other genes were identified at the 48 hr time point.

[c]ORF not annotated in *Saccharomyces* Genome Database.

In principle, altered BMV-directed Rluc expression observed in the 42 candidate genes might result from general defects in RNA4 translation or viral RNA synthesis, or from selective defects in replication, expression or function of the Rluc reporter gene. To identify genes that specifically affected BMV RNA synthesis and/or accumulation, secondary validation testing of the 42 candidate genes was performed using Northern blotting to analyze RNA3 replication and RNA4 production, as described in the next two sections.

2.2.2 Dox-repression of 19 essential genes facilitated BMV RNA accumulation

Of the 42 candidate genes identified in the reporter gene-based primary screens, 23 were genes whose repression enhanced BMV-directed Rluc expression relative to Fluc expression at least 6-fold in both passes at the same time point (Table 2.2). For secondary validation tests, these 42 candidate strains were transformed with the 1a- and $2a^{Pol}$-expressing plasmid pB12VG1 and with a plasmid expressing RNA3 retaining the BMV coat protein ORF (Fig. 2.1, pB3MS82). The levels of RNA3 and RNA4 replication products then were measured by Northern blotting. In particular, we used the level of RNA4 relative to 18S rRNA as the primary measure of any dox-induced change in BMV RNA-dependent RNA synthesis, through the ratio $[\text{RNA4/18S rRNA}]_{\text{dox-treated}}$/ $[\text{RNA4/18S rRNA}]_{\text{untreated}}$. RNA4 was used as the primary measure of BMV RNA synthesis since, unlike RNA3, RNA4 is only produced by viral RNA-dependent RNA synthesis and not also by DNA-dependent transcription (Fig. 2.1). Moreover, RNA4 level is the parameter most closely related to the Rluc expression measured in the primary screen (Fig. 2.1).

A statistically significant increase in BMV (+)RNA4 accumulation relative to 18S rRNA was confirmed for 19 of the 23 genes (~83% confirmation) at the commonly applied false discovery rate of 5% (Fig. 2.3 and Table 2.4). False discovery rate analysis is a robust statistical method that controls for multiple test variables by calculating an adjusted, more stringent *p*-value, termed a *q*-value (204). (+)RNA4 levels were enhanced 1.5- to 8-fold in the 19 confirmed

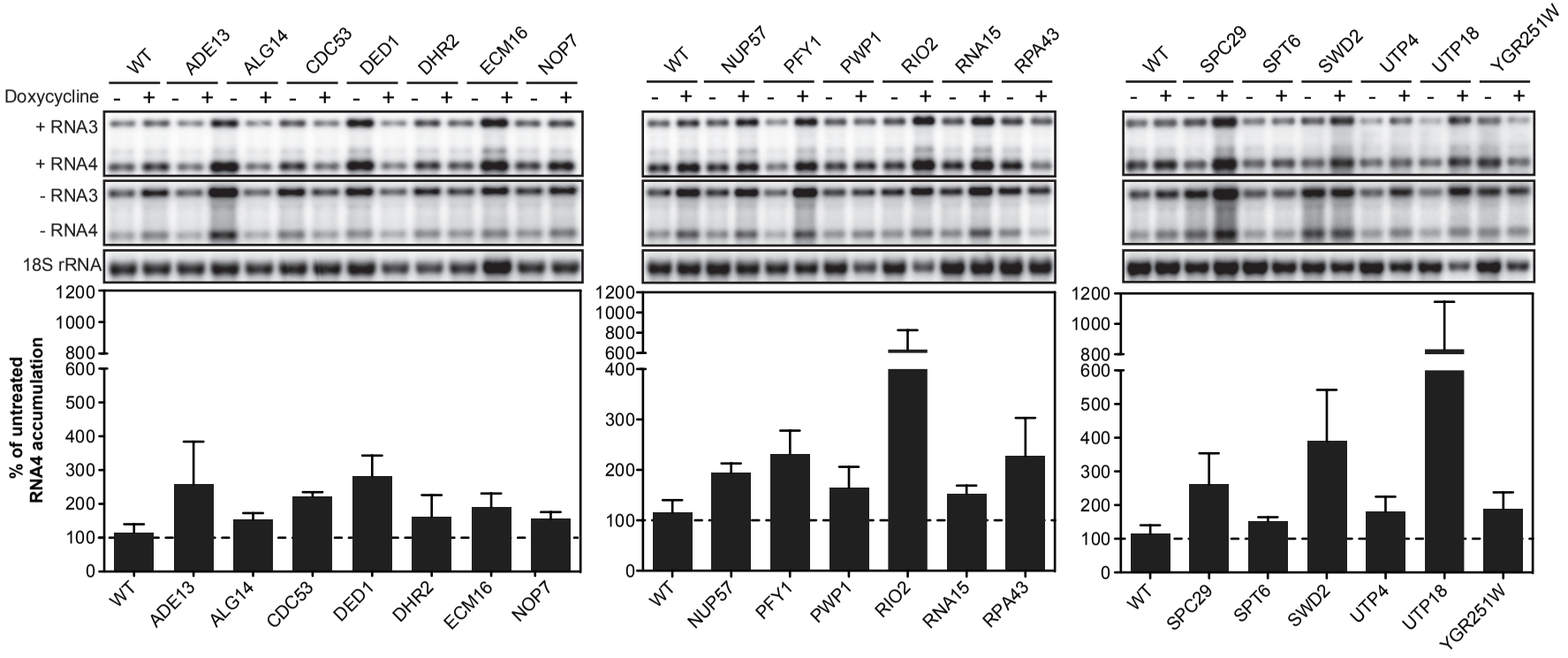

Figure 2.3. Dox-induced repression of 19 essential yeast genes enhances BMV RNA replication. Total RNA extracts were obtained from wild type R1158 and untreated and dox-treated (10 µg/ml) essential yeast strains expressing BMV 1a, 2a^{Pol} and RNA3. Accumulation of positive- and negative-strand RNA3 and subgenomic RNA4 was detected by Northern blotting using probes specific for BMV RNA3 and RNA4. Equal loading of total RNA was verified by probing for 18S rRNA. Values represent the mean of four independent experiments.

Table 2.4. Essential genes whose repression was confirmed to enhance BMV RNA accumulation in secondary validation testing.

ORF	Gene	(+)RNA4 (average % untreated)	q-value
YJL069C	*UTP18*	833 ± 312	0.011
YNL207W	*RIO2*	635 ± 190	0.003
YKL018W	*SWD2*	389 ± 153	0.006
YOR204W	*DED1*	282 ± 61	0.003
YPL124W	*SPC29*	261 ± 93	0.006
YLR359W	*ADE13*	258 ± 126	0.034
YOR122C	*PFY1*	232 ± 46	0.009
YOR340C	*RPA43*	227 ± 76	0.010
YDL132W	*CDC53*	222 ± 13	3.24E-04
YGR119C	*NUP57*	194 ± 19	0.006
YMR128W	*ECM16*	190 ± 41	0.011
YGR251W	N/A[a]	189 ± 45	0.014
YDR324C	*UTP4*	180 ± 49	0.003
YLR196W	*PWP1*	165 ± 41	0.011
YKL078W	*DHR2*	161 ± 65	0.036
YGR103W	*NOP7*	155 ± 21	0.011
YBR070C	*ALG14*	153 ± 20	0.006
YGL044C	*RNA15*	153 ± 16	0.003
YGR116W	*SPT6*	152 ± 12	0.003

[a]ORF not annotated in *Saccharomyces* Genome Database.

strains (Fig. 2.3 and Table 2.4). Similarly, levels of (-)RNA3, the replication intermediate that serves as a template for sgRNA4, were increased 1.4- to 5-fold in these strains (Table 2.5).

The 19 confirmed dox-repressed genes that enhanced BMV RNA accumulation encode proteins with functions in varied cellular processes, including ribosome biosynthesis (*DHR2, ECM16, NOP7, PWP1, RIO2, RPA43, UTP4, UTP18,* and *YGR251w*), cell cycle/DNA maintenance (*ADE13* and *SPC29*), mRNA metabolism (*RNA15, SPT6,* and *SWD2*), protein homeostasis (*PFY1*), translation (*DED1*), trafficking (*NUP57*) and lipid synthesis (*ALG14*) (Table 2.6). Possible relations of these functions to viral replication are considered further in the Discussion.

2.2.3 Dox-repression of five essential genes inhibited BMV RNA accumulation

The primary screens additionally identified 19 essential host genes that inhibited BMV-directed Rluc expression at least 6-fold in both passes at the same time point (Table 2.3). Northern blotting confirmed statistically significant decreases in BMV (+)RNA4 accumulation for 5 of 19 genes (~26% confirmation) at a false discovery rate of 5% (Fig. 2.4 and Table 2.7). (+)RNA4 levels were inhibited ~1.5- to 8-fold in these strains (Fig. 2.4 and Table 2.7). In addition to the severe inhibition of (+)RNA4 accumulation in P_{TET}-*HSF1*, P_{TET}-*PRE1*, and P_{TET}-*RPT6*, (-)RNA3 was inhibited 5.5-, 1.8-, and 5.5-fold in these strains, respectively (Fig. 2.4 and Table 2.8).

Interestingly, all five genes that inhibited BMV RNA replication (*ESS1, HSF1, JAC1, PRE1*, and *RPT6*) perform cellular functions that, in various ways, contribute to modulating host protein levels (Table 2.6).

2.2.4 BMV $2a^{Pol}$ protein levels are affected in some dox-repressed strains

One possible reason for altered RNA replication is deregulation of viral protein accumulation. To test this, accumulation of BMV RNA replication proteins 1a and $2a^{Pol}$ were

Table 2.5. Negative-strand RNA3 levels for essential yeast genes confirmed to enhance BMV RNA accumulation in secondary validation testing.

ORF	Gene	(-)RNA3 (average % untreated)
YJL069C	*UTP18*	501 ± 110
YOR340C	*RPA43*	265 ± 97
YNL207W	*RIO2*	263 ± 164
YKL018W	*SWD2*	220 ± 85
YOR122C	*PFY1*	219 ± 87
YGR251W	N/A[a]	198 ± 63
YGR103W	*NOP7*	198 ± 160
YLR359W	*ADE13*	194 ± 99
YBR070C	*ALG14*	185 ± 61
YDR324C	*UTP4*	185 ± 55
YGR119C	*NUP57*	177 ± 41
YKL078W	*DHR2*	176 ± 26
YGR116W	*SPT6*	175 ± 23
YMR128W	*ECM16*	139 ± 67
YOR204W	*DED1*	137 ± 41
YLR196W	*PWP1*	137 ± 32
YDL132W	*CDC53*	135 ± 16
YGL044C	*RNA15*	132 ± 38
YPL124W	*SPC29*	127 ± 71

[a]ORF not annotated in *Saccharomyces* Genome Database.

Table 2.6. Annotated functions of confirmed essential host genes affecting BMV RNA accumulation.

Gene[a]	Gene Description[a,b]
Protein Homeostasis	
ESS1	**Peptidylprolyl-cis/trans-isomerase; regulates phosphorylation of the RNA polymerase II large subunit**
HSF1	**Trimeric heat shock transcription factor**
JAC1	**Hsp40/DnaJ family J-protein that functions with Hsp70 in Fe-S cluster biogenesis in mitochondria**
PRE1	**Beta 4 subunit of the 20S core of the 26S proteasome**
RPT6	**One of six ATPases of the 19S regulatory particle of the 26S proteasome**
PFY1	Binds profilin, actin and phosphatidylinositol 4,5-bisphosphate; cytoskeleton organization
Translation	
DED1	ATP-dependent DEAD-box RNA helicase, required for translation initiation of all yeast mRNAs
Trafficking	
NUP57	Nucleoporin essential for trafficking nucleic acids, proteins, and RNA through the nuclear pore complex
Lipid synthesis	
ALG14	Component of UDP-GlcNAc transferase required for dolichyl-linked oligosaccharide synthesis
Ribosome Biosynthesis	
DHR2	DEAH-box ATP-dependent RNA helicase, required for 18S rRNA synthesis
ECM16	DEAH-box ATP-dependent RNA helicase specific to the U3 snoRNP, required for 18S rRNA synthesis
NOP7	Required for large ribosomal subunit maturation; required for exit from G0
PWP1	Protein with WD-40 repeats involved in rRNA processing
RIO2	Serine kinase involved in the processing of the 20S pre-rRNA into mature 18S rRNA
RPA43	RNA polymerase I subunit A43
UTP4	Subunit of U3-contaning complexes involved in production of 18S rRNA
UTP18	Possible U3 snoRNP protein involved in maturation of pre-18S rRNA
YGR251w	Required for 18S rRNA maturation
mRNA Metabolism	
RNA15	Component involved in the cleavage and polyadenylation of mRNA 3' ends
SPT6	Transcription elongation factor required for the maintenance of chromatin structure during transcription
SWD2	Required for methylation of histone H3 and RNA polymerase II transcription termination
Cell Cycle/DNA Maintenance	
ADE13	Adenylosuccinate lyase involved in the purine nucleotide synthesis
CDC53	A scaffolding subunit (cullin) for multiple E3 ubiquitin-ligase complexes; regulates G1-S cell cycle progression
SPC29	Inner plaque spindle pole body (SPB) component; required for SPB duplication

[a]Bold font indicates genes whose repression inhibits viral RNA accumulation; non-bold font indicates genes whose repression enhances viral RNA accumulation.

[b]Based on the *Saccharomyces* Genome Database at http://www.yeastgenome.org/.

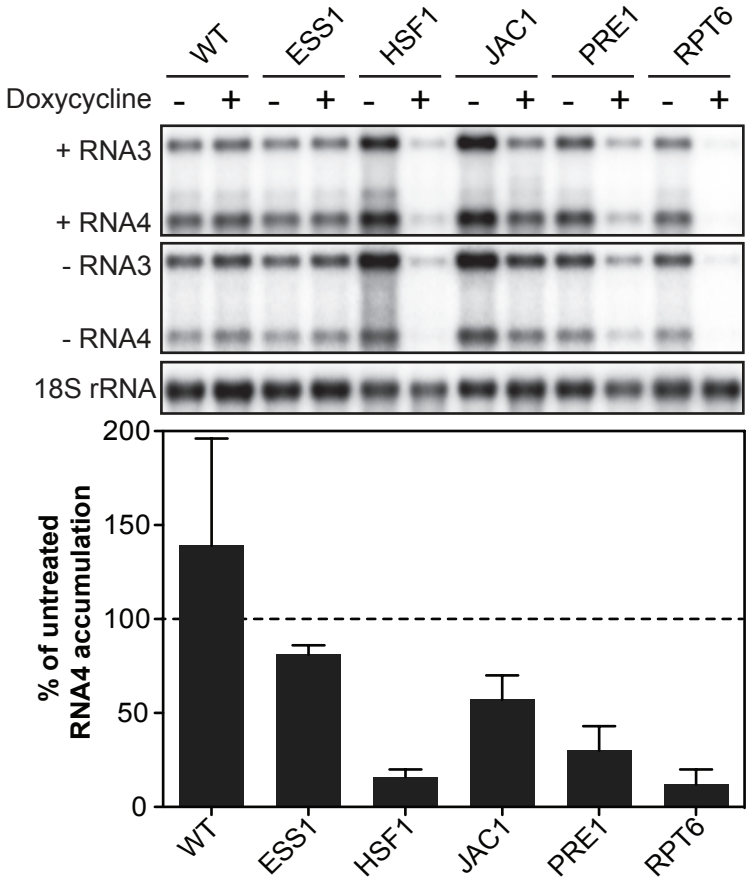

Figure 2.4. Dox-induced repression of five essential yeast genes inhibits BMV RNA replication. Total RNA extracts were obtained from wild type R1158 and untreated and dox-treated (10 µg/ml) essential yeast strains expressing BMV 1a, $2a^{Pol}$ and RNA3. Accumulation of positive- and negative-strand RNA3 and subgenomic RNA4 was detected by Northern blotting using probes specific for BMV RNA3 and RNA4. Equal loading of total RNA was verified by probing for 18S rRNA. Values represent the mean of four independent experiments.

Table 2.7. Essential genes whose repression was confirmed to inhibit BMV RNA accumulation in secondary validation testing.

ORF	Gene	(+)RNA4 (average % untreated)	q-value
YGL048C	*RPT6*	12 ± 8	0.024
YGL073W	*HSF1*	16 ± 4	0.004
YER012W	*PRE1*	30 ± 13	0.024
YGL018C	*JAC1*	57 ± 13	0.029
YJR017C	*ESS1*	81 ± 5	0.024

Table 2.8. Negative-strand RNA3 levels for essential yeast genes confirmed to inhibit BMV RNA accumulation in secondary validation testing.

ORF	Gene	(-)RNA3 (average % untreated)
YGL048C	*RPT6*	18 ± 9
YGL073W	*HSF1*	18 ± 9
YER012W	*PRE1*	55 ± 29
YGL018C	*JAC1*	63 ± 18
YJR017C	*ESS1*	92 ± 15

assayed by Western blotting. Addition of dox to growth medium had no detectable effect on BMV 1a and $2a^{Pol}$ accumulation in the wild type strain (Figs. 2.5 and 2.6). For 20 of 24 confirmed hits, BMV 1a levels in dox-treated strains were comparable to their untreated sample (Figs. 2.5 and 2.6). However, in P_{TET}-*ADE13,* P_{TET}-*DED1,* P_{TET}-*PRE1* and P_{TET}-*RPT6* dox-treated cells there was a detectable increase in 1a compared to the untreated strains (Figs. 2.5 and 2.6). Moreover, BMV $2a^{Pol}$ levels were significantly increased in P_{TET}-*HSF1*, P_{TET}-*PRE1* and P_{TET}-*RPT6* dox-treated strains (Fig. 2.6). In P_{TET}-*JAC1* dox-treated cells, $2a^{Pol}$ levels were elevated in the absence of dox, but reduced to near wild type levels in the presence of dox (Fig. 2.6). These results suggest that, with the potential exception of *HSF1*, *PRE1* and *RPT6*, viral protein regulation is unlikely to be the cause of altered viral RNA replication phenotypes upon depleting the products of the implicated genes.

2.3 DISCUSSION

We employed a high-throughput, systematic analysis of 741 dox-repressible essential yeast strains to identify 24 novel, essential host factors that alter BMV RNA replication. Our previous systematic analysis of ~4,500 non-essential yeast deletion strains identified 99 genes that inhibited or enhanced BMV RNA replication (119). Collectively, we have analyzed ~93% of all yeast genes (~5,800), and the 123 host genes identified to date that affect BMV RNA replication represent 2.3% of the yeast genome. As observed with tomato bushy stunt virus (TBSV) (96), another positive strand RNA virus, BMV replication is affected, directly or indirectly, by essential genes at a higher frequency (3.2%) than non-essential genes (2.2%).

For multiple reasons, our studies to date likely underestimate the number of host genes that contribute to BMV RNA replication. ~60% of non-essential yeast genes are genetically redundant, meaning that the functions of many gene deletions are partially compensated for by other genes (72, 220). Additionally, although the dox-repressible library is a powerful tool for

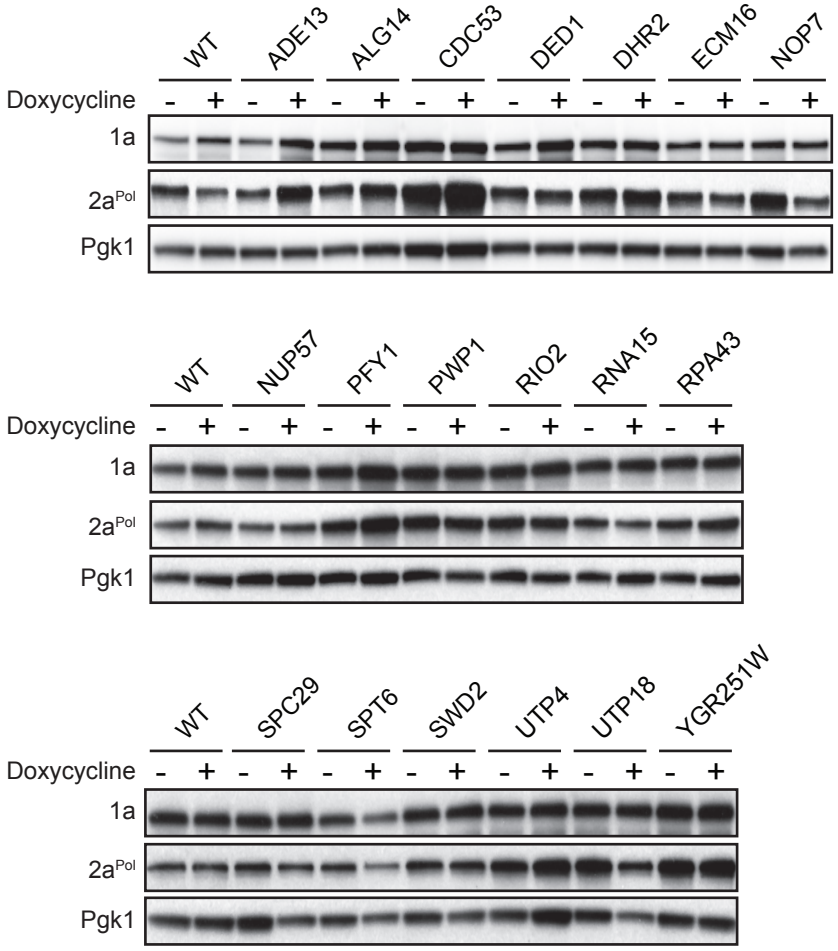

Figure 2.5. BMV 1a and 2a^{Pol} levels for dox-repressed essential yeast genes with enhanced BMV RNA replication. Accumulation of BMV 1a and 2a^{Pol} in wild type R1158 and untreated and dox-treated (10 µg/ml) essential yeast strains was measured by Western blot analysis. Total proteins were extracted from equal numbers of yeast cells and analyzed by SDS/PAGE. Equal loading of total protein was verified by measuring Pgk1p levels.

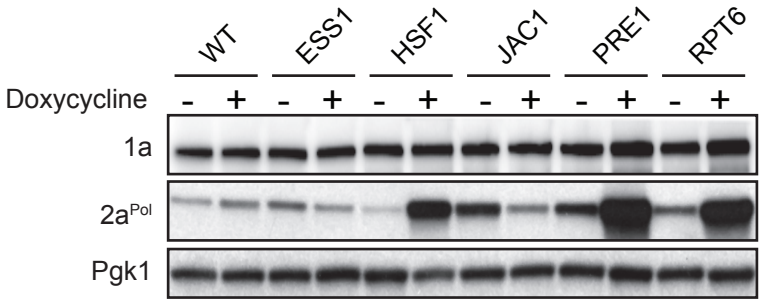

Figure 2.6. BMV 1a and 2a^{Pol} levels for dox-repressed essential yeast genes with inhibited BMV RNA replication. Accumulation of BMV 1a and 2a^{Pol} in wild type R1158 and untreated and dox-treated (10 µg/ml) essential yeast strains was measured by Western blot analysis. Total proteins were extracted from equal numbers of yeast cells and analyzed by SDS/PAGE. Equal loading of total protein was verified by measuring Pgk1p levels.

analyzing the effects of essential genes on virus replication, over 70% of the strains in this collection exhibit growth defects in the presence of dox and 14% exhibit growth defects in the absence of dox (149). Moreover, expressing viral components in some of these strains resulted in no or poor growth, interfering with meaningful analysis of these strains. Finally, in both the screens for non-essential genes (119) and essential genes (here), virus dependence on some host functions was likely masked by continuous expression of BMV replication proteins and RNA templates, compared to natural infections resulting from a single viral RNA template. This is analogous to studies in which high multiplicity of infection overcomes antiviral resistance in some cell lines (72, 154). The lower confirmation rate for the 19 candidate genes that inhibited BMV-directed Rluc expression may be because these primary screen candidates included false positives arising from the tendency of essential gene depletion to produce non-specific inhibitory effects and greater variability in results, as is also noted above in the Results section. Additionally, translation and protein expression are the basis of our primary screen luciferase assays, whereas secondary confirmation by Northern blotting analyzes RNA levels normalized to 18S rRNA. Subtle differences (e.g., growth conditions) not controlled for by Fluc in the primary screen or 18S rRNA in Northern analysis may also contribute to the lower confirmation rate observed. Despite such limitations, this study identified 24 novel, essential host genes from various cellular pathways with potentially diverse roles in BMV RNA replication.

Enhanced BMV RNA replication upon repression of an essential gene suggests that, when present, the host factor contributes to an inhibitory response in a cellular process/pathway that competes with the virus. For example, of the 19 genes whose repression stimulated BMV RNA replication, 9 genes (*DHR2*, *ECM16, NOP7*, *PWP1*, *RIO2*, *RPA43*, *UTP4*, *UTP18*, *YGR251W*) are functionally associated with ribosome biosynthesis (Table 2.6). All of these genes perform or participate in ATP-dependent processes and depleting products of the implicated genes may result in an increased pool of energy and/or nucleotides available to the virus (Fig. 2.3, Tables 2.4 and 2.6). Alternatively, depleting these genes may alter the

competition between viral and cellular translation. *UTP4* and *UTP18* function in rRNA processing, a cellular pathway that enhances TBSV replication (as shown by the effects of *UTP9* and *UTP15*) (96), but has the opposite effect on BMV RNA replication.

Depleting genes involved in processing cellular mRNA 3' ends *(RNA15*), regulating transcription (*SPT6*), modulating cellular gene expression (*SWD2*), and controlling nucleocytoplasmic trafficking (*NUP57*) may increase the availability of ribosomes and/or alter the levels of specific proteins, preferentially stimulating BMV RNA replication (Fig. 2.3, Tables 2.4 and 2.6) by disrupting cellular pathways that would compete with BMV RNA translation or replication under wild type conditions. Thus, experimental depletion of these genes is in some ways analogous to the global shutoff of host mRNA pathways, employed by many mammalian viruses through diverse mechanisms (70, 108, 233). Additional studies are necessary to define the role of these mRNA metabolism genes in BMV RNA replication.

In previous studies, we have observed that significantly disrupting the cell cycle and extended doubling times can non-specifically increase BMV RNA levels per cell, apparently because the virus has more time to accumulate RNA replication products prior to cell division (unpublished data). To avoid such false positives, we excluded from further analysis strains for which dox-treatment significantly slowed cell division (see Results above). Thus, although *SPC29* and *PFY1* encode proteins potentially related to cell division (respectively a spindle pole body protein and actin-binding protein) the doubling times of untreated and dox-treated P_{TET}-*SPC29 and* P_{TET}-*PFY1* cells were comparable and likely do not account for the increased levels of BMV RNA4 observed (Fig. 2.3. and Table 2.4). Alternatively, disrupting the cell cycle in P_{TET}-*SPC29*- and/or P_{TET}-*PFY1*-repressed cells may alter cell cycle signal transduction pathways or the localization of cellular factors that normally inhibit viral RNA replication.

Mutating general translation initiation factor *DED1* severely inhibits translation of BMV $2a^{Pol}$ from BMV genomic RNA2 in a fashion dependent on specific sequences in the RNA2 5' noncoding region (NCR) (161). Because the RNA2 5' NCR was not present in the BMV

expression constructs used in this study, we did not expect a detectable change in BMV RNA replication in the dox-repressed P_{TET}-*DED1* strain. However, we observed an increase in RNA replication (Fig. 2.3 and Table 2.4), suggesting that dox-repression of P_{TET}-*DED1* and global depletion of its gene products may have an alternative effect(s) on viral RNA replication compared to the previously analyzed *ded1-18* point mutant (161). For example, under our screen conditions, repressing P_{TET}-*DED1* may alter the production of viral or cellular proteins in ways that favor increased viral RNA accumulation. Further studies are necessary to define such potential additional role(s) for *DED1* in BMV RNA replication.

Reduced BMV RNA replication upon repression of an essential gene suggests that, when present, the host factor directly or indirectly facilitates viral RNA synthesis or accumulation. Interestingly, the five genes whose depletion inhibited BMV RNA replication (*ESS1*, *HSF1*, *JAC1*, *PRE1*, *RPT6*) have varied roles in protein stability or activation. For example, a small but reproducible (~20%) inhibition of BMV RNA replication resulted upon dox-repression of P_{TET}-*ESS1*, a peptidyl-prolyl cis-trans isomerase (PPI) (Fig. 2.4 and Table 2.7). Changes in isomerase activity can alter the structure, stability, or intracellular localization of client proteins (201), and deleting or mutating PPIs has variable effects on positive-strand RNA viruses (65, 109, 142, 240). For example, knockdown of cyclophilin A and loss of its PPIase activity severely inhibits hepatitis C virus replication (34, 109, 135). Conversely, siRNA-mediated knockdown of cyclophilin G mRNA stimulates hepatitis c virus replication (65). Collectively, these findings suggest multi-faceted, complex roles for PPIs in positive-strand RNA virus replication.

JAC1, a member of the Hsp40/DnaJ family of proteins, encodes a specialized J-protein co-chaperone that assists Hsp70 in iron-sulfur (Fe-S) cluster biogenesis (101, 180). Fe-S clusters are among the most versatile protein co-factors in the cell and participate in electron transfer, ribosome biogenesis, regulating gene expression and enzyme activity, and nucleotide metabolism (20, 129, 130). The inhibition of BMV replication upon dox-repressing P_{TET}-*JAC1*

(Fig. 2.4 and Table 2.7) may result from negatively affecting the activation and/or function of one or more cellular or viral factors required for BMV RNA replication. Previously, we showed that *YDJ1*, another J-protein co-chaperone of Hsp70 and Hsp90, is required to activate the BMV RNA replication complex, likely through modulating BMV $2a^{Pol}$ folding or assembly into the complex (213). Dox-repression of another heat shock protein, P_{TET}-*HSF1*, inhibited BMV RNA replication by 84% (Fig. 2.4 and Table 2.7). Thus, our data suggest that BMV utilizes multiple members of the heat shock protein family to facilitate RNA replication.

Dox-repressing P_{TET}-*PRE1*, a 20S proteasome core component, inhibited BMV RNA replication by 70% (Fig. 2.4 and Table 2.7). Similarly, repressing P_{TET}-*RPT6*, one of six ATPases of the 19S regulatory particle of the 26S proteasome, resulted in an ~90% reduction in BMV RNA replication (Fig. 2.4 and Table 2.7). Additionally, BMV $2a^{Pol}$ accumulation increased significantly in both P_{TET}-*PRE1* and P_{TET}-*RPT6* dox-repressed cells (Fig. 2.6). These results are consistent with previous findings that multiple non-essential ubiquitin-proteasome system components contribute to BMV RNA replication and that cells lacking *PRE9*, the only non-essential 20S proteasome component, also exhibit a substantial increase in BMV $2a^{Pol}$ levels (119). Our prior data show that having a substantial excess of $2a^{Pol}$ shifts replication compartments from small spherular compartments to double membrane layers, but does not inhibit viral RNA replication (197). Thus, the increase in $2a^{Pol}$ accumulation in dox-repressed P_{TET}-*PRE1* and P_{TET}-*RPT6* (Fig. 2.6) is not likely the cause of decreased RNA replication. However, prior results do not exclude the possibility that *PRE1* and *RPT6* depletion might affect BMV RNA replication by directly or indirectly modulating $2a^{Pol}$ localization, post-translational modification or interacting partners. The 26S proteasome localizes predominantly to the nuclear envelope-ER network (59), the site of BMV RNA replication (189, 196), and numerous viruses utilize the ubiquitin-proteasome system to facilitate infection or replication (15, 17, 18, 30, 182, 234). Studies to define the specific role(s) of the ubiquitin-proteasome system in BMV RNA replication are ongoing.

With the exception of *NUP57*, *RNA15*, *SPC29* and *YGR251w*, each of the essential genes identified in this study have recognized orthologs in *Arabidopsis thaliana* (http://www.arabidopsis.org/ and http://ppod.princeton.edu/), presenting the possibility that similar genes could function in BMV RNA replication in its natural plant hosts. For example, we have shown here that dox-repression of Hsp70 cofactor *JAC1* or heat shock protein transcription factor *HSF1* significantly inhibits BMV RNA replication. *Arabidopsis* encodes 18 Hsp70 family members and Hsp70s have been shown to affect the replication of other (+)RNA viruses in plants, including TBSV and turnip mosaic virus (99, 224).

Similarly, *PRE1* (*PBD1* and *PBD2* in *Arabidopsis)* and *RPT6* (*RPT6a* and *RPT6b* in *Arabidopsis*) are essential components of the highly conserved 26S proteasome and recent results from our laboratory show that BMV RNA replication in yeast and plant cells depends critically on the ubiquitin-proteasome pathway (B. Gancarz and P. Ahlquist, unpublished results) (119, 226).

In summary, our high-throughput analysis of essential yeast genes identified a diverse set of host factors that affect BMV RNA replication and significantly expanded our knowledge of cellular pathways utilized by BMV. Additional studies both in yeast and in BMV's natural plant hosts should reveal how these host factors affect the virus and provide new insights to host cell function and virus-host interactions. Although targeting some essential genes may result in deleterious effects on cells or patients, focusing on the relevant cellular pathways, rather than only individual genes, may overcome such issues. For example, two of the essential genes with the most substantial inhibitory effect on BMV RNA replication, *PRE1* and *RPT6*, are proteasome components, while other proteasome components are not essential (e.g. *PRE9*, identified in previous screen). Proteasome inhibitors have antiviral activity against multiple diverse viruses (including herpes simplex virus, hepatitis B virus, and HIV, among others), have been through multiple clinical trials, and are already approved for use in patients for some purposes. Many of

the genes identified function in pathways utilized by other viruses and thus may present potential cellular targets for developing broad-spectrum antivirals.

2.4 MATERIALS AND METHODS

2.4.1 *S. cerevisiae* strains and plasmids

The yeast Tet-Promoter Hughes Collection of essential yeast strains was purchased from Open Biosystems (Huntsville, AL). The tet-promoter mutant strains (designated here with the prefix P_{TET}) were provided in the haploid R1158 background (*MATa URA3::CMV-tTA MATa his3-1 leu2-0 met15-0*), which was constructed by a one-step integration of the cytomegalovirus (CMV) promoter-driven tTA* transactivator at the *URA3* locus (83). The kanR-tetO7-TATA was then integrated into the promoter of a different essential gene in strain R1158, allowing the repression of essential gene expression upon the addition of dox to growth medium (149).

pB12VG1 expresses BMV 1a and $2a^{Pol}$ from the *GAL1* and *GAL10* promoters, respectively (119). pB3BG29, based on pB3Rluc (119), uses a truncated *GAL1* promoter (GALL (153)) to express RNA3 with the coat protein ORF replaced by the *Renilla* luciferase (Rluc) ORF (from pRL-null; Promega, Madison, WI). pB3BG29 also expresses the firefly luciferase (Fluc) ORF (from pGL3-Basic; Promega, Madison, WI) from the *GAL10* promoter. To construct pB3BG29, the *Age*I-*Aat*II RNA3/Rluc-containing fragment of pB3Rluc (119) replaced the *Age*I-*Aat*II FHV RNA1/Rluc-containing fragment of pBDL250-Ren [B. Lindenbach, unpublished]. pB3MS82 expresses a BMV RNA3 derivative in which the coat protein gene has a four-nucleotide insertion and a point mutation, abolishing expression of the coat protein (12). The use of pB3MS82 in this study, as in many other studies (12, 52, 71, 133, 161, 227), allows analysis of RNA3 and RNA4 levels while avoiding any possible effects of coat protein expression and RNA encapsidation. pB12VG1 and pB3BG29 were used in reporter gene-based

primary screens and pB12VG1 and pB3MS82 were used in secondary validation testing by Northern blotting.

2.4.2 Yeast transformation and growth

96-well yeast transformations were based on a one-step procedure (35). The P_{TET} essential yeast strains were grown to saturation overnight at 30°C in 96-well plates (1 ml per well). The cells were pelleted, suspended in 100 μl of transformation mix (0.18 M LiAc, pH 5.5, 36% polyethylene glycol-3350, 90 mM DTT, 0.5 mg/ml sheared salmon sperm DNA, and 20 μg/ml of each plasmid) per well and incubated at 30°C for 60 min. Cells then were heat shocked at 42°C for 20 min, pelleted, re-suspended in 20 μl sterile water per well and 10 μl was plated on solid media. Transformants were selected by complementation of auxotrophic markers. 96-well plates of transformed yeast were re-formatted to contain 48 strains in duplicate per plate so that strains could be analyzed in the absence of dox (allowing essential gene expression) or in the presence of dox (repressing essential gene expression). Strains containing BMV expression plasmids were grown overnight in medium containing raffinose, subcultured to a starting OD_{600}=0.1 in medium containing raffinose ±10 μg/ml dox, grown for 24 hr subcultured to a starting OD_{600}=0.1 in medium containing galactose ±10 μg/ml dox. Cells were analyzed at 24 hr and 48 hr post gal-induction of virus expression. Strains were grown in 96-well plates for luciferase assays and 14 ml culture tubes for Northern analysis.

2.4.3 RNA analysis

For 96-well Fluc assays, 2.5 μl of cells were lysed in 1X Passive Lysis Buffer (Promega, Madison, WI), 25 μl of Luciferase Assay Substrate (Promega, Madison, WI) was injected and read for 1s with a 1.6s delay using a VictorV (PerkinElmer, Waltham, MA). For 96-well Rluc assays, 5 μl of cells were lysed in 1X Passive Lysis Buffer, 25 μl of *Renilla* Luciferase Assay Substrate (Promega, Madison, WI) was injected and read for 1s with a 1.6s delay using a

VictorV. To allow comparison between plates, the median of untreated samples and the median of dox-treated samples were calculated for each plate. Each untreated sample was then normalized to the untreated median whereas each dox-treated sample was normalized to the dox-treated median. For each pass of the 741 P_{TET} strains, we calculated BMV-directed Rluc expression as [$Rluc_{dox\text{-}treated}$/$Fluc_{dox\text{-}treated}$] normalized to the dox-treated median and [$Rluc_{untreated}$/$Fluc_{untreated}$] normalized to the untreated median. The dox-treated to untreated ratio of ratios was calculated and converted to fold change. High-throughput isolation of total RNA from yeast cells was performed as previously described (57). Northern blotting was performed as previously described (131) except that 2 µg RNA was separated in 1% (wt/vol) agarose-MOPS (morpholinepropanesulfonic acid)-formaldehyde gels. RNAs were detected using ^{32}P-labeled probes specific for positive- or negative-strand BMV RNA3 and RNA4 as previously described (124). The 18S rRNA probe was derived from pTRI RNA 18S templates (Ambion, Austin, TX). Probes were synthesized using an Epicenter Riboscribe probe synthesis kit (Madison, WI) with the appropriate enzyme, i.e., T7 or or SP6 polymerase. Northern blots were imaged on a Typhoon 9200 instrument (Amersham Biosciences, Piscataway, NJ) and band intensities were analyzed with ImageQuant software (Molecular Dynamics, Piscataway, NJ).

2.4.4 Protein extraction, Western blotting and total protein analysis

Total protein was extracted as previously described (124) and equal volumes of cell lysates were separated on 4-15% Criterion™ TGX™ precast polyacrylamide gels (Bio-Rad, Hercules, CA). Proteins were transferred to PVDF membrane and expression of target proteins was detected with the following antibodies and dilutions: rabbit anti-BMV 1a at 1:10,000, mouse anti-BMV $2a^{Pol}$ at 1:3,000, and mouse anti-Pgk1p (Molecular Probes, Carlsbad, CA) at 1:10,000 using HRP-conjugated secondary antibodies (Thermo Scientific, Rockford, IL) and Supersignal West Femto substrate (Thermo Scientific, Rockford, IL).

2.4.5 Statistical analysis

The tools in R statistical package (version R-2.11.1) (http://www.r-project.org/) (204) was used for statistical analysis of BMV RNA replication data obtained by Northern blotting. Log transformation was applied to $[\text{RNA4/18S rRNA}]_{\text{dox-treated}}$/ $[\text{RNA4/18S rRNA}]_{\text{untreated}}$ ratios from Northern blot data, where 18S rRNA served as normalization standard. One-sided *t*-statistics were used to identify the dox-treated strains whose RNA replication was statistically significantly altered compared to untreated strains. *p*-values from *t*-statistics were converted to *q*-values to control for false discovery rate (204).

Chapter 3[2]

BROMOVIRUS RNA REPLICATION REQUIRES MULTIPLE FUNCTIONS OF THE UBIQUITIN-PROTEASOME SYSTEM

3.1 INTRODUCTION

All positive-strand RNA viruses, which have limited genetic material, depend on host proteins, membranes, lipids and metabolites for genome replication (7, 157). The availability of these key host resources is controlled, in large part, by the ubiquitin-proteasome system (UPS), the predominant proteolytic system in all eukaryotic cells. Multiple positive-strand RNA viruses manipulate various features of the highly conserved UPS to favor their replication (17, 18, 30, 40, 54, 156, 182, 202). Accordingly, understanding the mechanistic implications of these virus-host interactions, although challenging, presents an opportunity for revealing novel targets for the development of broad-spectrum antivirals.

Brome mosaic virus (BMV), a member of the alphavirus-like superfamily of human, animal and plant pathogens, has been used as a model system to study many features of positive-strand RNA virus infection, including RNA replication and virus-host interactions (160). BMV has a three genomic RNAs and one subgenomic mRNA. RNA1 and RNA2 encode the replication factors 1a and 2a polymerase ($2a^{Pol}$), respectively. 1a contains an RNA capping domain (11, 12, 114) and NTPase/RNA helicase-like domain (227). $2a^{Pol}$ contains a central

---

[2] The work in this chapter is planned for submission to the Journal of Virology. B. L. Gancarz completed the work and writing in this chapter under the guidance of P. Ahlquist. Lance Rodenkirch of the W.M. Keck Laboratory for Biological Imaging at the University of Wisconsin-Madison assisted with confocal Microscopy. Leanne Olds and Halena VanDeusen assisted with illustrations.

RNA-dependent RNA polymerase (RdRp)-like domain and an N-terminal 1a-interacting domain (36, 102, 164). RNA3 encodes the 3a protein and the cell-to-cell movement protein, both of which are required for systemic infection in natural plant hosts. Coat protein is translated from subgenomic RNA4, initiated internally on negative-strand RNA3. In both natural plant hosts and *Saccharomyces cerevisiae*, which supports all known features of BMV RNA replication, 1a directs itself, $2a^{Pol}$ and viral RNA templates to perinuclear endoplasmic reticulum (ER) membranes, which are the sites of viral RNA replication (36, 49, 92, 164, 189, 190, 196).

The ability of BMV to recapitulate all known replication features in yeast has proved instrumental in identifying and characterizing its interactions with host cells (7, 52, 68, 119, 123, 124, 161, 162, 214, 226, 243). Previously, Kushner *et al.* screened a single-gene deletion library of non-essential yeast genes and identified 99 genes whose loss inhibited or enhanced BMV RNA replication ≥ 3-fold (119). Recently, we complemented these studies by screening a dox-repressible library of essential yeast strains and identifying 24 essential host genes whose depleted expression reproducibly inhibited or enhanced BMV RNA replication ≥ 6-fold (68). Notably, ~10% of the 123 genes that altered BMV RNA replication are members of the ubiquitin-proteasome system (UPS) (Tables 3.1 and 3.2).

The UPS is the major eukaryotic cellular pathway for protein degradation and regulates critical biological processes such as cell cycle control, signal transduction, transcription, and protein quality control, among others (61, 79, 80, 219). Ubiquitin is covalently attached to target proteins through a cascade of sequential reactions by activating enzymes (E1), conjugating enzymes (E2) and ligases (E3) (172, 175, 231) (Fig. 3.1A). The resulting product is an isopeptide bond between the carboxy terminus of ubiquitin and the ε-amino group of lysine residue in the protein substrate (80, 175, 231). The attachment of a single ubiquitin moiety to a substrate functions as a non-proteolytic signal, whereas substrates destined for degradation by the proteasome are conjugated to a polyubiquitin chains (176). The 26S proteasome is composed of a 28-subunit catalytic core particle (20S CP) and a 19-subunit regulatory particle

Table 3.1. *S. cerevisiae* UPS genes and their effect on BMV RNA replication.

	ORF[a]	Gene[a]	Alias(s)[a]	Description[a]	Non-essential (NE) or Essential (E)[a]	Effect on BMV RNA Replication[b]
19S Regulatory Particle						
Lid						
	YER021W	*RPN3*	*SUN2*	Non-ATPase	E	Not in library
	YDL147W	*RPN5*	*NAS5*	Non-ATPase	E	Not screened-growth defect
	YDL097C	*RPN6*	*NAS4*	Non-ATPase	E	Not in library
	YPR108W	*RPN7*		Non-ATPase	E	Not in library
	YOR261C	*RPN8*		Non-ATPase	E	Not screened-growth defect
	YDR427W	*RPN9*	*NAS7*	Non-ATPase	NE	No effect
	YHR200W	*RPN10*	*MCB1, SUN1*	Non-ATPase	NE	No effect
	YFR004W	*RPN11*	*MPR1*	Non-ATPase	E	Not screened-growth defect
	YFR052W	*RPN12*	*NIN1*	Non-ATPase	E	Not in library
	YDR363W-A	*SEM1*	*DSS1 HOD1*	Suppressor of Exocyst Mutations	NE	≥3-fold inhibition
Base						
	YHR027C	*RPN1*	*HRD2, NAS1*	Non-ATPase	E	Not in library
	YIL075C	*RPN2*	*SEN3*	Non-ATPase	E	Not in library
	YLR421C	*RPN13*		Non-ATPase	NE	No effect
	YKL145W	*RPT1*	*YTA3, CIM5*	AAA ATPase	E	Not in library
	YDL007W	*RPT2*	*YTA5, YHS4*	AAA ATPase	E	Not screened-growth defect
	YDR394W	*RPT3*	*YTA2, YNT1*	AAA ATPase	E	Not in library
	YOR259C	*RPT4*	*PCS1, SUG2 CRL13*	AAA ATPase	E	Not screened-growth defect
	YOR117W	*RPT5*	*YTA1*	AAA ATPase	E	Not in library
	YGL048C	*RPT6*	*CIM3, SUG1, SCB68, CRL3*	AAA ATPase	E	≥6-fold inhibition
20S Core Proteasome						
	YER012W	*PRE1*		Beta 4 subunit	E	≥6-fold inhibition
	YPR103W	*PRE2*	*PRG1, SRR2, DOA3*	Beta 5 subunit	E	Not in library
	YJL001W	*PRE3*	*CRL21*	Beta 1 subunit	E	No effect
	YFR050C	*PRE4*		Beta 7 subunit	E	No effect
	YMR314W	*PRE5*		Alpha 6 subunit	E	Not screened-growth defect
	YOL038W	*PRE6*		Alpha 4 subunit	E	Not screened-growth defect
	YBL041W	*PRE7*	*PRS3*	Beta 6 subunit	E	Not in library
	YML092C	*PRE8*		Alpha 2 subunit	E	No effect
	YOR362C	*PRE10*		Alpha 7 subunit	E	Not in library
	YGR135W	*PRE9*		Alpha 3 subunit	NE	≥3-fold inhibition
	YOR157C	*PUP1*		Beta 2 subunit	E	Not in library
	YGR253C	*PUP2*	*DOA5*	Alpha 5 subunit	E	Not in library
	YER094C	*PUP3*	*SCS32*	Beta 3 subunit	E	Not in library
	YGL011C	*SCL1*	*PRC2*	Alpha 1 subunit	E	Not in library
Proteasome-Interacting proteins						
	YGL004C	*RPN14*		19S base assembly	NE	No effect
	YDL020C	*UFD5*	*RPN4, SON1*	Transcription factor that stimulates proteasome gene expression	NE	≥3-fold inhibition
	YBR173C	*UMP1*	*RNS2*	Chaperone required for correct maturation of the 20S proteasome	NE	≥3-fold inhibition
	YKL213C	*DOA1*	*UFD3, ZZZ4*	Regulates cellular ubiquitin concentration	NE	≥3-fold inhibition

Ubiquitin-activating enzyme (E1)				
YKL210W	*UBA1*		E	Not screened-growth defect
Ubiquitin-conjugating enzymes (E2)				
YDR054C	*CDC34*	*DNA6, UBC3*	E	Not screened-growth defect
YGR133W	*PEX4*	*UBC10, PAS2*	NE	No effect
YGL058W	*RAD6*	*PSO8, UBC2*	NE	Not screened-growth defect
YDR177W	*UBC1*		E	No effect
YOR339C	*UBC11*		NE	No effect
YLR306W	*UBC12*		NE	No effect
YDR092W	*UBC13*		NE	No effect
YBR082C	*UBC4*		NE	Not in library
YDR059C	*UBC5*		NE	No effect
YER100W	*UBC6*	*DOA2*	NE	Not in library
YMR022W	*UBC7*	*DER2, QRI8*	NE	>3-fold inhibition
YEL012W	*UBC8*	*GID3*	NE	No effect
YDL064W	*UBC9*		E	No effect
Ubiquitin-protein ligases (E3)				
HECT (Homologous to E6-AP C terminus) class				
YJR036C	*HUL4*		NE	No effect
YGL141W	*HUL5*		NE	No effect
YER125W	*RSP5*	*UBY1, SMM1, NPI1, MUT2, MDP1*	E	Not screened-growth defect
YDR457W	*TOM1*		NE	No effect
YKL010C	*UFD4*		NE	>3-fold inhibition
RING (Really Interesting New Gene) class				
APC (Anaphase Promoting Complex) subclass				
YGR225W	*AMA1*	*SPO70*	NE	No effect
YGL116W	*CDC20*	*PAC5*	E	No effect
YGL003C	*CDH1*	*HCT1*	NE	No effect
ECS (ELC1, CUL3 and SOCS/BC-box) subclass				
YNL230C	*ELA1*		NE	No effect
YJR052W	*RAD7*		NE	No effect
SCF (SKP1, CDC53, and F-box) subclass				
YFL009W	*CDC4*		E	Not screened-growth defect
YMR094W	*CTF13*	*CBF3C*	E	No effect
YJL149W	*DAS1*		NE	No effect
YOR080W	*DIA2*	*YOR29-31*	NE	Not screened-growth defect
YJR090C	*GRR1*	*COT2, CAT80, SDC1, SSU2*	NE	Not screened-growth defect
YOL133W	*HRT1*	*HRT2, ROC1, RBX1*	E	No effect
YLR097C	*HRT3*		NE	No effect
YLR368W	*MDM30*	*DSG1*	NE	No effect
YIL046W	*MET30*	*ZRG11*	E	No effect
YJL204C	*RCY1*		NE	>3-fold enhancement
YBR280C	*SAF1*		NE	No effect
YNL311C	*SKP2*		NE	No effect
YML088W	*UFO1*		NE	No effect
YDR131C	N/A[c]		NE	No effect
YDR306C	N/A[c]		NE	No effect
YLR224W	N/A[c]		NE	No effect

YLR352W	N/A[c]		NE	No effect
SPRF (Single Protein RING Finger) subclass				
YMR119W	*ASI1*		NE	No effect
YNL008C	*ASI3*		NE	Not in library
YDL074C	*BRE1*		NE	No effect
YOL013C	*HRD1*	*DER3*	NE	No effect
YER068W	*MOT2*	*SIG1, NOT4*	NE	Not screened-growth defect
YDR313C	*PIB1*		NE	No effect
YCR066W	*RAD18*		NE	No effect
YLR032W	*RAD5*	*REV2, SNM2*	NE	No effect
YMR247C	*RKR1*	*LTN1*	NE	No effect
YDR143C	*SAN1*		NE	No effect
YIL030C	*SSM4*	*DOA10, KIS3*	NE	No effect
YKL034W	*TUL1*		NE	No effect
YGR184C	*UBR1*	*PTR1*	NE	≥3-fold inhibition
YLR024C	*UBR2*		NE	No effect
U-BOX (U-BOX is similar to RING domain) subclass				
YLL036C	*PRP19*	*PSO4*	E	No effect
YDL190C	*UFD2*		NE	No effect
Deubiquitinating enzymes (DUBs)				
JAMM (Joesphine's and JAB1/MPN/MOV34 Metalloenzymes) family				
YFR004W	*RPN11*	*MPR1*	E	Not screened-growth defect
YDL122W	*UBP1*		NE	No effect
YNL186W	*UBP10*	*DOT4*	NE	Not in library
YKR098C	*UBP11*		NE	No effect
YJL197W	*UBP12*		NE	No effect
YBL067C	*UBP13*		NE	No effect
YBR058C	*UBP14*	*GID6*	NE	No effect
YMR304W	*UBP15*		NE	Not screened-growth defect
YPL072W	*UBP16*		NE	Not in dataset
YOR124C	*UBP2*		NE	No effect
YER151C	*UBP3*	*BLM3*	NE	No effect
YER144C	*UBP5*		NE	No effect
YFR010W	*UBP6*		NE	≥3-fold inhibition
YIL156W	*UBP7*		NE	No effect
YMR223W	*UBP8*		NE	No effect
YER098W	*UBP9*		NE	No effect
OTU (Ovarian Tumor Proteases) family				
YFL044C	*OTU1*	*YOD1*	NE	No effect
YHL013C	*OTU2*		NE	No effect
UCH (Ubiquitin C-terminal Hydrolases) family				
YJR099W	*YUH1*		NE	No effect
USP (Ubiquitin-Specific Proteases) family				
YDR069C	*DOA4*	*UBP4 ,SSV7, NPI2, DOS1, MUT4*	NE	≥3-fold inhibition

[a]Based on the *Saccharomyces* Genome Database at http://www.yeastgenome.org/ and the *Saccharomyces cerevisiae* Ubiquitination Database (SCUD) at http://scud.kaist.ac.kr/.

[b]As reported previously in primary screens by Kusher *et al.* (2003) *Proc Natl Acad Sci*. 100, 15764-69 and Gancarz *et al.* (2011) *PLoS One*. 6, e23988.

[c]ORF not annotated in *Saccharomyces* Genome Database.

Table 3.2 Summary of UPS genes and their effect on BMV RNA replication.[a]

	UPS Genes			
	Non-essential	**Essential**	**Total**	**Percent of total strains**
Not in library	4	16	20	17.5
Not screened-growth defect	5	12	17	15.0
Not in dataset	1	0	1	0.9
No effect on BMV RNA replication	53	10	63	55.2
Inhibited BMV RNA replication	10	2	12	10.5
Enhanced BMV RNA replication	1	0	1	0.9
Total	**74**	**40**	**114**	

[a]See Table 3.1 to identify specific strains.

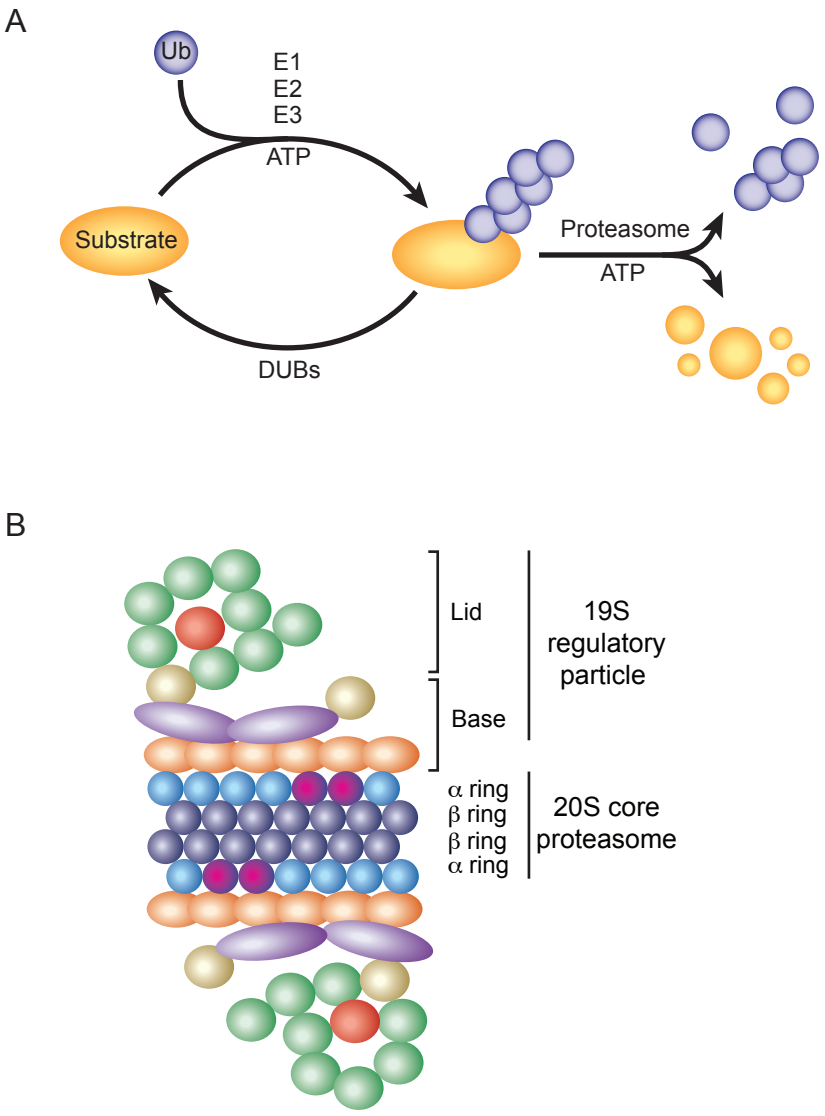

Figure 3.1. The ubiquitin-proteasome system for protein degradation and 26S proteasome. (A) The ubiquitin-proteasome system for proteolysis. The sequentential actions of E1s (ubiquitin-activating enzymes), E2s (ubiquitin-conjugating enzymes) and E3s (ubiquitin-ligating enzymes) covalently attach one or more ubiquitin molecules (Ub) to substrates in an ATP-dependent reaction. The ubiquitin tag serves as the predominant recognition motif for the 26S proteasome an subsequent proteolysis. Deubiquitinating enzymes (DUBs) can remove ubiquitin before substrate degradation inititates, allowing some substrates to escape degradation. (B) Schematic of the 26S proteasome. The proteasome is composed of a 28-subunit catalytic core particle (CP, or 20S particle), capped at each end with a 19-subunit regulatory particle (RP, or 19S particle). The CP is cylinder-like structure formed by four heptemaric stacked rings, with proteolytic activity localized to the inner β rings. The outer α ring proteins have RNase activity. The RP is composed of two distinct subcomplexes, the lid and base, and is responsible for substrate unfolding and translocation into the CP.

(19S RP) and the fundamental role of this ~2.5 MDa protein complex is to recognize, unfold and digest ubiquitinated protein substrates (26, 61) (Fig. 3.1B).

Here, we used microscopy combined with genetic and biochemical approaches to investigate the potential role(s) of nine previously identified UPS genes in BMV RNA replication (68, 119) (Fig. 3.2). These genes, whose loss inhibited BMV RNA replication ~6- to 100-fold, are components of the 20S core (*PRE1, PRE9*), 19S regulatory particle (*SEM1, RPT6*) and accessory proteins (*UBR1, UBP6, UMP1, UFD4, UFD5*). Our results show that at non-cytotoxic doses, proteasome inhibitor MG132 inhibited BMV RNA replication ≥4-fold in barley and yeast, confirming that the UPS is required for BMV RNA replication in its natural host. Additionally, our genetic studies revealed that the nine implicated UPS genes contribute to BMV RNA replication in multiple, mechanistically distinguishable ways.

3.2 RESULTS

3.2.1 Inhibiting the 26S proteasome inhibits BMV RNA replication

As described above, the UPS is comprised of the 26S proteasome as well as multiple accessory proteins (e.g. E1s, E2s, E3s, DUBs, chaperones, etc.). Multiple positive-strand RNA viruses use diverse mechanisms to manipulate the UPS for replicating their genome (30, 182, 202). To determine if BMV RNA replication required 26S proteasome activity, we assayed viral RNA accumulation after treating barley protoplasts and yeast cells expressing BMV replication components with non-cytotoxic doses of MG132, a synthetic, reversible inhibitor that targets the chymotrypsin-like activity of the 26S proteasome without influencing its ATPase or isopeptidase features (121, 155). Barley protoplasts were inoculated with infectious *in vitro* transcripts containing complete copies of wt RNA1, RNA2 and RNA3, which results in amplification of RNAs1-3 and synthesis of subgenomic (sg) RNA4 via a minus-strand RNA3 intermediate (6).

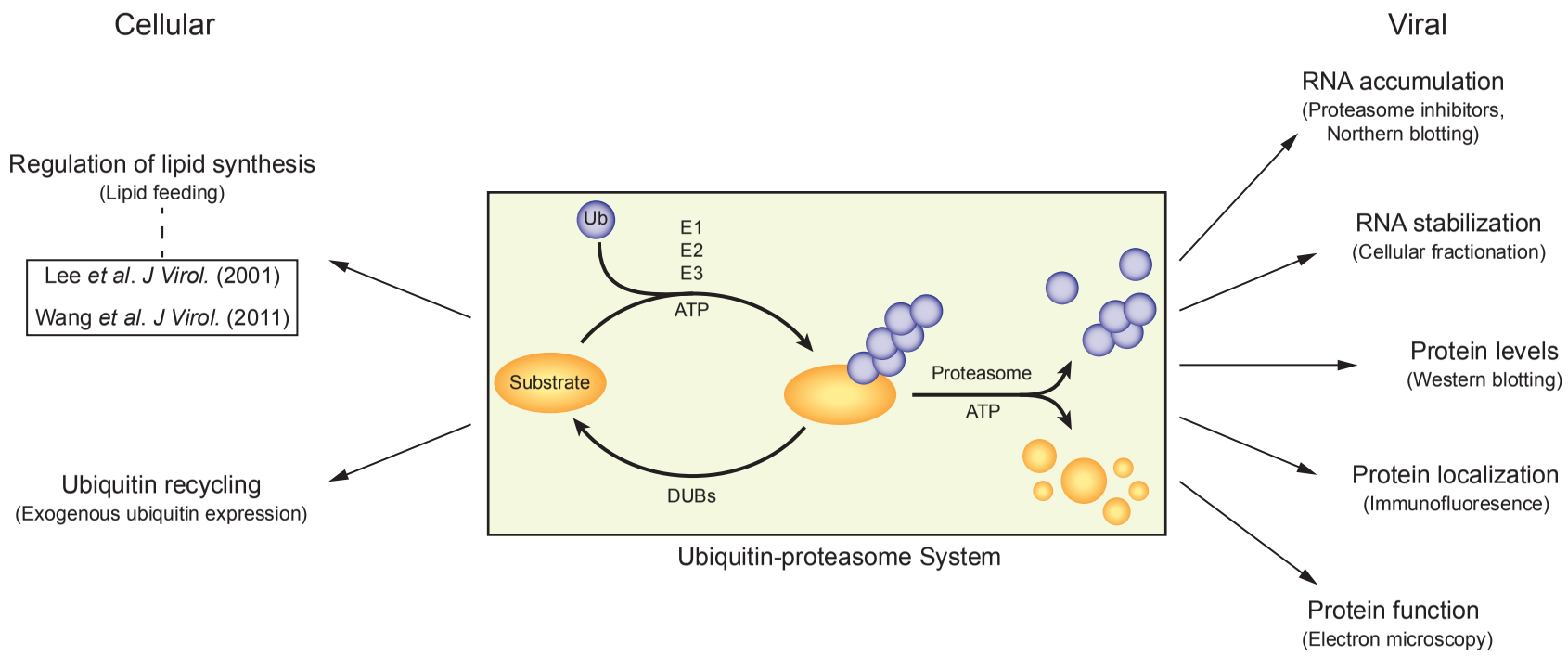

Figure 3.2. Experimental approaches used to determine the role of the UPS in BMV RNA replication. To mechanistically characterize how the UPS affects BMV RNA replication, we used a multi-faceted approach by evaluating cellular processes such as lipid synthesis and ubiquitin homeostasis, as well as various steps of the viral RNA replication process (RNA accumulation, RNA stabilization, protein translation and localization, etc.).

Similarly, in yeast cells expressing BMV 1a and $2a^{Pol}$ proteins, DNA plasmids were used to launch positive-strand RNA3 transcripts, which are used as templates for the synthesis of negative-strand RNA3, which, in turn, is copied to amplify positive-strand RNA3 and produce sgRNA4 (92). Therefore, in both protoplasts and yeast, the production of RNA4 is a true measure of viral RNA replication. Treating barley protoplasts expressing BMV with 10 μM or 20 μM MG132 for 12 hrs inhibited RNA4 accumulation 2-fold and ~4-fold, respectively (Fig. 3.3A), whereas treating with DMSO control buffer had no effect on RNA4 accumulation (Fig. 3.3A). Similarly, treating yeast cells expressing BMV with 50 μM MG132 for 18 hrs resulted in a 25-fold inhibition of RNA4 accumulation compared to 1 hr of MG132 treatment or DMSO control buffer treatment, which did not alter RNA4 accumulation (Fig. 3.3B). In barley protoplasts, 1a and particularly $2a^{Pol}$ protein levels were reduced by MG132 treatment (Fig. 3.3C) in parallel with the decrease in RNA replication (Fig. 3.3A). In contrast, in yeast, proteasome inhibition by MG132 did not affect levels of 1a protein and increased $2a^{Pol}$ levels (Fig. 3.3D). These differences are consistent with and likely reflect the highly distinct modes of 1a and $2a^{Pol}$ expression in these two cases. In plants, 1a and $2a^{Pol}$ were translated from BMV RNAs 1 and 2, whose levels are dependent on viral RNA replication. Accordingly, the decrease in 1a and $2a^{Pol}$ protein accumulation paralleled the MG132-induced decrease in viral RNA replication (Fig. 3.3A). In yeast, 1a and $2a^{Pol}$ were translated from non-replicating, DNA plasmid-expressed mRNAs that contain the 1a and 2a open reading frames between yeast 5' and 3' noncoding regions (119). Since the levels of these mRNAs are independent of viral RNA replication, 1a and $2a^{Pol}$ translation is likely little changed by MG132, and the effects of inhibiting proteasome action by MG132 are presumably dominated by their direct effects on 1a and $2a^{Pol}$ protein stability. The observed unchanged level of 1a and increased level of $2a^{Pol}$ is in keeping with our group's earlier findings that 1a protein has a longer half-life than $2a^{Pol}$ (unpublished results).

Since the 26S proteasome is the primary regulator of polyubiquitin-protein conjugate degradation (61), successful inhibition of the proteasome causes substrate turnover to

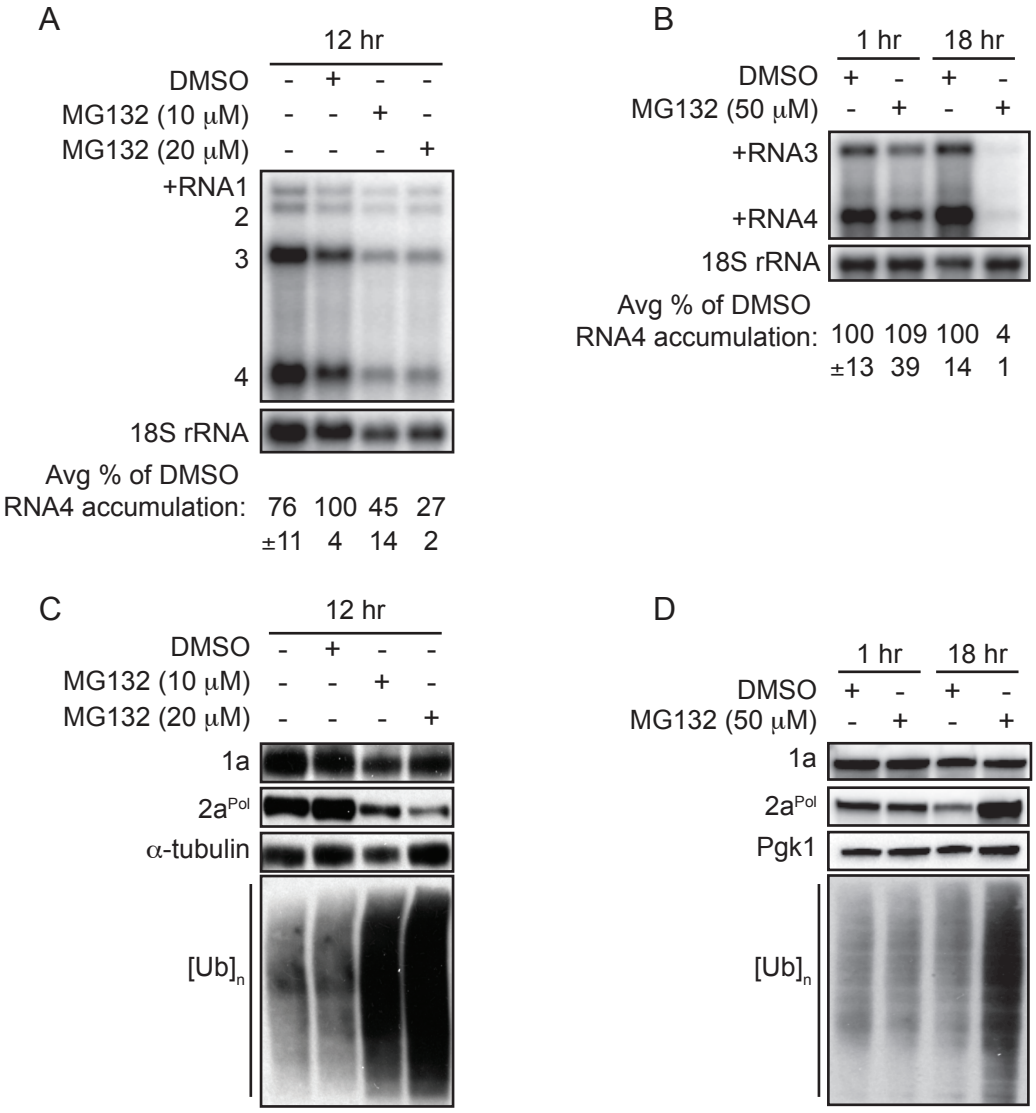

Figure 3.3. Proteasome inhibitor MG132 inhibits viral RNA accumulation in plants and yeast. (A) Accumulation of positive-strand RNAs 1, 2, 3 and 4 in untreated and MG132-treated barley protoplasts as detected by Northern blot.18S rRNA was measured as a loading control. (B) Accumulation of positive-strand RNA3 and RNA4 from untreated and MG132-treated yeast cells co-expressing 1a, $2a^{Pol}$, and RNA3 as detected by Northern blot.18S rRNA was measured as a loading control. In A and C, DMSO was a negative control for MG132 treatment. (C) Accumulation of BMV 1a and $2a^{Pol}$ in untreated and MG132-treated barley protoplasts as detected by Western blot. Total proteins were extracted from equal numbers of barly protoplasts and analyzed by SDS/PAGE. Equal loading of total protein was verified by measuring α-tubulin levels. (D) Accumulation of BMV 1a and $2a^{Pol}$ in untreated and MG132-treated yeast cells as detected by Western blot. Total proteins were extracted from equal numbers of yeast cells and analyzed by SDS/PAGE. Equal loading of total protein was verified by measuring Pgk1p levels. In C and D, MG132-mediated inhibition of proteasome function was verified by measuring the accumulation of ubiquitin-protein conjugates $[Ub]_n$.

decrease, resulting in accumulation of ubiquitin-conjugated proteins. To ensure 26S proteasome function was impaired by MG132 treatment, we assayed for the accumulation of Ub-protein conjugates by Western blotting, an established control for monitoring proteasome inhibition in plants, yeast and other eukaryotes (1, 117, 136, 202). As expected, there was a substantial increase in Ub-protein conjugates 12 or 18 hrs post-MG132 treatment in protoplasts and yeast, respectively (Figs. 3.3B and D).

3.2.2 BMV RNA replication is severely inhibited in UPS mutants

Previously, our laboratory analyzed ~5,800 yeast genes (93%) and identified 123 genes affecting BMV RNA replication, including nine genes in the UPS whose loss inhibited BMV RNA replication ~3- to 100-fold (68, 119). These UPS genes are components of the 20S core (*PRE1, PRE9*), 19S regulatory particle (*SEM1, RPT6*) and accessory proteins (*UBP6, UBR1, UMP1, UFD4, UFD5*) (Tables 3.1 and 3.2) (68, 119). Genes not essential for cell growth and viability are referred to throughout as non-essential genes, whereas genes required for cell growth and viability are referred to here as essential genes. In these studies, seven non-essential genes (*PRE9, SEM1, UBP6, UBR1, UMP1, UFD4 and UFD5*) were assayed in cells with a complete deletion of a single open reading frame (119). *PRE1* and *RPT6*, which are essential genes, were assayed in strains with a single essential gene promoter replaced by a doxycycline repressible promoter (P_{TET}), allowing repression of essential gene expression by adding doxycycline to the growth medium (68). The nine UPS genes discussed here were identified in two independent screens that each utilized a BMV RNA3 derivative expressing *Renilla* luciferase (Rluc) as a viral RNA replication reporter (68, 119). To eliminate the possibility that the BMV RNA replication defect was specific to the Rluc reporter, we performed secondary validation tests using strains transformed to express 1a, $2a^{Pol}$ and template RNA3. For essential genes, it is important to note that expression levels after substitution of the P_{TET} promoter are often different than expression levels from the endogenous gene promoter (149). Therefore, to

test and to control for possible effects of this promoter on viral RNA replication and/or gene expression, each dox-treated strain was compared to its untreated counterpart rather than to the parental wt strain. The levels of RNA3 and RNA4 replication products were measured by Northern blotting in strains for which essential genes were dox-depleted or non-essential genes were deleted. In particular, we used the level of RNA4 relative to 18S rRNA as the primary measure of any change in BMV RNA-dependent RNA synthesis, through the ratio [RNA4/18S rRNA]$_{\text{dox-treated}}$/ [RNA4/18S rRNA]$_{\text{untreated}}$ for essential strains and [RNA4/18S rRNA] for non-essential strains. RNA4 was used as the primary measure of any change in BMV RNA synthesis since, unlike RNA3, RNA4 is only produced by viral RNA-dependent RNA synthesis and not also by DNA transcription (see Fig. 2.1). Additionally, RNA4 accumulation is the parameter most closely related to the Rluc expression measured in both primary screens (see Fig. 2.1 and refs (68, 119).

In yeast cells with dox-repressed essential UPS genes P_{TET}-*RPT6* or P_{TET}-*PRE1*, (+)RNA4 accumulated to 2% and 10% of untreated (+)RNA4 levels, respectively (Fig. 3.4A, lanes 1, 2, 5 and 6). Similarly, in all non-essential UPS deletion mutants, (+)RNA4 accumulated to only <3% of wt (+)RNA4 levels (Fig. 3.4B, lanes 1, 3, 5, 7, 9, 11, 13 and 15). These results agreed well with previous Rluc-based measurements (68, 119). Negative-strand RNA3 synthesis was also substantially inhibited in all UPS mutants, indicating a defect in this earlier replication step (Figs. 3.4A and B).

3.2.3 BMV RNA replication is restored completely in mutant *PRE1* and partially in mutants *RPT6, UBP6 and UBR1* by supplementing unsaturated fatty acids

BMV RNA replication in yeast and plants requires *OLE1* Δ9 fatty acid desaturase, which converts saturated fatty acids (SFA) to unsaturated fatty acids (UFA) (123, 124). In yeast, transcription of *OLE1* and other lipid synthesis genes is regulated by ubiquitin/proteasome-dependent activation and release of two homologous, membrane-anchored cytosolic

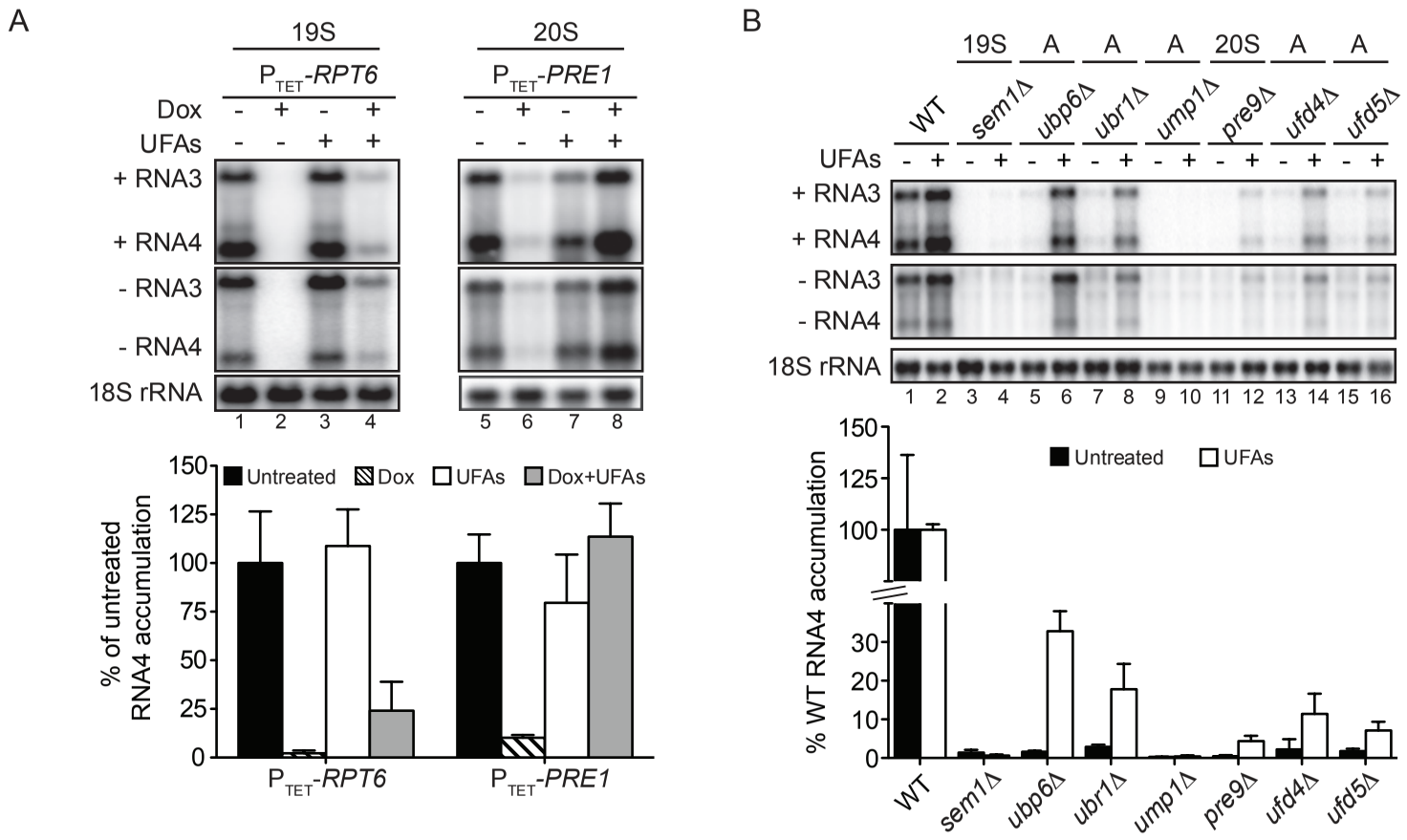

Figure 3.4. Depleting essential or deleting non-essential UPS genes inhibits BMV RNA replication. Accumulation of positive-strand RNA4 is severely inhibited in yeast strains with dox-repressed essential genes (A) and yeast strains in which non-essential genes are deleted (B). BMV RNA replication is partially partially complemented in mutant *RPT6* and completely complemented in mutant *PRE1* (A,right panel) by supplementing 1 mM unsaturated fatty acids (an equimolar mixture of palmitoleic acid and oleic acid) in growth medium partially . In A and B, total RNA was extracted from yeast cells expressing BMV 1a, $2a^{Pol}$ and RNA3. RNA was detected by Northern blotting using a BMV RNA4-specific probe. Equal loading of total RNA was verified by probing for 18S rRNA. 19S, component of the 19S regulatory particle of the 26S proteasome; 20S, component of the 20S core proteasome; A, UPS accessory protein; P_{TET}, tetracycline-repressible promoter; Dox, doxycycline (10 µg/ml); UFAs, unsaturated fatty acids.

transcription factors, Mga2 and Spt23, which then translocate to the nucleus and initiate lipid synthesis gene transcription (244). To test if the BMV RNA replication defects observed in UPS mutants were linked to *OLE1* activation, we analyzed *OLE1* mRNA levels. In *RPT6*- and *PRE1*-depleted cells, *OLE1* mRNA accumulation was reduced 6- and 25-fold, respectively (Fig. 3.5A). In *ump1Δ* cells, a ~50% reduction in *OLE1* mRNA levels was observed compared to wt cells (Fig. 3.5B, lane 5), but in all other UPS mutants, *OLE1* mRNA accumulation was comparable to wt levels (Fig. 3.5B). Next we tested if supplementing UFA products of *OLE1* (an equimolar mixture of palmitoleic acid and oleic acid) in the growth medium restored (+)RNA4 accumulation. Adding 1 mM UFAs did not affect the growth of wt or UPS mutant strains (data not shown). Supplementing UFAs completely restored BMV RNA replication in UPS mutant *PRE1* (Fig. 3.4A, lane 8 vs. lane 6), increasing (+)RNA4 accumulation more than 10-fold, to ~110% of untreated P_{TET}-*PRE1* RNA replication levels (Fig. 3.4A, lane 5). This result is similar to the full complementation of BMV RNA replication in the *ole1w* and *ole1*Δ mutants that can be observed with UFA addition (123, 124), implying that UPS mutant *PRE1* affects BMV RNA replication primarily through the UPS-dependent activation of the lipid synthesis pathway. However, in *RPT6*-depleted cells, providing UFAs only partially restored BMV RNA replication to ~25% of that in untreated P_{TET}-*RPT6* cells (Fig. 3.4, lane 4 vs. lane 2). Similarly, in *ubp6Δ* and *ubr1Δ* cells, UFAs partially restored RNA replication to ~32% and 17% of that in WT cells supplemented with UFAs, respectively (Fig. 3.4B, lanes 6 and 8 vs. lane2). Thus, *RPT6*, *UBP6* and *UBR1*, in addition to the other UPS mutants not complemented by UFAs (*SEM1, PRE9, UFD4* and *UFD5*), must contribute to BMV RNA replication through UPS-dependent mechanisms independent of UFA regulation.

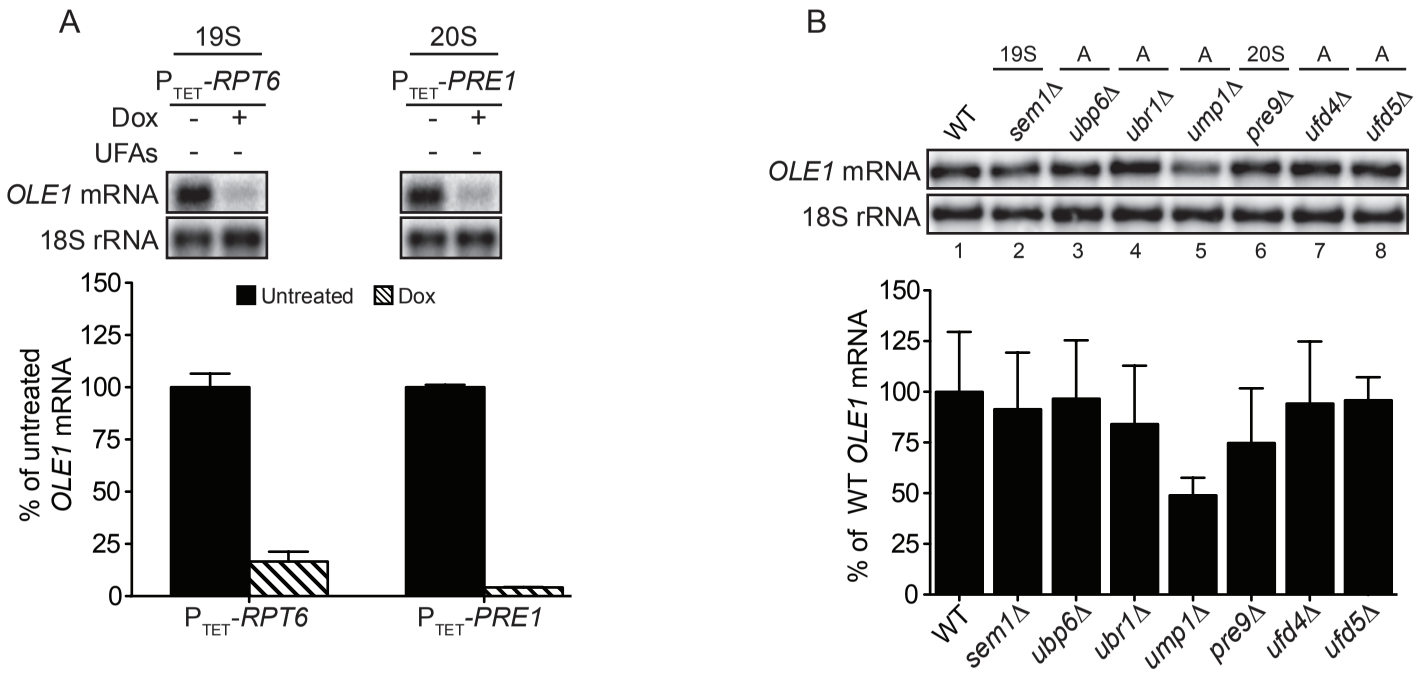

Figure 3.5. *OLE1* mRNA accumulation in UPS mutants. (A) Accumulation of *OLE1* transcript is severely inhibited in dox-repressed essential genes *RPT6* and *PRE1*. (B) *OLE1* transcript accumulates to levels higher than observed in wt yeast in all non-essential deletion mutants. In A and B, total RNA was extracted from yeast cells expressing BMV 1a, $2a^{Pol}$ and RNA3. *OLE1* mRNA was detected by Northern blotting with an *OLE1*-specific probe. Equal loading of total RNA was verified by probing for 18S rRNA. 19S, component of the 19S regulatory particle of the 26S proteasome; 20S, component of the 20S core proteasome; A, UPS accessory protein; P_{TET}, tetracycline-repressible promoter; Dox, doxycycline (10 µg/ml); UFAs, unsaturated fatty acids.

3.2.4 BMV RNA replication is partially restored in four UPS mutants by expressing exogenous ubiquitin

Ubiquitination of target protein substrates regulates diverse biological processes including protein trafficking, protein turnover, cell signaling, transcription and immune responses, among others (232). Disrupting UPS accessory proteins Doa4, Ufd3 and Ubp6, results in depleted pools of free Ub (97, 126, 192, 208) and inhibited BMV RNA replication (119). Since Doa4 and Ufd3, which are components of the UPS, were being analyzed in independent studies (226) these genes were not included in analyses presented here. Western blotting confirmed a decrease in free Ub levels in *ubp6*Δ (Fig. 3.6B, lane 5), whereas free Ub levels appeared largely unaffected in all other UPS mutants (Fig. 3.6B). However, detecting variations in free Ub levels can be masked by growth conditions (208). To determine if reduced free Ub levels caused the observed BMV RNA replication defect in any of the nine UPS mutants analyzed here, we expressed exogenous Ub from plasmid pYEP96, which provides wt Ub levels (Figs. 3.7A and B). In *ubp6*Δ, *ubr1*Δ, *pre9*Δ, *ufd4*Δ and *ufd5*Δ cells, Ub supplementation partially restored (+)RNA4 levels to 71%, 81%, 31%, 80% and 63% of wt cells supplemented with Ub, respectively (Fig. 3.7B). The mutants in which BMV RNA replication was complemented most substantially (*UBP6, UBR1, UFD4* and *UFD5*) all encode UPS accessory proteins that perform Ub-dependent functions (Table 3.1), implying that Ub-dependent processes contribute to BMV RNA replication.

3.2.5 Disrupting UPS genes *RPT6*, *PRE1*, *UBR1* and *UMP1* increases $2a^{Pol}$ accumulation

To determine if the inhibition of BMV RNA replication in UPS mutants was due to altered viral protein levels, we measured the accumulation of BMV RNA replication proteins 1a and $2a^{Pol}$ by Western blotting. BMV 1a levels in dox-treated P_{TET}-*PRE1* and P_{TET}-*RPT6* strains were comparable to their untreated counterparts (Fig. 3.8A, 1a blot, lanes 1, 2, 5 and 6). Similarly, 1a levels in the other UPS mutants were comparable to wt levels (Fig. 3.8B, 1a blot, lanes 5, 7, 9,

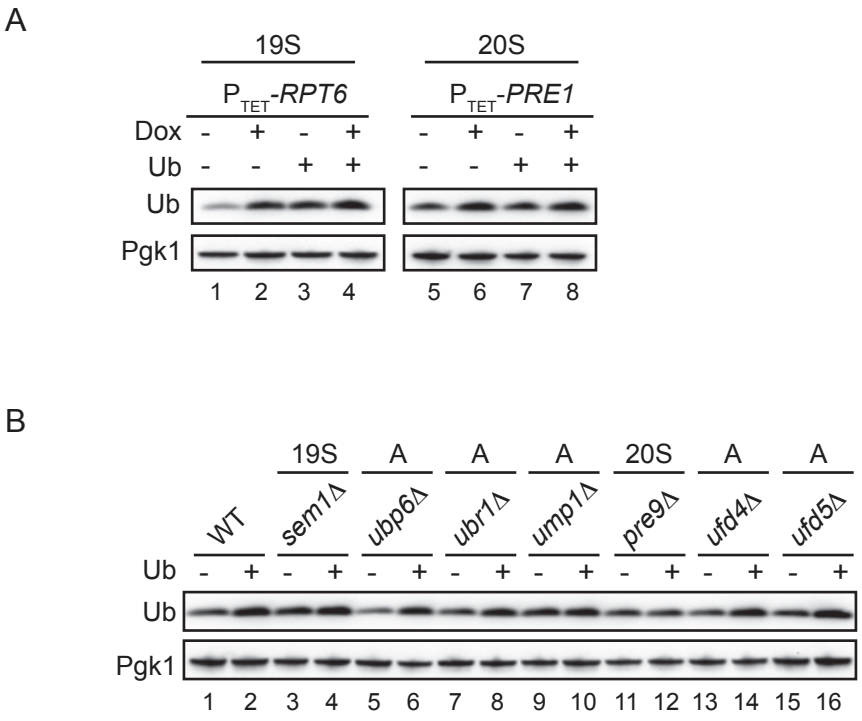

Figure 3.6. Free ubiquitin levels in UPS mutants in the absence or presence of exogenous ubiquitin expression. In A and B, total proteins were extracted from equal numbers of yeast cells and analyzed by SDS/PAGE. Monoubiquitin was detected with an anti-ubiquitin monoclonal antibody. Equal loading of total protein was verified by measuring cytosolic protein Pgk1 levels. 19S, component of the 19S regulatory particle of the 26S proteasome; 20S, component of the 20S core proteasome; A, UPS accessory protein; P_{TET}, tetracycline-repressible promoter; Dox, doxycycline (10 µg/ml); Ub, ubiquitin.

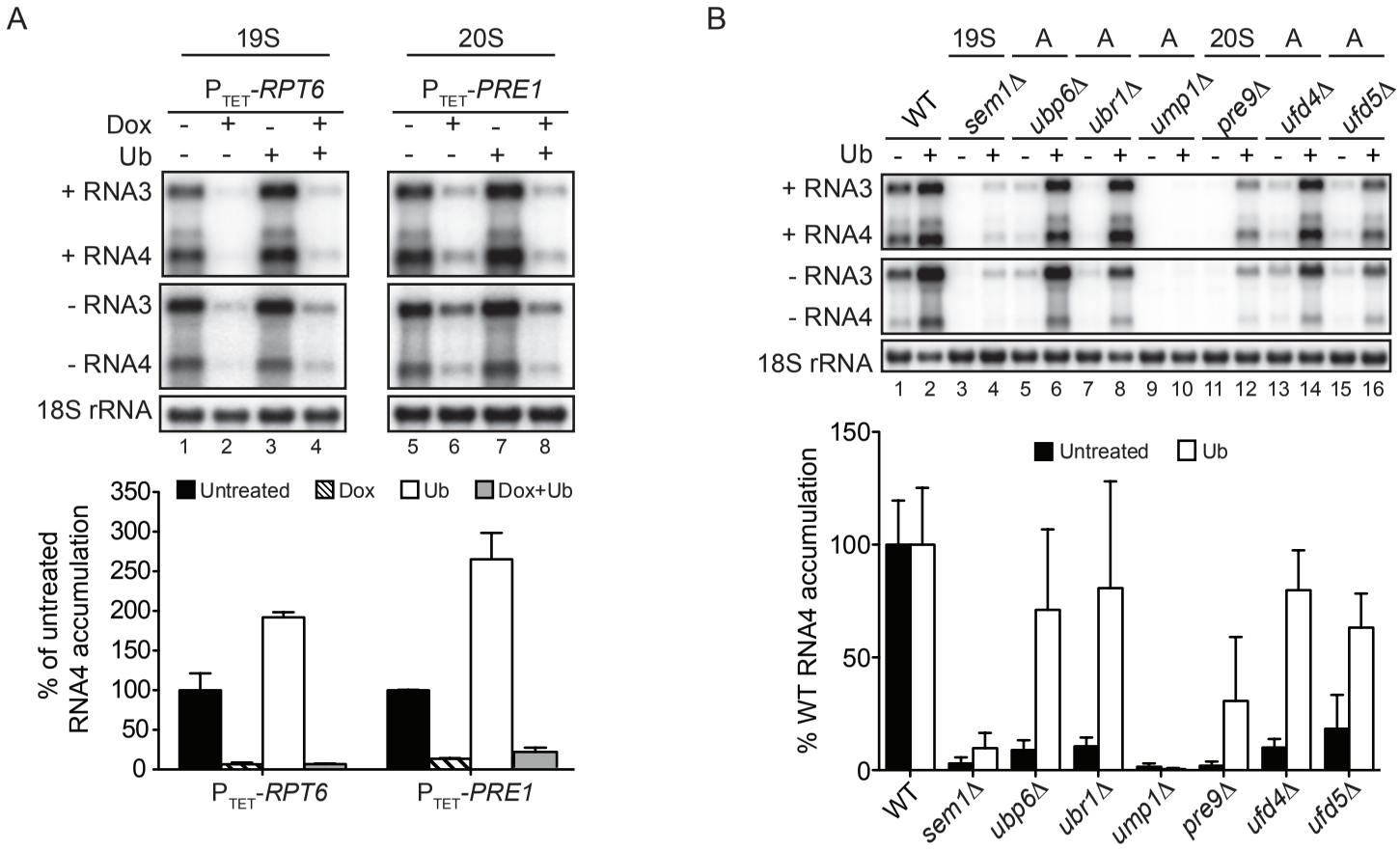

Figure 3.7. Viral RNA replication is partially complemented in UPS mutants *ubp6*Δ, *ubr1*Δ, *pre9*Δ, *ufd4*Δ, and *ufd5*Δ by expressing exogenous ubiquitin. In A and B, total RNA was extracted from yeast cells expressing BMV 1a, $2a^{Pol}$, and RNA3 in the presence or absence of a plasmid expressing ubiquitin. RNA was detected by Northern blot using a BMV RNA4-specific probe. 18S rRNA was measured as a loading control. 19S, component of the 19S regulatory particle of the 26S proteasome; 20S, component of the 20S core proteasome; A, UPS accessory protein; P_{TET}, tetracycline-repressible promoter; Dox, doxycycline (10 µg/ml); Ub,

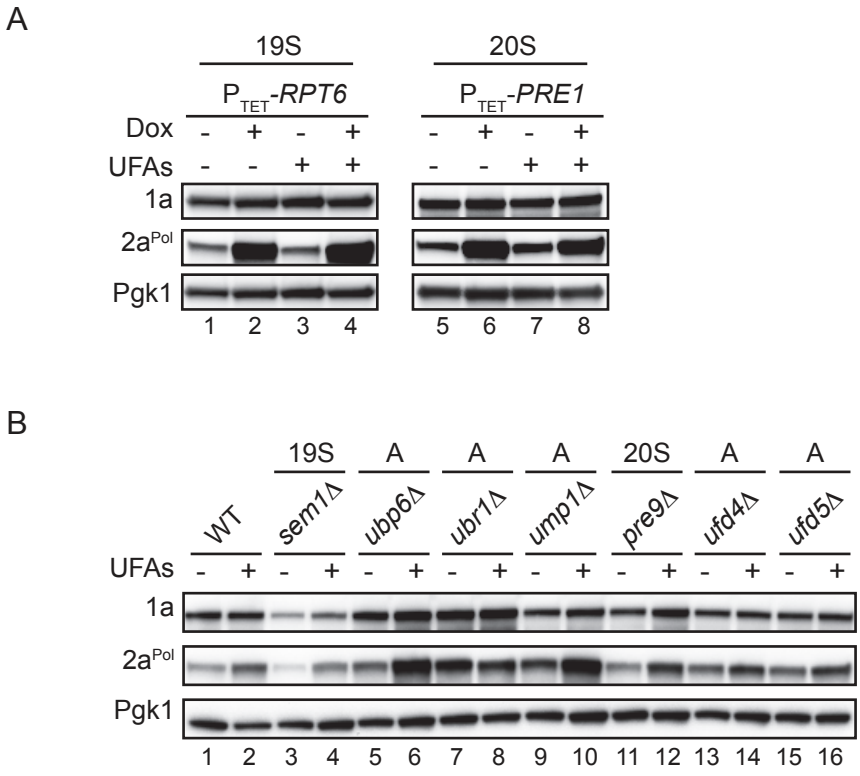

Figure 3.8. BMV 1a and 2a^{Pol} levels in UPS mutants in the absence or presence of unsaturated fatty acids. In A and B, total proteins were extracted from equal numbers of yeast cells and analyzed by SDS/PAGE. Accumulation of BMV 1a and 2a^{Pol} was detected with anti-BMV 1a, anti-BMV 2a^{Pol}, and anti-Pgk1. Equal loading of total protein was verified by measuring cytosolic protein Pgk1 levels. 19S, component of the 19S regulatory particle of the 26S proteasome; 20S, component of the 20S core proteasome; A, UPS accessory protein; P_{TET}, tetracycline-repressible promoter; Dox, doxycycline (10 µg/ml); UFAs, unsaturated fatty acids.

11, 13 and 15), with the exception of *sem1*Δ, which showed a slight, but reproducible, decrease in 1a accumulation (Fig. 3.8B, 1a blot, lanes 1 and 3). In stark contrast, BMV $2a^{Pol}$ levels were significantly increased in P_{TET}-*PRE1* and P_{TET}-*RPT6* dox-treated strains compared to their untreated samples (Fig. 3.8A, $2a^{Pol}$ blot, lanes 1, 2, 5 and 6). UPS mutants *ubr1*Δ and *ump1*Δ exhibited a large increase in $2a^{Pol}$ compared to wt (Fig. 3.8B, $2a^{Pol}$ blot, lanes 1, 7 and 9), compared to mutants *ubp6*Δ, *ufd4*Δ and *ufd5*Δ, which showed more moderate increases in $2a^{Pol}$ accumulation (Fig. 3.8B, $2a^{Pol}$ blot, lanes 1, 5, 13 and 15). Similar to 1a levels in *sem1*Δ, $2a^{Pol}$ levels were also slightly decreased compared to wt cells (Fig. 3.8B, $2a^{Pol}$ blot, lanes 1 and 3). Supplementing UFAs or expressing exogenous Ub had no effect on 1a or $2a^{Pol}$ accumulation in dox-treated P_{TET}-*RPT6* and P_{TET}-*PRE1* strains (Figs. 3.8A and 3.9A, respectively). Additionally, dox-depleting P_{TET}-*RPT6* and P_{TET}-*PRE1* in the presence of UFAs still resulted in a significant accumulation of $2a^{Pol}$, suggesting the observed increase in $2a^{Pol}$ levels in UPS mutants *RPT6* and *PRE1* is not linked to lipid synthesis, but to some other UPS-dependent process(es). UFA supplementation did, however, increase levels of $2a^{Pol}$ in wt cells and UPS mutants *sem1*Δ, *ubp6*Δ, *ump1*Δ and *pre9*Δ (Fig. 3.8B, $2a^{Pol}$ blot, lanes 2, 4, 6, 10 and 12). Similarly, expressing exogenous Ub moderately increased $2a^{Pol}$ levels in UPS mutants *sem1*Δ, *ump1*Δ, *pre9*Δ and *ufd5*Δ. 1a levels in all UPS mutants were unaffected by addition of UFAs or expressing exogenous Ub (Figs. 3.8 and 3.9, respectively). These results suggest that altered regulation of the stability of $2a^{Pol}$ and/or other proteins may be the cause of, or contribute to, viral RNA replication phenotypes observed upon depleting/deleting products of the implicated genes.

3.2.6 UPS mutants *ubr1*Δ, *pre9Δ*, *ufd4*Δ and *ufd5*Δ exhibit 1a-independent RNA3 stabilization

In yeast cells, BMV RNA3 has an *in vivo* half-life of <10 min in the absence of 1a (91). In the presence of 1a, however, RNA3 accumulation is increased 8- to 20-fold and its half-life is extended to >3 hrs (91, 227). Increased stability of RNA3 is a result of its 1a-dependent

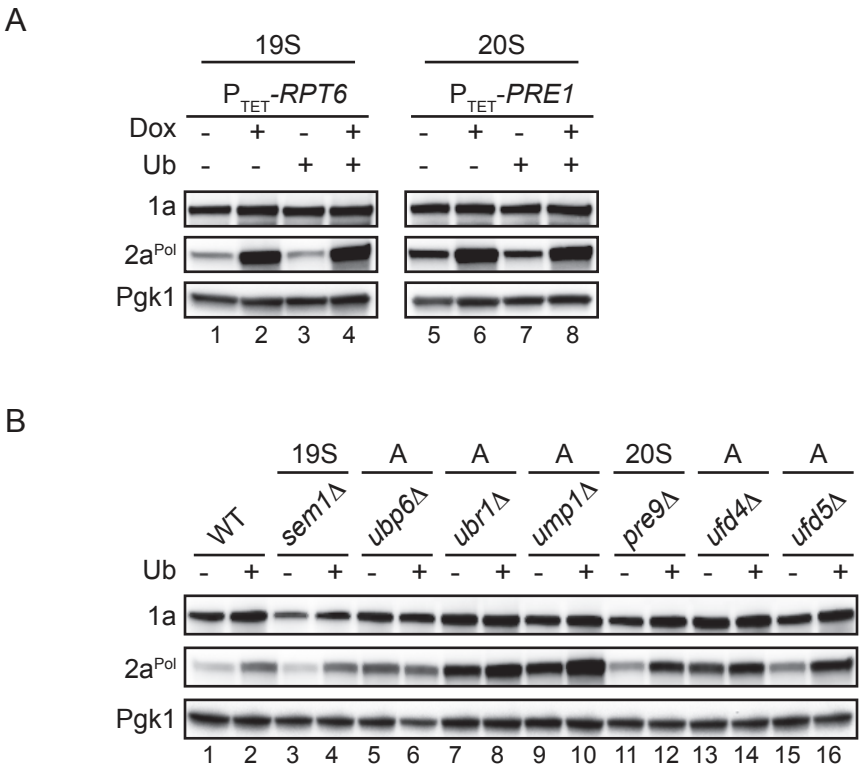

Figure 3.9. BMV 1a and 2a^{Pol} levels in UPS mutants in the absence or presence of exogenous ubiquitin expression. In A and B, total proteins were extracted from equal numbers of yeast cells and analyzed by SDS/PAGE. Accumulation of BMV 1a and 2a^{Pol} was detected with anti-BMV 1a, anti-BMV 2a^{Pol}, and anti-Pgk1. Equal loading of total protein was verified by measuring cytosolic protein Pgk1 levels. 19S, component of the 19S regulatory particle of the 26S proteasome; 20S, component of the 20S core proteasome; A, UPS accessory protein; P$_{TET}$, tetracycline-repressible promoter; Dox, doxycycline (10 µg/ml); Ub, ubiquitin.

recruitment to a membrane-associated, nuclease resistant state, which likely represents its localization to membrane-bounded, spherular replication compartments (196). For these experiments, we generated UPS deletion mutants *sem1*Δ*, ubr1*Δ, *ump1*Δ, *ufd4*Δ*, pre9*Δ and *ufd5*Δ in the *S. cerevisiae* strain YPH500, used in multiple previous studies of BMV RNA replication (52, 190, 196, 197), as we had difficulty detecting 1a-induced RNA3 accumulation in the BY4743 deletion mutant library background strain. Despite extensive efforts, we could not generate the YPH500 *ubp6Δ* strain, suggesting this deletion inhibits cell growth in YPH500 cells. Although the UPS mutants are responsive to 1a, demonstrated by the observed 1a-induced RNA3 accumulation in each deletion strain (Fig. 3.10A, lanes 2, 4, 6, 8, 10, 12 and 14), RNA3 accumulation in the presence of 1a is, overall, decreased compared to wt, with the exception of *pre9Δ* cells, which accumulate higher levels of RNA3 (153%) compared to wt cells in the presence of 1a (Fig. 3.10B). Additionally, *ubr1*Δ and *ufd4*Δ cells accumulated significantly more RNA3 transcript *in the absence of 1a* (2000% and 563%, respectively) compared to wt cells lacking 1a (Fig. 3.10C), whereas a more moderate 1a-independent RNA3 accumulation was observed in *pre9Δ* (~270%) and *ufd5Δ* (173%) cells compared to 1a-independent RNA3 accumulation in wt cells (Fig. 3.10C). Thus, loss of UPS accessory proteins Ubr1, Pre9, Ufd4 and Ufd5 exhibits 1a-independent affects on BMV RNA3, suggesting that these proteins may modulate recruitment of RNA3 to a membrane associated state under normal cellular conditions.

3.2.7 1a induces membrane association of RNA3 in UPS mutant *RPT6*

To further explore UPS-mediated BMV RNA membrane association, we used cellular fractionation to more directly determine if RNA3 was membrane-associated in the BY-derived P_{TET} essential strains because generating YPH500 P_{TET} strains requires multiple technically challenging steps compared to generating deletion mutants. The cellular fractionation results presented here are for UPS mutant *RPT6* and experiments analyzing *PRE1* are in progress.

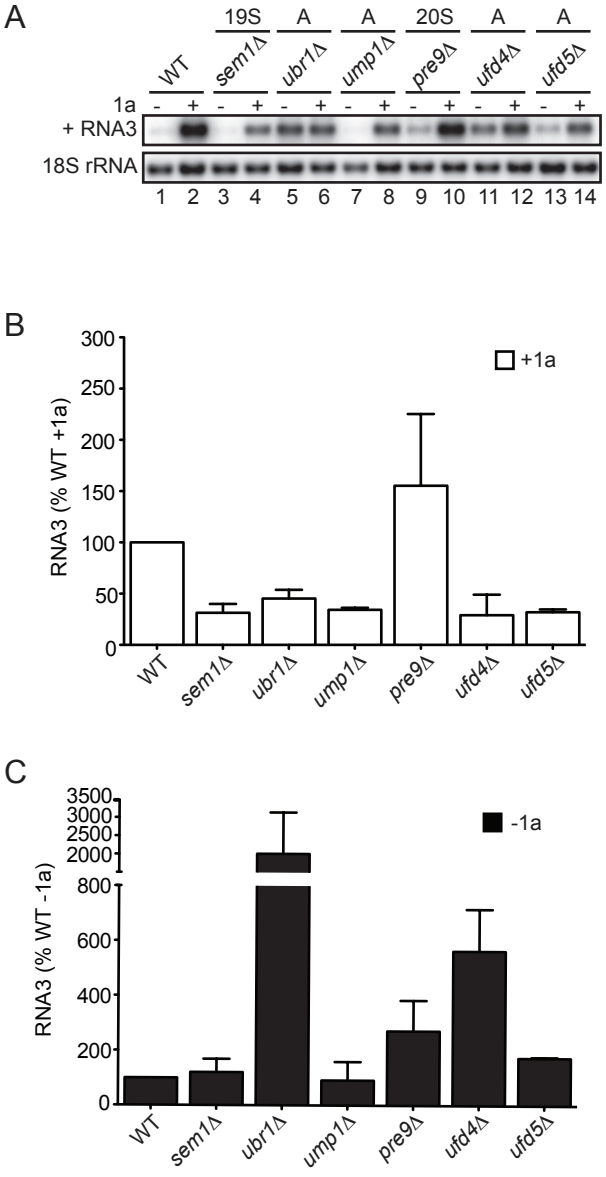

Figure 3.10. UPS mutants *ubr1*Δ, *pre9*Δ, *ufd4*Δ *and ufd5*Δ exhibit 1a-independent RNA stabilization. (A) The ratio of BMV RNA accumulation in the presence or absence of 1a in wt and deletion mutant yeast cells. (B) RNA3 accumulation in the presence of 1a. (C) RNA3 accumulation in the absence of 1a. For A, B and C, total RNA was extracted from yeast cells and RNA3 accumulation in the absence or presence of 1a was detected by Northern blotting using a BMV RNA-specific probe. Equal loading of of total RNA was verified by probing for 18S rRNA. 19S, component of the 19S regulatory particle of the 26S proteasome; 20S, component of the 20S core proteasome; A, UPS accessory protein.

Yeast cells were spheroplasted, lysed and centrifuged at low speed to separate a soluble supernatant and membrane-containing pellet fraction. In the absence of 1a, BMV RNAs, like most if not all yeast mRNAs and rRNAs, are recovered in the soluble fraction (37, 196). However, co-expressing 1a and RNA3 induces selective membrane association of BMV RNAs that can be measured by cell fractionation. Moreover, fractionation provides a direct measure of RNA3 template recruitment to membranes, an early RNA replication step that precedes and is closely linked to RNA stabilization (described above in 3.2.6) and $2a^{Pol}$-dependent negative-strand RNA synthesis (37, 196, 206). In wt and P_{TET}-*RPT6* untreated and dox-treated cells lacking 1a, RNA3 was predominantly in the supernatant (Fig. 3.11, histogram panels 1, 3, 5 and 7, supernatant fraction). In contrast, in wt untreated and dox-treated yeast cells expressing 1a, 70% and 67% of RNA3, respectively, was recovered in the pellet (Fig. 3.11, histogram panels 2 and 4, pellet fraction). Similarly, RNA3 was efficiently recovered in the membrane pellet of untreated (73%) and dox-treated (84%) P_{TET}-*RPT6* cells (Fig. 3.11, histogram panels 6 and 8, pellet fraction). Thus, UPS mutant *RPT6* does not inhibit BMV RNA replication by disrupting early, 1a-mediated recruitment of the RNA3 replication template to a membrane-associated state.

3.2.8 BMV $2a^{Pol}$ localization is disrupted in UPS mutants *RPT6, SEM1 and UMP1*

In plant cells and yeast, BMV 1a and $2a^{Pol}$ colocalize predominantly at the perinuclear ER in a concentrated, crescent-shaped pattern (189, 190). Since the decrease in BMV RNA replication upon depleting or deleting UPS genes was not due to decreased levels of viral proteins, with the possible exception of mutant *SEM1* (Fig. 3.8B, lane 3), we investigated if the localization of viral proteins was altered in the absence of any of the UPS proteins in cells co-expressing 1a and $2a^{Pol}$. In wt untreated and dox-treated yeast, 1a and $2a^{Pol}$ localized normally to the perinuclear ER membrane, indicating the presence of dox did not effect normal localization of BMV replication proteins (Fig. 3.12, panels A-B and Fig. 3.13, panels A-B).

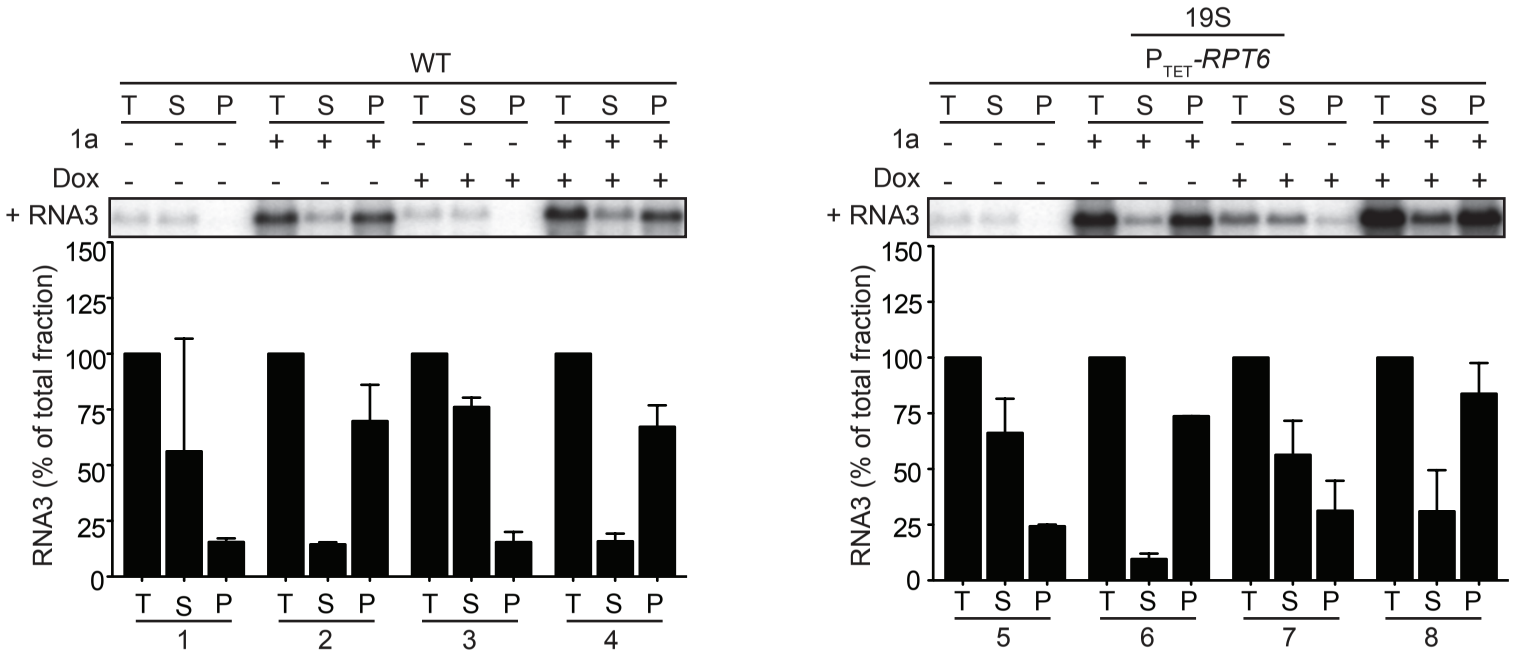

Figure 3.11. RNA3 is recruited to a membrane-associated state in UPS mutant *RPT6*. Untreated and dox-treated (10 µg/ml) wild type R1158 and P_{TET}-*RPT6* yeast cells expressing RNA3 only or RNA 3 and 1a were spheroplasted and lysed to yield a total RNA fraction (T). The lysate was centrifuged to obtain membrane-depleted supernatant (S) and membrane enriched pellet fractions (P). RNA was isolated from each fraction by hot phenol-chloroform extraction. Equal volumes of T, S and P fractions were analyzed by Northern blotting and RNA3 was detected using a probe specific for BMV RNA3. The accumulation of RNA3 in each T, S, P set was normalized to that in the T fraction for the corresponding set. 19S, component of the 19S regulatory particle of the 26S proteasome.

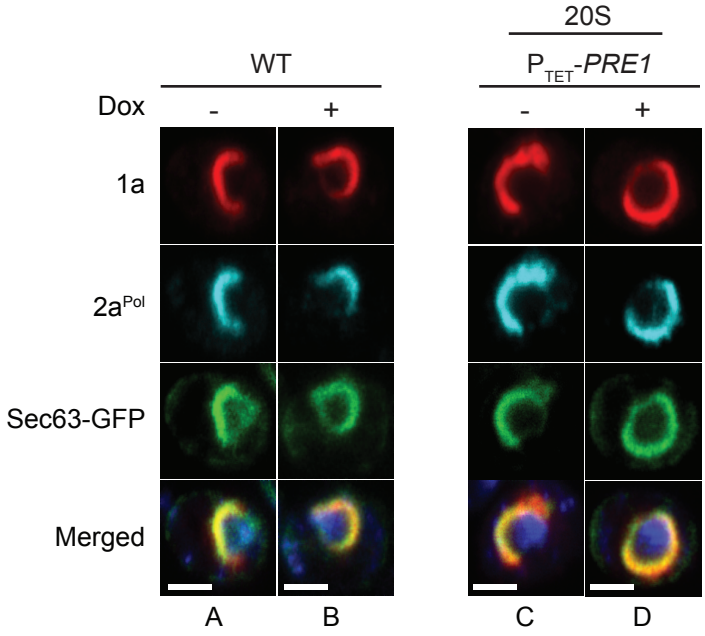

Figure 3.12. BMV 1a and 2a^{Pol} co-localize to the perinuclear ER membrane in UPS mutant *PRE1*. Confocal fluorescence images of *PRE1* untreated and dox-depleted yeast cells co-expressing BMV 1a, 2a^{Pol}, and the ER marker Sec63-GFP. Representative images for 1a (red), 2a^{Pol} (cyan), Sec63-GFP (green), and merged signals (bottom) are shown and each panel represents one cell. 20S, component of the 20S core proteasome; P_{TET}, tetracycline-repressible promoter; Dox, doxycycline (10 µg/ml). Scale bars, 0.5 µm.

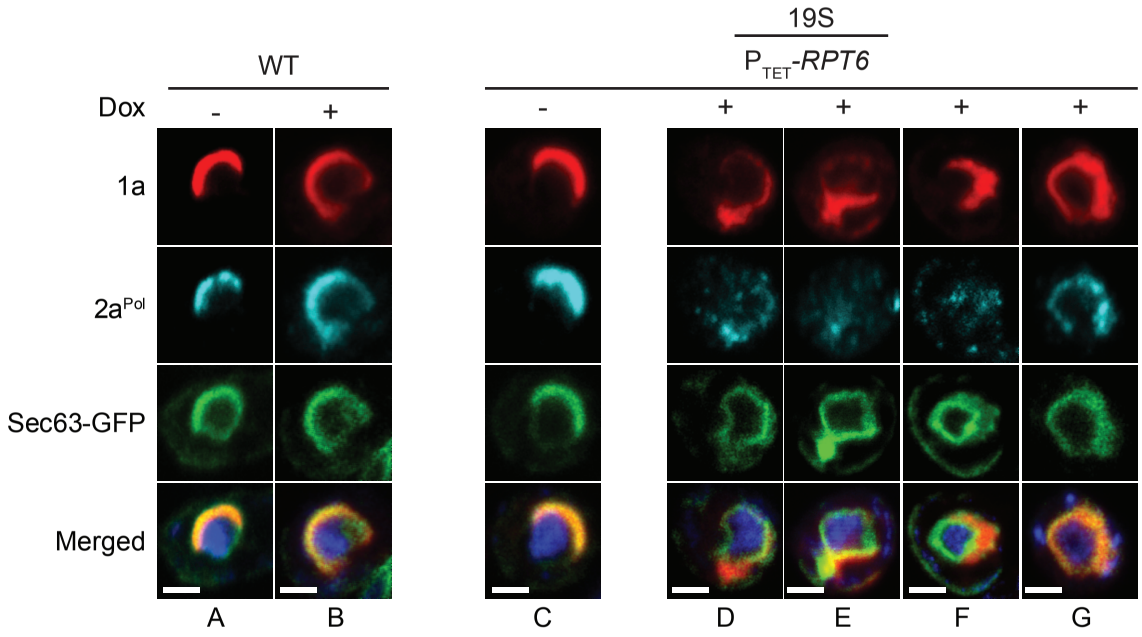

Figure 3.13. 2a^{Pol} perinuclear ER membrane localization is disrupted in UPS mutant *RPT6*. Confocal fluorescence images of P$_{TET}$-*RPT6* untreated and dox-depleted yeast cells co-expressing BMV 1a, 2a^{Pol}, and the ER marker Sec63-GFP. Representative images for 1a (red), 2a^{Pol} (cyan), Sec63-GFP (green), and merged signals (bottom) are shown and each panel represents one cell. 19S, component of the 19S regulatory particle of the 26S proteasome; P$_{TET}$, tetracycline-repressible promoter; Dox, doxycycline (10 µg/ml). Scale bars, 0.5 µm.

Similarly, localization of 1a and $2a^{Pol}$ was not altered in untreated or dox-depleted P_{TET}-*PRE1* (Fig. 3.12, panels C-D) or in untreated P_{TET}-*RPT6* cells (Fig. 3.13, panel C). However, in dox-treated P_{TET}-*RPT6* cells, while in rare instances normal 1a localization was seen (Fig. 3.13, panel A), aberrant 1a localization patterns were observed in the majority of cells (Fig. 3.13, panels D-G). 1a localization either extended away from the nucleus (Fig. 3.13, panel D-E) or was noticeably more diffuse (Fig. 3.13, panels F-G). Despite these perturbed localization patterns, 1a was associated with the ER membrane, as it colocalized with cellular ER marker Sec36-GFP (Fig. 3.13, panels D-G, merged images). Even more striking was the severe disruption of $2a^{Pol}$ localization in dox-treated P_{TET}-*RPT6* cells compared to P_{TET}-*RPT6* untreated cells (Fig. 3.13, panels D-G vs. panel C). Additionally, in cells exhibiting perturbed $2a^{Pol}$ localization, 1a and Sec63-GFP localization patterns are also slightly perturbed (Fig. 3.13, panels D-G vs. panel C). As with 1a, $2a^{Pol}$ localization in some cells was perinuclear ER-associated, but did not retain the concentrated, crescent shape localization pattern observed in wt and P_{TET}-*RPT6* untreated cells (Fig. 3.13, panel G vs. panels A and C). In other cells, complete disruption of $2a^{Pol}$ localization was evident (Fig. 3.13, D-F). A similar diffuse $2a^{Pol}$ localization pattern was also observed in mutants *sem1Δ* (Fig. 3.14 panels B-D) and *ump1*Δ (Fig. 3.14 panels G-H), although in cells lacking Ump1 this observation was less frequent compared to the aberrant $2a^{Pol}$ localization patterns observed in *sem1Δ* cells and *RPT6*-depleted cells. 1a and $2a^{Pol}$ in all other non-essential deletion mutants co-localized to the perinuclear ER membrane as in wt cells (Fig. 3.14).

3.3 DISCUSSION

Many, if not all, viruses exploit the highly conserved UPS at various stages of infection to regulate viral proteins, enhance their own replication and/or evade cellular antiviral responses (53, 54, 94, 203). Although recent reports highlight the importance of this cellular pathway in

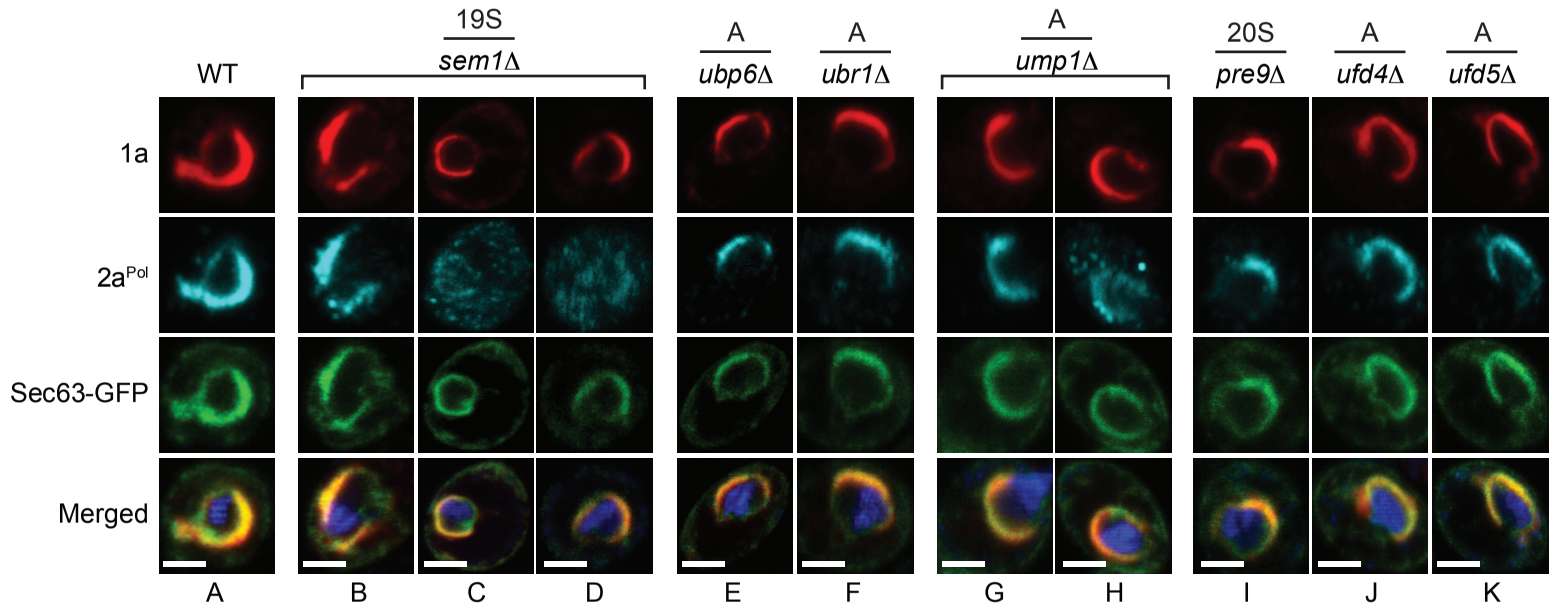

Figure 3.14. 2a^{Pol} perinuclear ER membrane localization is disrupted in UPS mutants *SEM1* and *UMP1*. Confocal fluorescence images of wt and nonessential proteasome deletion mutant yeast cells co-expressing BMV 1a, 2a^{Pol}, and the ER marker Sec63-GFP. Representative images for 1a (red), 2a^{Pol} (cyan), Sec63-GFP (green), and merged signals (bottom) are shown and each panel represents one cell. 19S, component of the 19S regulatory particle of the 26S proteasome; 20S, component of the 20S core proteasome; A, UPS accessory protein. Scale bars, 1.0 µm.

(+)RNA virus-host interactions (17, 18, 30, 40, 54, 156, 182, 202), in many cases the underlying mechanistic roles for the UPS are not entirely resolved due to the complexity of interactions between the UPS and the multiple steps of viral infection. Previously, our laboratory identified 123 genes affecting BMV RNA replication, including nine genes in the UPS whose loss inhibited viral RNA replication ~6- to 100-fold (68, 119). Here we investigated the role(s) of nine implicated UPS genes, which are components of the 20S core (*PRE1, PRE9*), 19S regulatory particle (*SEM1, RPT6*) and accessory proteins (*UBR1, UBP6, UMP1, UFD4 and UFD5*) in BMV RNA replication. As detailed below, our studies revealed that the UPS contributes to viral RNA replication in at least three mechanistically distinct ways: (i) UPS-dependent activation of lipid synthesis genes; (ii) UPS-dependent processes complementable by ubiquitin; and (iii) UPS-dependent processes not complementable by lipids or ubiquitin (Table 3.3).

3.3.1 26S proteasome activity is required for BMV RNA replication in plants and yeast

Proteasome inhibitor studies with the widely used peptide aldehyde MG132 showed that activity of the 26S proteasome is required for bromovirus RNA replication in barley protoplasts and yeast (Figs. 3.3A and B). Additionally, disrupting the proteasome affects $2a^{Pol}$ accumulation (Fig. 3.3D). Our data are consistent with reports demonstrating that West Nile virus (69) and rotavirus (136) require functional proteasomes for efficient genome replication at a post-entry step and that UPS regulates multiple viral polymerases (30, 40, 202, 228). From these data we conclude that BMV requires active 26S proteasomes for RNA synthesis and regulation of its RNA-dependent RNA polymerase.

3.3.2 BMV RNA replication is linked to proteasome-dependent activation of lipid synthesis genes

Cellular membrane lipid composition is critical for BMV and many other (+) RNA viruses, which form RNA replication compartments by dramatically rearranging host membranes (49,

Table 3.3. Summary of UPS mutant phenotypes.

					Accumulation		Localization		
		RNA replication	Lipid complementation	Ubiquitin complementation	1a	2a^{Pol}	1a	2a^{Pol}	1a-independent RNA3 stabilization
Class I. UPS-dependent activation of lipid synthesis genes									
ubr1Δ[a]	**E3 ligase**	3%	**17%**	81%	Normal	Increased	Normal	Normal	Yes
P$_{TET}$-*RPT6*	**19S RP**	2%	**25%**	7%	Normal	Increased	Diffuse[b]	Diffuse	Not available for assay
ubp6Δ[a]	**Deubiqutinatinase**	2%	**32%**	71%	Normal	Increased	Normal	Normal	Not available for assay
P$_{TET}$-*PRE1*	**20S CP**	10%	**110%**	13%	Normal	Increased	Normal	Normal	Not available for assay
Class II. UPS-dependent processes complemented by ubiquitin									
pre9Δ	**20S CP**	1%	2%	**31%**	Normal	Normal	Normal	Normal	Yes
ufd5Δ	**Transcription factor**	3%	3%	**63%**	Normal	Normal	Normal	Normal	Yes (moderate)
ubp6Δ	**Deubiquitinase**	2%	32%	**71%**	Normal	Increased	Normal	Normal	Not available for assay
ufd4Δ	**E3 ligase**	4%	8%	**80%**	Normal	Normal	Normal	Normal	Yes
ubr1Δ	**E3 ligase**	3%	17%	**81%**	Normal	Increased	Normal	Normal	Yes
Class III. UPS-dependent processes not complemented by lipids or ubiquitin									
ump1Δ	**Chaperone**	0.3%	**0.4%**	**1%**	Normal	Increased	Normal	Diffuse[b]	No
sem1Δ	**19S RP**	1.0%	**0.6%**	**10%**	Decreased	Decreased	Normal	Diffuse[b]	No

[a]BMV RNA replication was partially complemented by lipids and ubiquitin and so is present in Class I and Class II.

[b]Localization pattern was observed in a fraction of cells.

145, 193, 196). Mutations in fatty acid desaturase *OLE1* inhibit BMV RNA replication ≥20-fold, but are fully complemented by supplementing UFAs, the products of Ole1p, in growth medium (123, 124). Activation of *OLE1* requires ubiquitination and subsequent proteasomal processing of transcription factors Mga2 and Spt23 (244). In cells depleted of essential gene *RPT6*, one of the six ATPases of the 19S regulatory particle, and *PRE1*, a β-subunit of the 20S catalytic core proteasome, BMV RNA replication was abolished (Fig. 3.4A, lanes 2 and 6) and accumulation of *OLE1* fatty acid desaturase mRNA levels was significantly inhibited (Fig. 3.5A). BMV RNA replication in *RPT6*- and *PRE1*-depleted cells was unaffected by expressing exogenous Ub (Fig. 3.7, lanes 4 and 8), which restores activation of Mga2 in cells depleted of free Ub (226). This is consistent with the observation that dox-treated *RPT6* and *PRE1* cells do not exhibit depleted free Ub levels (Fig. 3.6A) and these data suggest that a defect in Mga2 and Spt23 is not a likely explanation for RNA replication defects in mutants *RPT6* and *PRE1*. In *PRE1*-depleted cells, RNA replication was fully complemented by UFA feeding (Fig 3.4A, lane 8), providing a mechanistic explanation for the observed replication defect in *PRE1*-depleted cells. Moreover, these data support and expand recently published results by Wang *et al.*, which link additional UPS genes to lipid homeostasis and BMV RNA replication (226). Supplementing UFAs in the growth medium only partially complemented the RNA replication defect observed cells lacking Rpt6, Ubp6 or Ubr1 (Fig. 3.4A, lane 4 and Fig. 3.4B, lanes 6 and 8) showing that *RPT6, UBP6* and *UBR1* contribute one or more additional UPS-dependent, lipid-independent function(s) to BMV RNA replication.

3.3.3 Ub-dependent processes are required for BMV RNA replication

Ubiquitination is a post-translational modification in which single ubiquitin molecules or polyubiquitin chains are attached to client proteins, ultimately dictating their cellular fate (231). Polyubiquitin chains are required for substrate recognition and subsequent degradation by the proteasome, whereas monoubiquitination determines the localization and activity of proteins

(61, 231). Multiple UPS accessory proteins in our study perform ubiquitin-dependent functions or are ubiquitin substrates: Ubp6 is a deubiqutinating enzyme and a proteasome accessory component (14, 126); Ubr1 is a RING-type E3 ligase that recognizes substrates in the N-end rule pathway (85, 235), whereas Ufd4 is a HECT-type E3 enzyme that functions in the ubiquitin-fusion pathway (97) and recently it was shown that Ubr1 and Ufd4 interact, both physically and functionally (84); and Ufd5 is a transcriptional activator of proteasome genes (237) that is subsequently degraded by the proteasome via ubiquitin-dependent and -independent mechanisms (98). Although only *ubp6*Δ showed a deficiency in free Ub levels (Fig. 3.6B, lane 5), BMV RNA replication was substantially complemented in UPS mutants *upb6*Δ, *ubr1*Δ, *ufd4*Δ and *ufd5*Δ by expressing exogenous Ub (Fig. 3.7B). These data reveal a role or roles for Ub-dependent processes in BMV RNA replication, although whether these processes contribute to activating viral or cellular proteins required for BMV, to degrading antiviral cellular factors, or to other aspects of viral RNA replication remains unclear. Since many (+)RNA viruses employ strategies to downregulate expression of their RNA-dependent RNA polymerase (RdRp) (4), one possibility is that Ub-dependent processes affect BMV RNA replication by modulating turnover of the viral polymerase, which has been reported for (+)RNA viruses coxsackievirus B3 (202) and TYMV (30, 40). Consistent with this idea is the observation that $2a^{Pol}$ accumulates to higher than wt levels in UPS mutants *upb6*Δ, *ubr1*Δ, *ufd4*Δ and *ufd5*Δ (Fig. 3.9B, lanes 5, 7, 13 and 15). Alternatively, these genes may directly or indirectly modulate $2a^{Pol}$ localization. Indeed, in cells lacking 19S regulatory particle component Rpt6, deubiqutinase Ubp6 or ubiquitin ligase Ubr1, which physically interacts with Rpt6 (236), although $2a^{Pol}$ levels were significantly increased, 1a failed to recruit the viral polymerase to sites of RNA replication complex formation (Figs. 3.13 and 3.14). These observations suggest the opposing processes of ubiquitination and deubiquitination may be important for proper localization of $2a^{Pol}$ to membrane-associated RNA replication complexes.

3.3.4 Lipid-independent, Ub-independent processes are required for BMV RNA replication

BMV RNA replication defects in the majority of UPS mutants analyzed here can be linked to processes that activate lipid metabolism genes (*RPT6*, *PRE1, UBP6 and UBR1*) or require ubiquitin (*UBP6*, *UBR1*, *UFD4*, *UFD5*). However, deleting Sem1p, a non-ATPase component of the 19S regulatory particle lid (64), or Ump1p, a molecular chaperone that is required for maturation of the 20S catalytic core (184), exhibited lipid- and ubiquitin-independent RNA replication defects (Fig. 3.3B, lanes 4 and 10 and Fig. 3.7B, lanes 4 and 10, respectively). Consistent with its role in activating the 20S core proteasome, allowing subsequent degradation of Ub-conjugated proteins, *ump1*Δ cells exhibited an increase in $2a^{Pol}$ accumulation comparable to that observed in MG132-treated yeast, which also lack 20S catalytic core activity, but $2a^{Pol}$ localization was perturbed in a fraction of *ump1*Δ cells (Figs. 3.8A, lane 9; Fig. 3.3D and Fig. 3.14, panels G-H). These observations underscore the importance of active proteasomes for viral RNA replication and implicate the necessity of lipid- and ubiquitin-independent processes for BMV RNA replication, specifically in modulating viral polymerase accumulation and/or activity.

3.3.5 1a-independent RNA3 stabilization

The phenotypic classes of proteasome mutants discussed above affect RNA replication and/or viral protein accumulation. An additional, striking observation was that an early replication step prior to genome replication was altered in some mutants. In wt cells, expressing 1a increases the half-life of RNA3 from ~5 min to > 3hr in the presence of 1a (91) and stimulates an 8- to 30-fold increase in RNA3 accumulation, depending on the level of 1a expression (196). This 1a-dependent increase in RNA3 accumulation *in vivo* is associated with 1a-mediated transfer of RNA3 to a membrane-associated state, which represents its localization to spherular RNA replication complexes formed on the perinuclear ER membrane (196). 1a-dependent RNA3 stabilization was observed in all mutants assayed (Fig. 3.10A, lanes 4, 6, 8,

10, 12 and 14). However, in mutants *ubr1*Δ, *pre9*Δ, *ufd4*Δ and *ufd5*Δ, RNA3 was stabilized in the *absence* of 1a as well (Fig. 3.10C). These results suggest a potential UPS-dependent role in early steps of BMV RNA replication, during which RNA3 is recruited from translation to RNA replication (91). It is possible that disrupting the UPS causes mislocalization of RNA3 in the absence of 1a. Alternatively, 20S proteasome RNAase activity, which has specificity for viral RNAs (94, 178), may be disrupted, a model seems most likely for mutant *PRE9*, which is a component of the 20S core proteasome.

3.3.6 Summary

Our systematic analysis of nine UPS genes in yeast revealed at least three mechanistically distinct contributions of the UPS to BMV RNA replication: (i) UPS-dependent activation of lipid synthesis genes; (ii) UPS-dependent processes complementable by ubiquitin; and (iii) UPS-dependent processes not complementable by lipids or ubiquitin. Moreover, proteasome inhibitor studies in barley protoplasts suppressed BMV RNA replication, confirming that UPS-dependent processes are required in natural host cells. Further studies will determine more directly how the implicated UPS genes affect BMV RNA replication and should significantly advance our understanding of cellular functions and pathways and virus-host interactions. The UPS is a highly conserved eukaryotic cellular pathway manipulated by multiple diverse viruses that pose significant health concerns, including including hepatits C virus, influzenza virus, and HIV, among others and presents a useful opportunity to explore broader approaches for virus control.

3.4 MATERIALS AND METHODS

3.4.1 Yeast strains

Essential yeast strains. The yeast Tet-Promoter Hughes Collection of essential yeast strains was purchased from Open Biosystems (Huntsville, AL). The tet-promoter mutant strains (designated here with the prefix P_{TET}) were provided in the haploid R1158 background (*MATa URA3::CMV-tTA MATa his3-1 leu2-0 met15-0*), which was constructed by a one-step integration of the cytomegalovirus (CMV) promoter-driven tTA* transactivator at the *URA3* locus (83). The kanR-tetO7-TATA was then integrated into the promoter of a different essential gene in strain R1158, allowing the repression of essential gene expression upon the addition of dox to growth medium (149).

Non-essential yeast strains. BY4743 (*MAT*a/α *his3Δ1/his3Δ1 leu2Δ0/leu2Δ0 LYS2/lys2Δ0 met15Δ0/MET15 ura3Δ0/ura3Δ0)* and its various single-gene deletion derivatives and YPH500 (*MATα ura3–52 lys2–801 ade2–101 trp1-Δ63 his3-Δ200 leu2-Δ1*) were used. The following strains were generated in YPH500 for this work: *sem1*Δ (YPH500 *sem1::kanMX4*), *ubr1*Δ (YPH500 *ubr1::kanMX4*), *ump1*Δ (YPH500 *ump1::kanMX4*), *pre9*Δ (YPH500 *pre9::kanMX4*), *ufd4*Δ (YPH500 *ufd4::kanMX4*), *ufd5*Δ (YPH500 *ufd5::kanMX4*). Several attempts were made to generate YPH500 *ubp6*Δ (YPH500 *ubp6::kanMX4*), but viable colonies could not be recovered. Genomic insertions were made using an amplified *KanMX4* cassette flanked by 5' and 3' homologous recombination regions.

3.4.2 Plasmids

To express BMV 1a and $2a^{Pol}$ for assaying BMV RNA replication, pB12VG1 was used (119). *CUP1* promoter-driven BMV RNA3 was launched from pB3VG128-H in medium lacking copper. To assay 1a-mediated RNA3 stability, pB3MS82 was used, which expresses BMV RNA3 from a *GAL1* promoter. Both pB3VG128-H and pB3MS82 express a BMV RNA3

derivative in which the coat protein gene has a four-nucleotide insertion and a point substitution, abolishing expression of the coat protein (12). The use of pB3VG128-H and pB3MS82 in this study, as in many other studies (12, 52, 71, 133, 161, 227), allows analysis of RNA3 and RNA4 levels while avoiding any effects of possible variations in coat protein expression and RNA encapsidation. For immunfluoresence and electron microscopy, BMV 1a and $2a^{Pol}$ were expressed from *GAL1* promoter-driven centromeric plasmids pB1YT3H (11) and pB2YT5-2 (12), respectively. The sec63-GFP fusion protein was expressed from plasmid pPS1530 or pBG30, both of which are derivatives of pJK59 (a gift from P. Silver, Department of Biological Chemistry and Molecular Pharmacology, Harvard University).

For barley protoplast experiments, pB1TP3, pB2TP5, and pB3TP8 were used which contain complete cDNA copies of wild type BMV RNA1, RNA2, and RNA3, respectively. Additionally, these plasmids each contain a T7 RNA polymerase promoter, allowing *in vitro* synthesis of infectious BMV transcripts (5, 93).

3.4.3 Yeast transformation and growth

The lithium acetate-polyethylene glycol (PEG) method was used to transform plasmids into yeast strains (58).

Essential strain growth. Essential yeast strains containing BMV expression plasmids were grown overnight at 30°C in synthetic medium containing 2% raffinose as a carbon source, subcultured to a starting optical density at 600 nm (OD_{600})=0.1 in medium containing raffinose ±10 μg/ml dox and grown for 24 hr. Cells then were subcultured to a starting OD_{600}=0.1-0.2 in medium containing 2% galactose as a carbon source ±10 μg/ml dox. Cells were grown for 2 passages (36 to 48 hr) and harvested when the OD_{600} was between 0.4-1.0. Leucine, histidine, methionine or combinations thereof were omitted to maintain plasmid selection.

Non-essential strain growth. Non-essential yeast strains containing BMV expression plasmids were grown overnight at 30°C in synthetic medium containing 2% glucose as a carbon

source, subcultured to a starting starting OD_{600}=0.08-0.2 in medium containing 2% galactose as a carbon source. Cells were grown for 2 passages (36 to 48 hr) and harvested when the OD_{600} was between 0.4-1.0. Leucine, hisitidine, uracil or combinations thereof were omitted to maintain plasmid selection.

To make medium supplemented with unsaturated fatty acids, Tergitol NP-40 was added to a final concentration of 1% to solubilize the fatty acids. Equimolar amounts of palmitoleic acid (16:1) and oleic acid (18:1) were added to Tergitol NP-40-containing medium to a final concentration of 1 mM (205).

3.4.4 Preparation and transfection of barley mesophyll protoplasts

Barley (*Hordeum vulgare*), cultivar Robust, seeds were obtained from Johnny's Selected Seeds (http://www.johnnyseeds.com/). The procedures described below for isolating and inoculating barley protoplasts are a combination of procedures described by Kroner and Ahlquist (10) and Rao (186).

Plant growth. Barley seeds were planted in peat moss and vermiculite (1:1) and watered with 0.5x Hoagland's solution once each day. Protoplasts were isolated from 7 day-old seedlings (avg. height 10-11 cm) grown at 24°C in a growth chamber set at a 16 hr photoperiod.

Preparation of leaves and protoplast extraction. Two 1.2 g aliquots of 7 day-old barley leaves were harvested using a sharp razor blade to cut leaves 4-5 cm above potting medium. Dry or yellow leaves were never harvested. Leaves were cut lengthwise and then crosswise into 0.5-1 mm^2 sections. Sliced material was transferred and distributed into a petri dish containing freshly made 25 ml enzyme solution [2% cellulase R-10 (Yakult Pharmaceutical Industry Co, LTD., Tokyo, Japan), 0.1% macerozyme R-10 (Yakult Pharmaceutical Industry Co, LTD., Tokyo, Japan), 0.1% BSA (A4503; Sigma-Aldrich, St. Louis, MO) in 0.55 M mannitol, pH 5.9; final pH of solution adjusted to 5.9 with citric acid and filtered sterilized with 0.2 µm filter) and incubated in the dark for 3 hrs at 30°C. Leaf sections were gently swirled every 30 min to

ensure that leaf tissue was digested. The enzyme-digested leaf solution was transferred into a 250 ml sterile beaker and swirled for 20 sec to release protoplasts. The solution was poured through a 70 µm nylon cell strainer (352350; BD Biosciences, San Jose, California) into a 50 ml polypropylene conical tube. The 25 ml protoplast-containing filtrate was split equally into three 14 ml polystyrene round bottom tubes (352057; BD Biosciences, San Jose, California) by gentle pouring and tubes were centrifuged at 50 x g for 3 min to pellet leaf tissue and debris. A transfer pipet was used to remove as much supernatant as possible without disturbing the protoplast pellet. 8 ml of 0.55 M mannitol, pH 5.9 was slowly added down the side of the tube and 2 ml 0.55 M sucrose was underlaid beneath the digested leaf material. Tubes were centrifuged at 100 x g for 8 min to separate protoplasts from cell debris. The dark green band of protoplasts at the mannitol/sucrose interface was collected with a transfer pipet and transferred to a 50 ml polypropylene conical tube. All centrifugation steps were performed in an Allegra™ 6R centrifuge with a GH-3.8 swinging bucket rotor (Beckman Coulter, Inc., Brea, CA).

Yield and viability count. A 25 µl aliquot of protoplasts was added to 2.5 µl 5mg/ml fluorescein diacetate (F7378; Sigma-Aldrich, St. Louis, MO) and incubated at room temperature for 5 min. The stained protoplast solution was applied to a hemacytometer and visualized under a bright field light source (total cell count) and a fluorescent light source (viable cell count). Average yields were 1 to 4 x 10^5 protoplasts per ml. The ratio of viable cells to total cells was calculated to obtain an estimate of the percent viable cells. The number of viable protoplasts per cubic centimeter was determined (10 cells/mm^2=10^5 cells/cm^3) and used to estimate the number of viable protoplasts per milliliter.

Transfection of protoplasts with viral RNA. BMV RNA1, RNA2, and RNA3 were *in vitro* transcribed and capped using the T7 mMESSAGE mMACHINE® Kit (Ambion, Austin, TX) from EcoRI-linearized plasmids pB1TP3, pB2TP5, and pB3TP8, respectively (93). For each inoculation, 10^5 protoplasts were transferred to a 14 ml polystyrene culture tube and centrifuged at 50 x g for 4 min. The supernatant was removed while leaving the pellet undisturbed. The

protoplasts were re-suspended by gently tapping the bottom of the tube and the volume of the protoplast solution was adjusted to 100 µl with 0.55 M mannitol, pH 5.9. 5 µg each of BMV RNA1, RNA2, and RNA3 and 110 µl of PEG-$CaCl_2$ solution [40% PEG 4000 (81240; Sigma-Aldrich, St. Louis, MO), 3mM $CaCl_2$] were added to the protoplasts. The tube was tapped gently to thoroughly mix PEG-$CaCl_2$, RNAs, and protoplasts and incubated on ice for 15 min. 1 ml of 0.55 M mannitol, pH 5.9 was added to stop the transfection reaction, protoplasts were pelleted at 50 x g for 4 min, supernatant was removed and cells were gently re-suspended in 1 ml protoplast medium. Protoplast medium was freshly made by diluting 100x $CaCl_2$ solution, 1000x KK solution and 1000x CKM solution (see below for recipes) to 1x in 20 ml 0.55 M mannitol, pH 5.9 containing 0.2 M MES, pH 6.5 and 10 µg gentamicin (15710-064; Gibco, Grand Island, NY). The final pH was checked to ensure that it was 6.5 and the medium was filter sterilized with a 0.45 µm filter prior to use. Stock solutions for protoplast medium were made as follows and stored for up to one month: 100x $CaCl_2$ solution (100 ml: 14.7 g $CaCl_2$ in 0.55 M mannitol, pH 5.9, adjust final pH to 6.5 with 0.01 M KOH, autoclave), 1000x KK solution (100 ml: 2.72 g KH_2PO_4 and 10.11 g KNO_3 in sterile water, adjust final pH to 6.5 with 10 M KOH, autoclave) and 1000x CKM solution (100 ml: 0.0025 g $CuSO_4$, 0.017 g KCl, 24.65 g $MgSO_4$ in 0.55 M mannitol, pH 5.9, adjust final pH to 5.8 with 0.01 M KOH, autoclave).

Tubes containing transfected protoplasts were placed in 24°C incubator under fluorescent light measuring 25 μEm^{-2} sec^{-1} of intensity at the bottom of the tube (e.g. closest to protoplasts in medium), as measured with a quantum light meter (model MQ-100; Apogee Instruments Inc., Logan, UT). Protoplasts were collected 12- 18 hrs post transfection for RNA and protein analysis. All centrifugation steps were performed in an Allegra™ 6R centrifuge with a GH-3.8 swinging bucket rotor (Beckman Coulter, Inc., Brea, CA).

3.4.5 Proteasome inhibitor treatments

Yeast. Due to the naturally impermeable cell wall of wild type yeast, special growth conditions were utilized for proteasome inhibitor treatments in yeast (132, 170). Specifically, L-proline was used instead of ammonium sulfate as the sole nitrogen source in growth medium and sodium dodecyl sulfate (SDS) was added to growth medium during inhibitor treatment. These conditions are thought to facilitate the transient opening of the cell wall/plasma membrane, rendering the cells permeable to protease inhibitors (132). Wt yeast cells expressing 1a, $2a^{Pol}$ and RNA3 were grown overnight at in synthetic medium (0.17% yeast nitrogenous base without ammonium sulfate) supplemented with 0.1% proline and 2% glucose as a carbon source (dex-proline) to induce expression of BMV. Cells were subcultured to a starting OD600=0.6 in dex-proline medium containing 0.003% SDS (132). After 3 hrs, cells were subcultured to a starting OD_{600}=0.25 in synthetic medium containing supplemented with 0.1% proline and 2% galactose as a carbon source (gal-proline) containing the control buffer dimethyl sulfoxide (DMSO) or 50 μM MG132 dissolved in DMSO (474790; Calbiochem/EMD Millipore, Billerica, Massachusetts). Cells were treated with MG132 for 1 hr or 18 hrs. Cells treated for 1 hr were pelleted, washed twice with synthetic medium containing 0.17% ammonium sulfate as nitrogen source and 2% galactose as carbon source (gal-AS) to remove DMSO or MG132, resuspended in gal-AS and returned to 30°C for and additional 17 hrs. 5 OD_{600} units of cells from each treatment were collected 18 hrs post-galactose induction and RNA and protein were isolated and analyzed as previously described. For all media used, leucine, histidine and uracil were omitted to maintain plasmid selection.

Barley protoplasts. Protoplasts were isolated and transfected with BMV RNAs as described above. Control buffer DMSO, 10 μM or 20 μM MG132 dissolved in DMSO was added to protoplasts immediately post-transfection and incubated for 12 hrs. RNA and protein were isolated and analyzed as previously described.

3.4.6 RNA extraction and analysis

Total RNA was isolated from yeast cells and barley protoplasts using acidic hot phenol and ethanol precipitation as described elsewhere (125). Northern blotting was performed as previously described (131) except that 2 µg of RNA total per sample was separated in 1% (wt/vol) agarose-MOPS (morpholinepropanesulfonic acid)-formaldehyde gels. BMV RNAs were detected using ^{32}P-labeled probes specific for positive- or negative-strand BMV RNA3 and RNA4 as previously described (124). The 18S rRNA probe was derived from pTRI RNA 18S templates (Ambion, Austin, TX). Probes were synthesized using an Epicenter Riboscribe probe synthesis kit (Madison, WI) with the appropriate enzyme, i.e., T7 or or SP6 polymerase. Northern blots were imaged on a Typhoon 9200 instrument (Amersham Biosciences, Piscataway, NJ) and band intensities were analyzed with ImageQuant software (Molecular Dynamics, Piscataway, NJ).

3.4.7 Protein extraction, Western blotting, and total protein analysis

BMV 1a and 2a^{Pol} and cellular pgk1. Yeast cells were grown to an OD_{600} of 0.4-1.0 and 2.5 OD_{600} units of cells were harvested. Total protein was extracted from yeast and barley protoplasts as previously described (124) and equal volumes of cell lysates were separated on 4-15% Criterion^{TM} TGX^{TM} precast polyacrylamide gels (Bio-Rad, Hercules, CA). Proteins were transferred to PVDF membrane, which were blocked for 1 hr with non-fat dry milk (5% in TBS containing 0.1% Tween 20) prior to antibody incubation as described below.

Ubiquitin and α-tubulin. Yeast and barley were grown as described above and total protein was extracted as previously described (124). Equal volumes of cell lysates were separated on 4-12% Bis-Tris Criterion^{TM} precast polyacrylamide gels (Bio-Rad, Hercules, CA) with 1X MOPS running buffer to detect ubiquitin-protein conjugates or MES running buffer to detect monoubiquitin. Proteins were transferred to PVDF membrane and the membrane was heat-inactivated by autoclaving in transfer buffer at 121°C for 20 min to enhance antigenic site

recognition (202) prior to blocking with heat-inactivated BSA (5% in TBS containing 0.1% Tween 20) for 1 hr. Membranes were incubated with antibodies as described below.

Antibodies. Expression of target proteins was detected by incubating the above membranes with the following antibodies and dilutions: rabbit anti-BMV 1a at 1:10,000, mouse anti-BMV $2a^{Pol}$ at 1:3,000, mouse anti-Pgk1p (A6457; Molecular Probes, Carlsbad, CA) at 1:10,000, mouse anti-Ub (P4D1; Santa Cruz Biotechnology, Santa Cruz, CA) at 1:1,000, mouse anti-α-tubulin (T-9026; Sigma-Aldrich, St. Louis, MO) at 1:1,000 using HRP-conjugated secondary antibodies (Thermo Scientific, Rockford, IL) and Supersignal West Femto substrate (Thermo Scientific, Rockford, IL). Chemiluminescence was detected with a Bio-Rad ChemiDoc™ XRS (Bio-Rad, Hercules, CA).

3.4.8 Cell fractionation assays

Yeast spheroplasts were prepared from 2.5 OD_{600} units of cells and were lysed in lysis buffer (50mM Tris-Cl, pH 7.4, 10 mM vanadyl ribonucleoside complex [S1402S; New England Biolabs, Ipswich, MA] per sample). Half of the lysate was retained as the total (T) fraction. The other half of the lysate was centrifuged at 4°C for 5 min at 20,000 x *g* to separate the supernatant fraction (S) from the membrane-enriched pellet fraction (P). RNA was extracted from the T, S and P fractions using acidic hot phenol and ethanol precipitation as described elsewhere (125). Equal volumes of RNA preparations from each fraction were analyzed by Northern blotting.

3.4.9 Confocal laser microscopy

Confocal microscopy was performed essentially as described (123, 190). Briefly, yeast cells expressing BMV 1a, $2a^{Pol}$, or both, and Sec63-GFP were fixed with 4% formaldehyde, speroplasted with lyticase, and permeabilized with 0.1% Triton-X 100. Speroplasts were transferred to 1% polyetheylenimine-coated 8 well µ-sildes (80826; ibidi, Verona, WI) and

incubated for 30 min in IM buffer (1% non-fat dry milk, 0.05% BSA, 150 mM NaCl, 50 mM HEPES, 0.5% Tween-20, 0.02% NaZ, and 0.2% gelatin) to inhibit non-specific antibody binding. Rabit anti-1a, mouse anti-2a^{Pol}, or both primary antibodies were diluted 1:100 in IM buffer and incubated with cells at 4°C overnight in a humid chamber. After four washes with IM buffer, Alexa Fluor® goat anti-rabbit 568 (A11011; Molecular Probes, Carlsbad, CA), Alexa Fluor® goat anti-mouse 647 (A21235; Molecular Probes, Carlsbad, CA), or both were added at a 1:100 dilution and incubated at 37°C for 1 hr in a humid chamber. After four washes with IM buffer, the nucleus was stained with DAPI in PBS (1:5,000) for 10 min at room temperature. Sec63p-GFP was visualized by its intrinsic fluorescence. Confocal microscopy was performed on a Nikon A1R high-speed confocal microscope at the W. M. Keck Laboratory for Biological Imaging at the University of Wisconsin-Madison. Images were generated using ImageJ or Fiji (http://rsbweb.nih.gov/ij/, http://fiji.sc/wiki/index.php/Fiji).

Chapter 4[3]

EVIDENCE IMPLICATING PHOSPHORYLATION OF BMV 2a^{Pol} IN RNA REPLICATION

4.1 INTRODUCTION

Despite their varied genetic organization, virion morphologies and host ranges, a universal feature of all positive-strand RNA viruses is their dependence on host subcellular membranes, proteins and signaling pathways for efficient genome replication (7, 49, 68, 119, 123, 124, 157). Positive-strand RNA viruses are the largest genetic class of viruses and include important human pathogens such as hepatitis C virus, SARS coronavirus and West Nile virus (217). Multiple reports highlight the emerging role of phosphorylation in regulating multiple aspects of positive-strand RNA virus replication for Dengue virus (106), cucumber mosaic virus (110, 111) and sindbus virus (45, 120, 127), among others (89), but the mechanistic role(s) of this important cellular pathway remains poorly understood for many positive-strand RNA viral proteins (110, 152, 187, 200).

Brome mosaic virus (BMV) is a representative member of the alphavirus-like superfamily and has been extensively studied as a model for positive-strand RNA virus replication, viral protein interactions and virus-host interactions (3, 52, 68, 119, 123, 124, 161, 162, 213, 226,

---

[3] B. L. Gancarz completed the work and writing in this chapter under the guidance of P. Ahlquist. Halena VanDeusen provided assistance with illustrations.

243). BMV has a tripartite genome. Genomic RNA1 encodes the multifunctional 1a replication protein that has N-terminal m^7G methyltransferase activity required for viral RNA capping (11, 12, 114) and a C-terminal NTPase/helicase-like domain (227). RNA 2 encodes the RNA-dependent RNA (RdRp) polymerase, $2a^{Pol}$, which has N-terminal 1a helicase-binding domains (13, 36, 102, 148). RNA3 encodes the 3a cell-to-cell movement protein and coat protein, which is translated from a subgenomic mRNA, RNA4, initiated internally on negative-strand RNA3. 3a and coat proteins direct systemic spread in natural plant hosts, but are dispensable for RNA replication (13, 148).

In both natural plant hosts and the yeast *Saccharomyces cerevisiae* BMV RNA replication depends on 1a, $2a^{Pol}$ and specific *cis*-acting RNA signals (206); localizes to ER membranes (189, 190); generates a substantial excess of positive- to negative-strand RNA (92); and directs subgenomic mRNA synthesis (92). BMV replication in yeast has facilitated detailed, mechanistic studies of viral protein-protein, protein-RNA interactions and has significantly advanced our understanding of virus-host interactions. Our studies in Chapter 3 revealed the importance of multiple functions of the ubiquitin-proteasome system in BMV RNA replication and suggest that host-mediated post-translational modifications of BMV replication proteins may also be essential for efficient RNA synthesis.

Phosphorylation is the most abundant post-translation modification and functions as a molecular switch to induce rapid changes in protein function, localization and/or stability, ultimately modulating major biological processes including signal transduction, gene expression and protein complex formation, among others (24, 107, 179, 216). The reversible process of protein phosphorylation is controlled by opposing activities of protein kinases and phosphatases. Kinases share a conserved catalytic domain, which catalyzes the transfer of the γ-phosphate from ATP to serine, threonine and tyrosine residues (Fig. 4.1) and phosphatases regulate the removal of phosphate groups from substrate proteins. Here, we investigated the potential role(s) for phosphorylation in BMV RNA replication, with specific focus on the RNA-

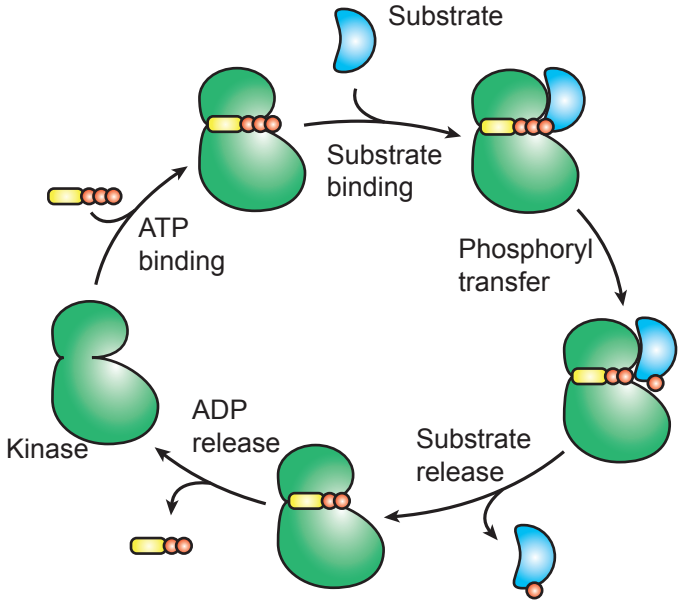

Figure 4.1. The general cascade of protein phosphorylation by a kinase. ATP binds to the active site of the kinase, followed by subsequent substrate binding to the kinase active site. Once this complex has formed, the terminal γ–phosphate of ATP (orange) is transferred to a serine (Ser), threonine (Thr) or tyrosine (Tyr) residue of the protein substrate. After phosphorylation, the substrate is released from the kinase and, finally, ADP is released from the kinase active site. It is important to note that these steps can vary between kinases. For example, a kinase may bind a protein substrate prior to ATP binding and others release ADP before dissociation of the substrate.

dependent RNA polymerase (RdRp) $2a^{Pol}$. We provide the first evidence that BMV $2a^{Pol}$ is phosphorylated in vivo and demonstrate the $2a^{Pol}$ threonine (T) residue at position 168 is necessary for BMV RNA replication. Additionally, we identify a novel host factor required for BMV RNA replication, cyclin-dependent kinase Pho85. Moreover the observation that deleting of Pho80, a cyclin partner of Pho85, substantially inhibits BMV RNA replication suggests a link between the Pho80-Pho85 holokinase and T168.

4.2 RESULTS

4.2.1 *In silico* predictions reveal 19 putative phosphorylation sites in BMV $2a^{Pol}$

BMV $2a^{Pol}$ is 94 kDa protein comprised of 822 amino acids (Figs. 4.2A and B), including 62 serine residues, 49 threonine residues and 26 tyrosine residues, collectively representing 137 potential phosphorylation sites. To reveal the most likely candidate sites for serine and threonine phosphorylation in BMV $2a^{Pol}$, *in silico* predictions were performed using the NetPhosYeast 1.0 server (87), a sister server of the first mammalian phosphorylation site prediction tool NetPhos (25), which predicts serine and threonine phosphorylation sites (phosphosites) in yeast proteins with high specificity and sensitivity (25, 87). This server was chosen since we have used the yeast *Saccharomyces cerevisae* as a model system to extensively analyze the function of BMV RNA replication proteins, 1a and $2a^{Pol}$ (36, 37, 47, 51, 91, 133, 190, 196, 227). For each input sequence, the NetPhosYeast 1.0 server outputs a list of potential phosphorylation sites with a corresponding score (a number between 0 and 1), which represents the phosphorylation potential of a residue. A score above 0.5 indicates the residue is a predicted phosphorylation site (87). Using this approach, 19 putative phosphosites (four threonine residues and 15 serine residues) were identified in the $2a^{Pol}$ protein (Fig. 4.2C and Table 4.1). The highest predicted phosphorylation site is T163, with a phosphorylation potential

A

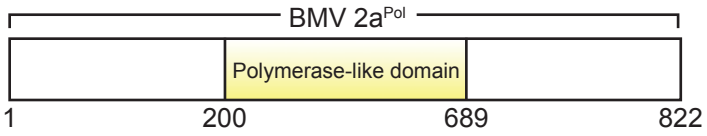

B

```
MSSKTWDDDFVRQVPSFQWIIDQSLEDEVEAASLQVQEPADGVAIDGSLA   50
SFKLAIAPLEIGGVFDPPFDRVRWGSICDTVQQMVQQFTDRPLIPQAEMA   100
RMLYLDIPGSFVLEDEIDDWYPEDTSDGYGVSFAADEDHASDLKLASDSS   150
NCEIEEVRVTGDTPKELTLGDRYMGIDEEFQTTNTDYDITLQIMNPIEHR   200
VSRVIDTHCHPDNPDISTGPIYMERVSLARTEATSHSILPTHAYFDDSYH   250
QALVENGDYSMDFDRIRLKQSDVDWYRDPDKYFQPKMNIGSAQRRVGTQK   300
EVLTALKKRNADVPEMGDAINMKDTAKAIAKRFRSTFLNVDGEDCLRASM   350
DVMTKCLEYHKKWGKHMDLQGVNVAAETDLCRYQHMLKSDVKPVVTDTLH   400
LERAVAATITFHSKGVTSNFSPFFTACFEKLSLALKSRFIVPIGKISSLE   450
LKNVRLNNRYFLEADLSKFDKSQGELHLEFQREILLALGFPAPLTNWWSD   500
FHRDSYLSDPHAKVGMSVSFQRRTGDAFTYFGNTLVTMAMIAYASDLSDC   550
DCAIFSGDDSLIISKVKPVLDTDMFTSLFNMEIKVMDPSVPYVCSKFLVE   600
TEMGNLVSVPDPLREIQRLAKRKILRDEQMLRAHFVSFCDRMKFINQLDE   650
KMITTLCHFVYLKYGKEKPWIFEEVRAALAAFSLYSENFLRFSDCYCTEG   700
IRVYQMSDPVCKFKRTTEERKTDGDWFHNWKNPKFPGVLDKVYRTIGIYS   750
SDCSTKELPVKRIGRLHEALERESLKLANDRRTTQRLKKKVDDYATGRGG   800
LTSVDALLVKSHCETFKPSDLR                               850
```

C

```
.SS.T.........................S.................   50
.........................S.......................   100
.............................................S..S   150
............T.....................T.............   200
.....................................S.............   250
.........................................S......T..   300
..................................................   350
..................................................   400
.....................S............................   450
..................................................   500
.......S........S.S.........................S.....   550
..................................................   600
..................................................   650
.................................S................   700
..................................................   750
...S..............................................   800
```

Figure 4.2. Predicted phosphorylation sites in BMV 2a^{Pol}. (A) Schematic representation of the 822 aa BMV 2a^{Pol} protein. In A, B and C, the yellow box corresponds to the conserved polymerase-like domain of BMV 2a (~ aa 200-689). (B) BMV 2a^{Pol} amino acid sequence. (C) Potential phosphosites in BMV 2a^{Pol} as predicted by CBS YeastPhos 1.0 server at http://www.cbs.dtu.dk/services/NetPhosYeast/. See Fig. 4.3 and Table 4.1 for additional information about the 19 predicted phosphorylation sites.

Table 4.1 Summary of the 19 putative serine and threonine phosphorylation sites in BMV 2a^{Pol}.[a]

Site		Sequence	Score
163	T	VTGDTPKEL	0.900
421	S	TSNFSPFFT	0.785
508	S	DSYLSDPHA	0.740
2	S	---MSSKTW	0.705
33	S	VEAASLQVQ	0.672
150	S	ASDSSNCEI	0.671
683	S	LAAFSLYSE	0.670
185	T	QTTNTDYDI	0.647
76	S	VEAASLQVQ	0.640
298	T	RRVGTQKEV	0.628
147	S	VRWGSICDT	0.615
235	S	TEATSHSIL	0.612
519	S	GMSVSFQRR	0.570
754	S	SSDCSTKEL	0.550
545	S	IAYASDLSD	0.544
291	S	MNIGSAQRR	0.535
3	S	--MSSKTWD	0.532
517	S	KVGMSVSFQ	0.531
5	T	MSSKTWDDD	0.512

[a] As predicted using the CBS YeastPhos 1.0 server at http://www.cbs.dtu.dk/services/NetPhosYeast/.

score of 0.9 (Fig. 4.3 and Table 4.1). These results indicate that BMV 2a^{Pol} is likely a phosophoprotein.

4.2.2 BMV 2a^{Pol} is phosphorylated *in vivo*

To examine whether the 2a^{Pol} protein was phosphorylated *in vivo*, we used ^{32}P-labeling, a highly selective and sensitive technique for screening of protein phosphorylation (44, 216). Wt yeast cells co-expressing BMV 1a, 2a^{Pol} and RNA3 (e.g. RNA replication conditions) or expressing 2a^{Pol} only were grown in the presence of ^{32}P-orthophosphate for 6 or 12 hr. Yeast cells were lysed in buffer containing phosphatase inhibitors to minimize the unwanted removal of radio-labeled phosphate groups potentially attached to 2a^{Pol}. Protein A sepharose beads bound to anti-2a^{Pol} antibody were used to precipitate 2a^{Pol} and immunoprecipitates were eluted from protein A sepharose beads, analyzed by SDS-PAGE and ^{32}P signal was detected by phosphorimaging. In cells expressing 2a^{Pol} without other viral factors, a band corresponding to the molecular weight of 2a^{Pol} (~94 kDa) was detected at both time points (Fig. 4.4, lanes 3 and 4). However, in wt yeast cells replicating BMV RNA (Fig. 4.4, lanes 1 and 2), a ^{32}P signal was not detected at 6 or 12 hrs post-induction of virus expression in the presence of ^{32}P-orthophosphate. These data show that BMV 2a^{Pol} is phosphorylated *in vivo* and suggest that RNA replication may require a specific form of the viral polymerase.

4.2.3 Phosphatase treatment of 2a^{Pol} results in a detectable reduction of phosphate levels

To confirm and extend our *in vivo* ^{32}P-labeling results, we used the phosphospecific Pro-Q Diamond fluorescent stain to determine if 2a^{Pol} is phosphorylated in the absence or presence of calf intestinal phosphatase treatment (CIP), an enzyme that catalyzes the removal of phosphate groups from serine, threonine and tyrosine residues. Pro-Q Diamond stain allows direct, in-gel detection of phosphoamino acids and has been extensively used for phosphoprotein analyses in yeast, plant and mammalian cells (38, 43, 134, 141, 143, 166, 183).

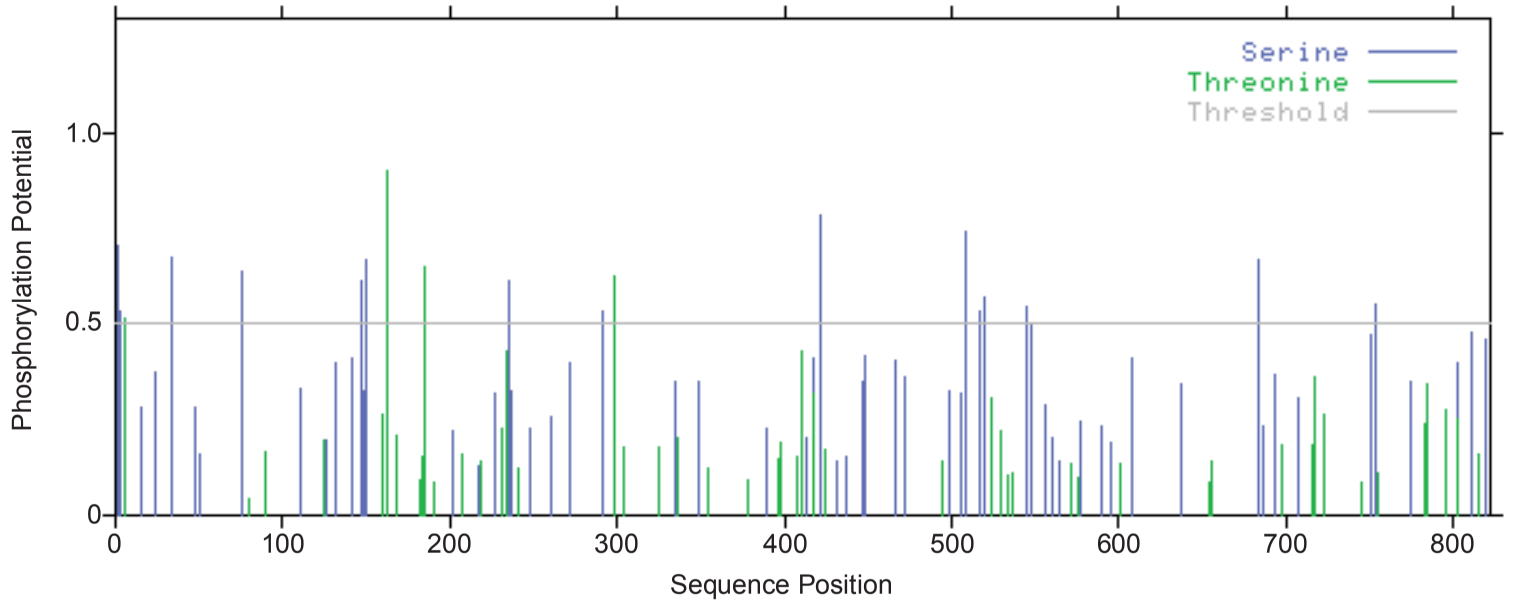

Figure 4.3. Graphic display of putatative serine and threonine phosphorylation sites in BMV 2a^{Pol}. Graphic output of the 19 predicted phosphorylation sites in BMV 2a^{Pol} as predicted by CBS YeastPhos 1.0 server at http://www.cbs.dtu.dk/services/NetPhosYeast/. A numeric score between 0 and 1, which represents phosphorylation potential, is plotted on the y-axis. When the score is above 0.5 (indicated by the grey threshold line) the residue is a predicted phosphorylation site.

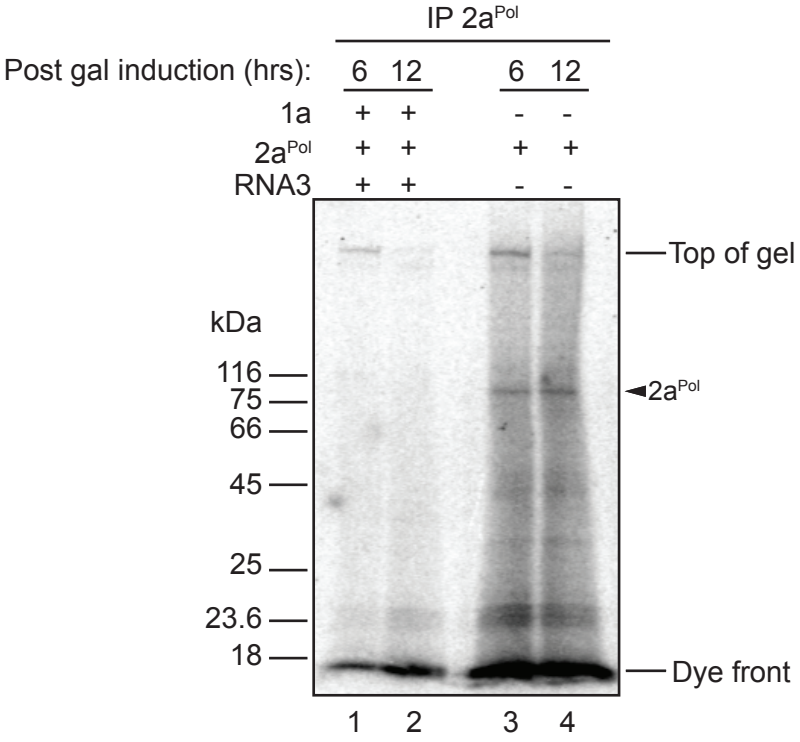

Figure 4.4. Phosphorimaging of SDS-PAGE shows ^{32}P-labeled BMV 2a^{Pol} as 94 kDa band. Wt yeast cells co-expressing BMV 1a, 2a^{Pol} and RNA3 or 2a^{Pol} only from *GAL1*-driven promoters were grown in the presence of ^{32}P-orthophosphate (10 μCi/ml) for 6 or 12 hrs post-galactose induction of viral components. Yeast cells were lysed and the cleared lysates were subjected to immunoprecipitation using an anti-2a^{Pol} antibody (IP 2a^{Pol}). The resulting immunoprecipitates were analyzed on an SDS-PAGE gel. ^{32}P signal was detected by phosphorimaging. Positions of molecular weight markers (kDa) are on the left. The position of 2a^{Pol} is designated with black arrowhead on the right.

$2a^{Pol}$ was purified from yeast whole cell lysates using immunoprecipitation (IP) as described above except that in this experiment, and all additional experiments, two antibodies that recognize different epitopes in $2a^{Pol}$ were used to increase the IP efficiency (validated by comparing the amount of $2a^{Pol}$ immunprecipitated by one vs. two antibodies using Western blotting, data not shown). As a negative control, a mock IP was performed on wt yeast cells lacking the $2a^{Pol}$ expression plasmid. After treating half of the eluted immunoprecipitates with CIP the samples were analyzed by SDS-PAGE and Pro-Q Diamond staining (Fig. 4.5A). A phosphospecific band was not detected in the mock IP sample (Fig. 4.5, lane 1), but $2a^{Pol}$ was positively stained (Fig. 4.5, lane 2) and this signal was a moderately, but reproducibly, reduced by CIP treatment (Fig. 4.5A, lane 3). The reduction in the phosphostaining signal observed is CIP treatment-specific, as confirmed by equivalent amounts of $2a^{Pol}$ in untreated and CIP-treated samples using SYPRO Ruby total protein gel stain (Fig. 4.5B, lanes 2 and 3). Further optimization of CIP treatment conditions and treatment with alternative phosphatases are being tested to seek a more substantial reduction in the $2a^{Pol}$ phosphospecific stain signal.

Since the residue with the highest phosphorylation potential, as predicted by the NetPhosYeast 1.0 server, was T163 (Figs. 4.2 and 4.3, Table 4.1), we next assessed if BMV $2a^{Pol}$ could be detected using a phosphothreonine-specific antibody. Wt yeast cells expressing $2a^{Pol}$, GFP-$2a^{Pol}$, an empty vector (negative control) or free GFP (negative control) were lysed and cleared lysates were subjected to IP using anti-$2a^{Pol}$ antibodies (Fig. 4.6A) or an anti-phosphothreonine (pThr) antibody (Fig. 4.6B). Immunoprecipitates were analyzed on SDS-PAGE. As shown in Fig. 4.6A (lanes 1, 2, 7-8), immunoblotting with an anti-$2a^{Pol}$ antibody recognized a single major band at ~94 kDa in cells expressing $2a^{Pol\ WT}$. In cells expressing GFP-$2a^{Pol}$, the anti-$2a^{Pol}$ antibody-reactive band shifted to a higher position, consistent with the expected molecular mass of the fusion protein (~124 kDa) (Fig. 4.6A, lanes 3 and 4) and confirming the derived pThr signal is from is $2a^{Pol}$ and not a cross-reacting band. As expected, a band was not detected in lysates from cells expressing an empty vector (Fig. 4.6A, lanes 5 and

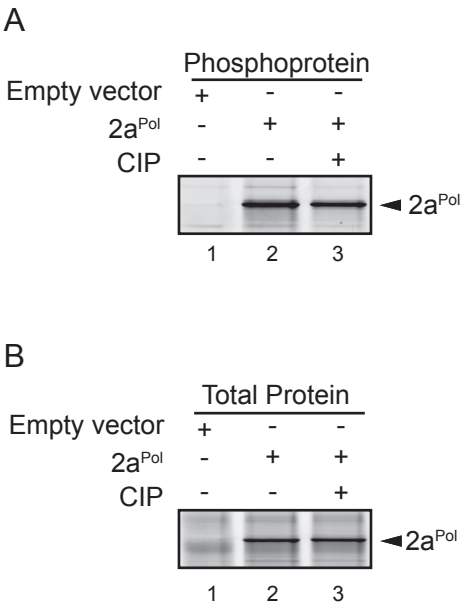

Figure 4.5. Phosphatase treatment of BMV 2a^{Pol} causes a detectable reduction in phosphorylation signal. Wt yeast cells expressing 2a^{Pol} or no plasmid (control) were lysed and the cleared lysates were subjected to immunoprecipitation using anti-2a^{Pol} antibodies. Half of the resulting immunoprecipitates were treated with calf intestinal phosphatase (CIP) (10U/sample) for 2 hrs at 37°C. Untreated and CIP-treated immunoprecipitates were analyzed by SDS-PAGE and the gel was stained with Pro-Q Diamond phosphoprotein gel stain (A) followed by SYPRO Ruby total protein gel stain (B). The position of 2a^{Pol} is designated with a black arrowhead on the right.

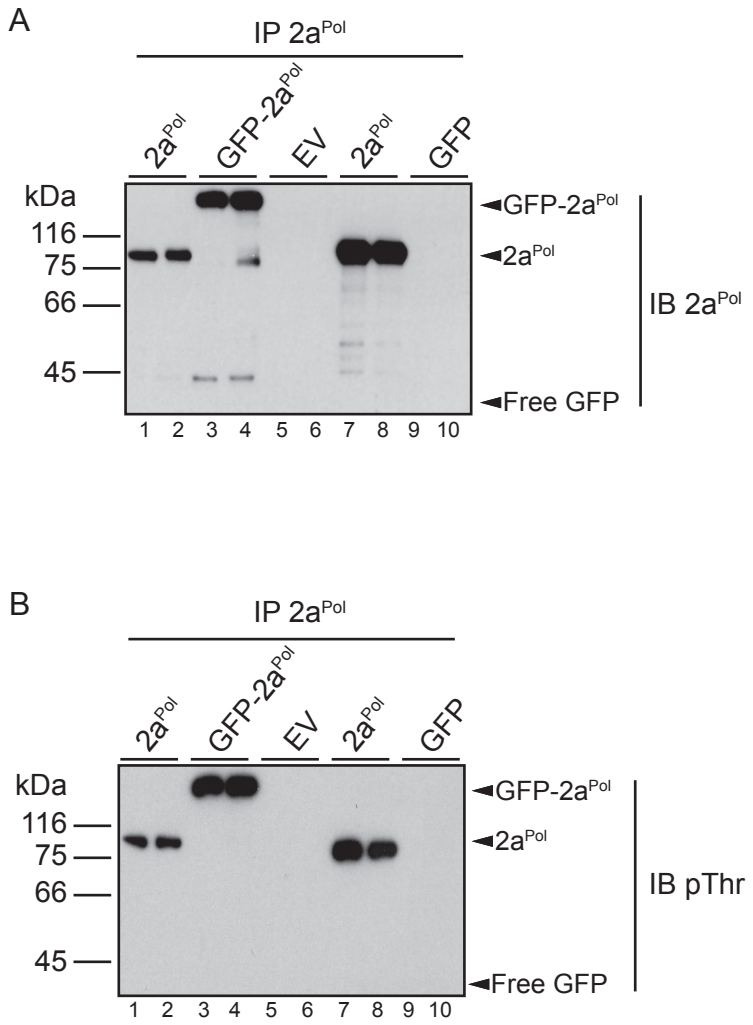

Figure 4.6. Detection of BMV 2a^{Pol} using a phosphothreonine-specific antibody. Wt yeast cells expressing 2a^{Pol}, GFP-2a^{Pol}, in which GFP was fused to the N-terminus of 2a, empty vector (EV) or free GFP (GFP). Yeast cells were lysed and the cleared lysates were subjected to immunoprecipitation using anti-2a^{Pol} (IP 2a^{Pol}) antibodies. The resulting immunoprecipitates were analyzed on SDS-PAGE and immunoblotted using anti-2a^{Pol} (IB 2a^{Pol}) (A) or anti-phosphothreonine (IB pThr) (B) antibodies. Positions of molecular weight markers (kDa) are on the left. The positions of 2a^{Pol}, GFP-2a^{Pol} and free GFP are designated with black arrow-heads on the right. As expected, free GFP was not detected in A or B as immunoprecipitation was performed with anti-2a^{Pol} and immunoblotting was performed with anti-2a^{Pol} or anti-pThr.

6) or free GFP (Fig. 4.6A, lanes 9 and 10). Similarly, after immunoprecipitating with anti-$2a^{Pol}$ antibodies, $2a^{Pol}$ and GFP-$2a^{Pol}$ were strongly detected with an anti-pThr antibody (Fig. 4.6B, lanes 1-4), but no signal was observed in lysates from yeast expressing an empty vector (Fig. 4.6B, lanes 5 and 6) or free GFP (Fig. 4.6B, lanes 9 and 10). These data demonstrate that BMV $2a^{Pol}$ is phosphorylated on a threonine residue(s), consistent with initial phosphosite server predictions (Figs. 4.2 and 4.3, Table 4.1).

4.2.4 T168 is essential for BMV RNA replication

Although $2a^{Pol}$ T163 had the highest phosphorylation potential score (Table 4.1), we took a broad initial approach and made triple alanine or aspartic acid substitutions of T160, T163 and T168, as neighboring residues can substantially influence kinase-substrate binding (28, 151, 210, 216) (Fig. 4.7A). Alanine substitution is the classical mutation used to abolish phosphorylation of an amino acid residue since alanine lacks the –OH group that acts as a phosphate acceptor site. Conversely, substituting aspartic acid, which is similar to phosphothreonine in structure and charge, can be an effective phosphomimetic. We used Pro-Q Diamond staining to determine if the triple amino acid substitutions affected $2a^{Pol}$ phosphorylation. $2a^{Pol\ WT}$, $2a^{Pol\ T160A,\ T163A,\ T168A}$ or $2a^{Pol\ T160D,\ T163D,\ T168D}$ were immunoprecipitated from wt yeast cells using anti-$2a^{Pol}$ antibodies and analyzed by SDS-PAGE and Pro-Q Diamond staining, as described above. A strong phosphospecific signal was detected in lysates from yeast expressing $2a^{Pol\ WT}$ (Fig. 4.7A, lanes 1-3) and this signal was reduced in lysates from yeast expressing the $2a^{Pol}$ triple alanine mutant (Fig. 4.7, lanes 4-6) or the $2a^{Pol}$ triple aspartic acid mutant (Fig. 4.7, lanes 7-9). The detected reduction in phosphorylation signal in the triple alanine mutant indicates that at least one of the mutated residues is a phosphorylated residue (phosphosite). However, since the signal was not completely diminished, additional $2a^{Pol}$ phosphosites likely exist, consistent with the 19 predicted phosphorylation sites (Figs. 4.2C and 4.2 and Table 4.1). The lower phosphostaining intensity observed in the triple aspartic acid

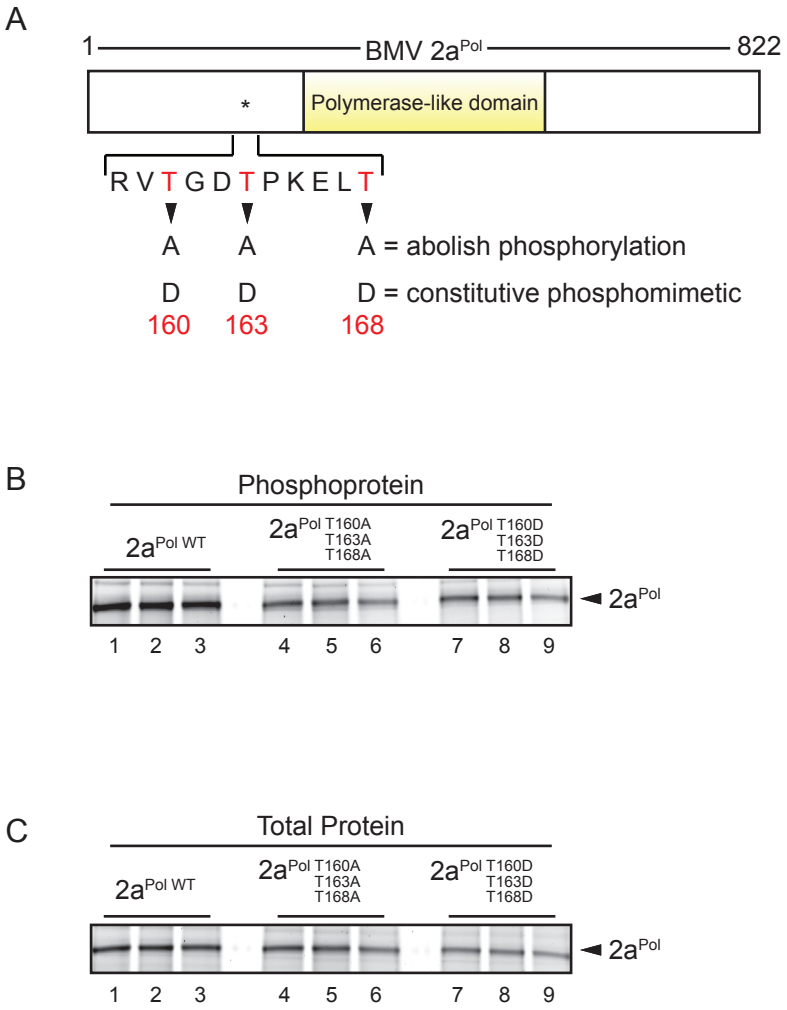

Figure 4.7. Mutating BMV 2a^{Pol} T160, T163 and T168 to alanine or aspartic acid results in decreased BMV 2a^{Pol} phosphorylation. (A) Schematic representation of BMV 2a^{Pol} with threonines (T) at positions 160, 163 and 168 in red. The asterisk (*) indicates T163 which is the residue with the highest probability of being phosporylated according to prediction software (see Figs. 4.2 and 4.3 and Table 4.1). (B) Triple alanine (A) or aspartic acid (D) subsititutions were made at T160, T163 and T168. Wt yeast cells expressing 2a$^{Pol\ WT}$ or the indicated 2a^{Pol} mutant were lysed and the cleared lysates were subjected to immunoprecipitation using anti-2a^{Pol} antibodies. Immunoprecipitates were analyzed by SDS-PAGE and the gel was stained with Pro-Q Diamond phosphoprotein gel stain (A) followed by SYPRO Ruby total protein gel stain (B). The position of 2a^{Pol} is designated with a black arrowhead on the right.

mutant is more difficult to interpret since there appears to be less total protein in these cell lysates compared to those collected from cells expressing $2a^{Pol\ WT}$, as indicated by SYPRO Ruby total protein staining (Fig. 4.7C, lanes 7-9 vs. lanes 1-3). While this result is consistent with these residues being phosphosites, the triple aspartic acid mutations may cause altered protein stability and thus be less informative than the alanine substitutions.

In yeast expressing BMV 1a and $2a^{Pol}$ proteins, DNA plasmids can be used to launch positive-strand RNA3 transcripts to provide RNA replication templates for synthesis of negative-strand RNA3, which in turn is copied to amplify levels of positive-strand RNA3 and to produce an additional RNA species, subgenomic RNA4 (92). Thus, the production of RNA4 is a true measure of viral RNA synthesis. To assess a potential role for $2a^{Pol}$ T160, T163 and/or T168 in BMV RNA replication, we assayed the accumulation of positive- and negative-strand RNA accumulation in wt yeast co-expressing 1a, RNA3 and $2a^{Pol\ WT}$, $2a^{Pol\ T160A,\ T163A,\ T168A}$ or $2a^{Pol\ T160D,\ T163D,\ T168D}$. As shown in Fig. 4.8A, wt yeast co-expressing 1a, RNA3 and $2a^{Pol\ WT}$ accumulated high levels of positive-stand RNA4 (lanes 1-3). However, positive-strand RNA4 accumulation was reduced to <1% of replication in yeast cells co-expressing 1a, RNA3 and either $2a^{Pol\ T160A,\ T163A,\ T168A}$ or $2a^{Pol\ T160D,\ T163D,\ T168D}$ (Fig. 4.8B, top panel, lanes 6-9). Negative-strand RNA3 synthesis was comparably inhibited by the $2a^{Pol}$ triple alanine mutations (Fig. 4.8B, middle panel, lanes 6-9). These results suggest that one or more of the mutated residues is critical for BMV RNA replication. To identify the specific threonine(s) that are important for viral RNA replication, T160, T163 and T168 were substituted to alanine individually or in pairwise combinations and assayed for positive-and negative-strand RNA accumulation in yeast cells co-expressing 1a and RNA3 and $2a^{Pol\ WT}$ or the specified $2a^{Pol}$ mutant (Fig. 4.8B). The $2a^{Pol}$ triple alanine mutant analyzed in Fig. 4.8A was included as a control. As shown in Fig. 4.8B, positive-strand RNA4 accumulated to wt levels in yeast expressing 1a, RNA3 and $2a^{Pol}$ mutants with single or double alanine substitutions at T160 or T163 (lanes 3-6 and 9-10 vs. lanes 1-2). However, in yeast expressing 1a, RNA3 and any $2a^{Pol}$ mutant containing an alanine substitution

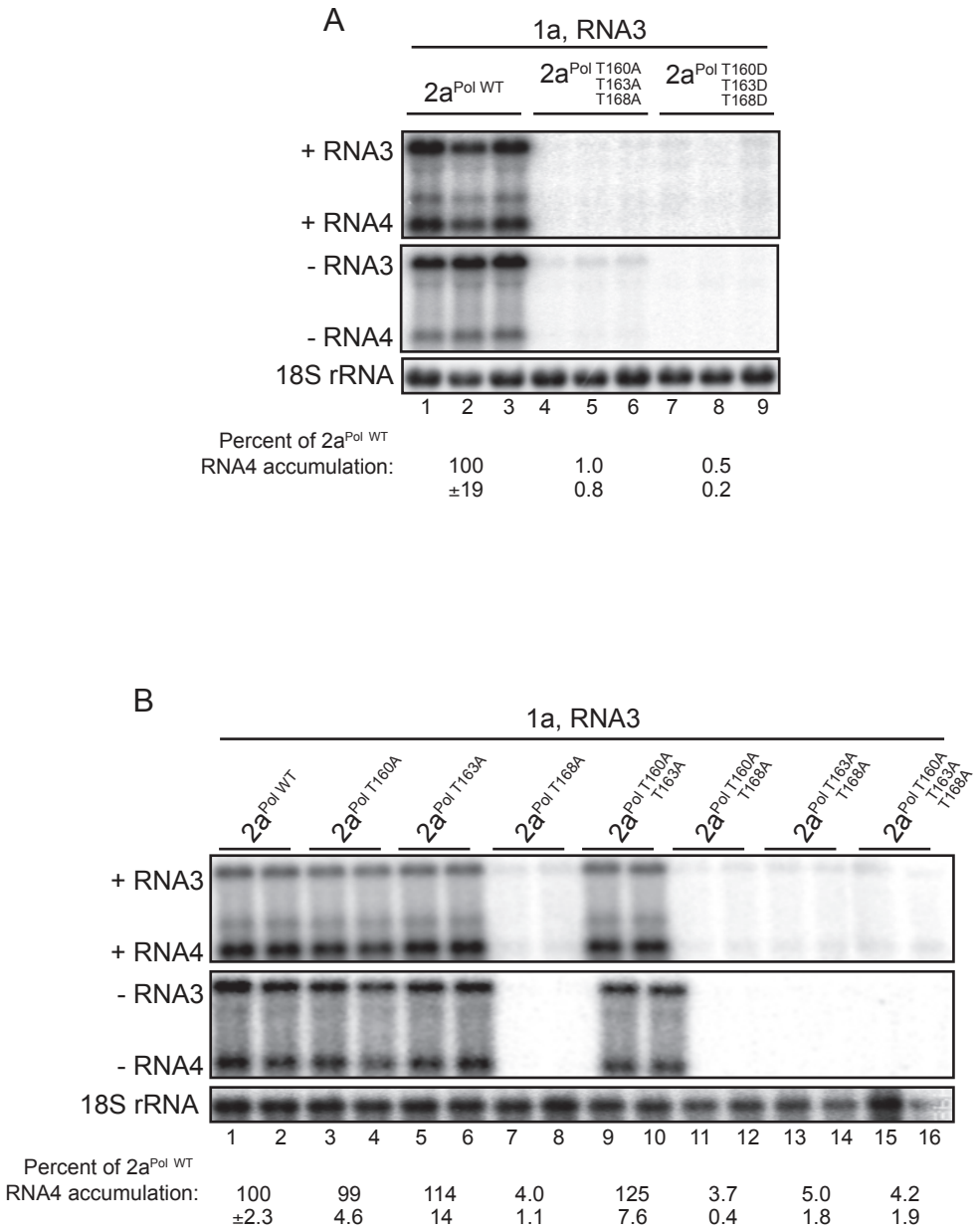

Figure 4.8. BMV RNA replication is inhibited by 2a^{Pol} T168A mutation. (A) Triple alanine (A) or aspartic acid (D) BMV 2a^{Pol} mutants. (B) BMV 2a^{Pol} T160, T163 and T168 were mutated individually or in combinations, as indicated above, to alanine (A). In A and B, BMV RNA accumulation in wt yeast co-expressing 1a, RNA3 and the indicated 2a^{Pol} mutant was analyzed. Total RNA was extracted from cells and RNA was detected by Northern blotting using a BMV RNA4-specific probe. Equal loading of total RNA was verified by probing for 18S rRNA.

at T168, positive-strand RNA4 accumulated to only ≤ 5% of replication levels in yeast expressing 1a, RNA3 and $2a^{Pol\ WT}$ and negative-strand RNA3 synthesis was also inhibited (Fig. 4.8B, lanes 7-8, 11-12 and 13-16 vs. 1-2). Taken together, our data suggests that T168 may be a critical phosphosite required for BMV RNA replication.

4.2.5 BMV RNA replication requires cyclin-dependent kinase Pho85

The data presented thus far indicates that BMV $2a^{Pol}$ is a phosphoprotein and that the threonine residue at position 168, which is a putative phosphosite, is critical for BMV RNA replication. To predict the putative kinase that may phosphorylate T168, we used the Scansite 2.0 *Motif Scan* program, which scans a vertebrate protein database of 65 conserved motifs and identifies short amino acid sequences that are phosphorylated by protein Ser/Thr- or Tyr-specific kinases, recognized by modular signaling domains, or mediate specific protein-protein or protein-phospholipid interactions (http://scansite.mit.edu/) (165). Using BMV $2a^{Pol}$ aa 155-175 as input sequence, *Motif Scan* predicted kinases Cdk1 and Cdk5, however, it should be noted that specificities of these kinases was predicted for T163. Both Cdk1 and Cdk5 are members of the mammalian cyclin dependent kinase (Cdk) family, which are key regulators of eukaryotic cell cycle progression (82, 194). In yeast, Cdk1 and Cdk5 are encoded by, Cdc28 and Pho85, respectively, which are homologous cyclin dependent kinases and share more than 50% of their sequence identity (81, 82, 212). Comparing the BMV $2a^{Pol}$ amino acid sequence in the T160/T163/T168 region to the Pho85 consensus sequence (S/T-P-X-I/L), revealed strong sequence similarities (Fig. 4.9A).

To determine if Pho85 is important for BMV RNA replication, we analyzed viral RNA accumulation in wt and *pho85*Δ cells expressing 1a, $2a^{Pol\ WT}$ and RNA3. As shown in Fig. 4.9B, positive-strand RNA3 and RNA4 accumulation was inhibited ~10-fold in *pho85*Δ cells compared to levels in wt yeast and the replication defect observed was completely complemented by

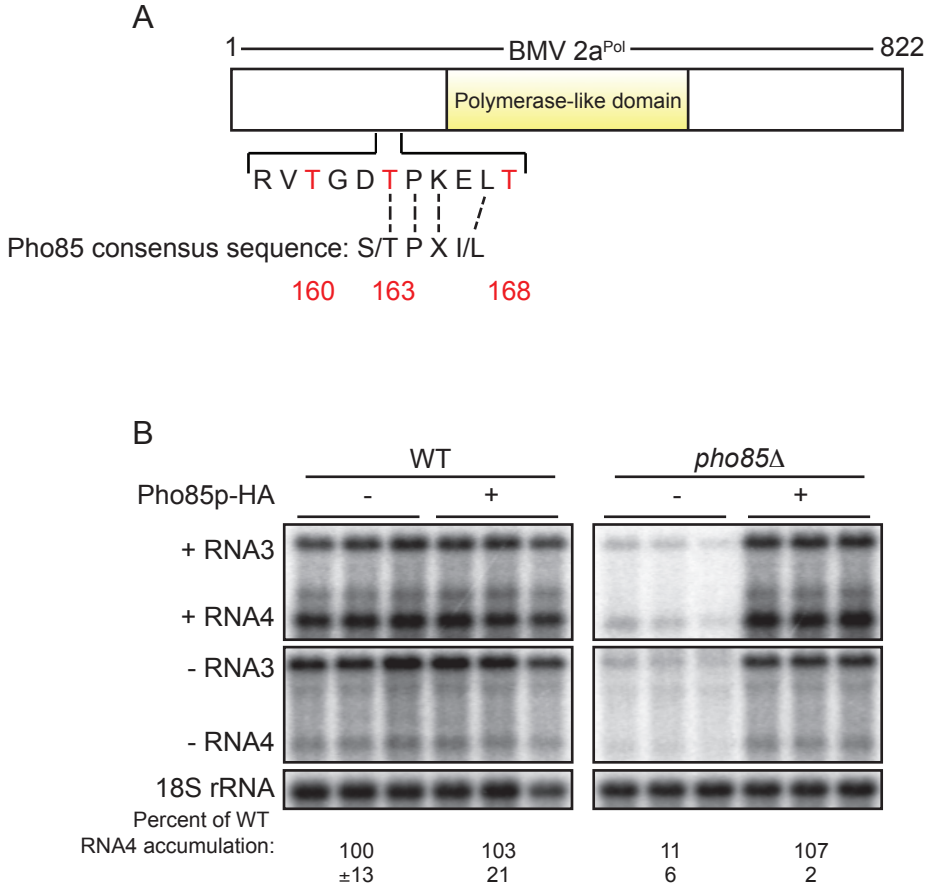

Figure 4.9. Pho85p is required for BMV RNA replication. (A) Schematic comparing the amino acid sequence containing BMV 2a^{Pol} T160, T163 and T168 to the Pho85 kinase consensus sequence for substrate recognition and phosphorylation (S/TPXI/L). (B) BMV RNA accumulation is inhibited in *pho85*Δ cells and the replication defect is complemented by Pho85p-HA.Total RNA was extracted from yeast co-expressing BMV 1a, 2a^{Pol} and RNA3 in the absence or presence of HA-Pho85p. BMV positive- and negative-strand RNAs were detected by Northern blotting using a BMV RNA4-specific probe. Equal loading of total RNA was verified by probing for 18S rRNA.

expressing Pho85p-HA. Importantly, these results show Pho85 is novel host gene required for BMV RNA replication.

4.2.6 BMV RNA replication is inhibited in cells lacking Pho85 cyclins Pcl6 or Pho80

The multifunctional Pho85 kinase interacts with 10 Pho85 cyclins (Pcls), which are grouped into two subfamilies based on sequence homology. The Pcl1,2 subfamily includes Pcl1, Pcl2, Pcl5, Pcl9 and Clg1 and primarily regulates cell cycle progression and morphogenesis (Fig. 4.10A). The Pho80 subfamily includes Pcl6, Pcl7, Pcl8, Pcl10 and Pho80 and is a key regulator of signaling environmental changes and metabolism (Fig. 4.10A). Since Pho85 association with different cyclins modulates distinct cellular processes (32, 81, 140), we assayed BMV RNA replication in Pcl deletion mutants as a means to determine if Pho85-regulated cellular functions are important for BMV RNA replication (Fig. 4.10A). Unfortunately, deletion mutants of Pcl5 and Pcl10 were not available in the yeast single-deletion mutant knockout library and thus were not analyzed here. In Pcl1,2 subfamily mutants *pcl1Δ*, *pcl2Δ*, *pcl9Δ* and *clg1Δ* and Pho80 subfamily mutants *pcl7Δ* and *pcl8Δ*, positive-strand RNA4 accumulated to wt levels or slightly higher (Fig. 4.10B). In cells lacking Pcl6 a modest 50% reduction in positive-strand RNA4 accumulation was observed compared to that in wt cells (Fig. 4.10B). However, *pho80Δ* cells exhibited a significant ~10-fold reduction in BMV RNA replication (Fig. 4.10B), indicating a more prominent role for Pcl Pho80 in BMV RNA replication. This reduction correlates with the 10-fold reduction in RNA replication observed in *pho85*Δ cells (Fig. 4.9B). Taken together, these data suggest that the Pho80-Pho85 cyclin-dependent kinase complex is primarily responsible for the *PHO85* effect on BMV RNA replication.

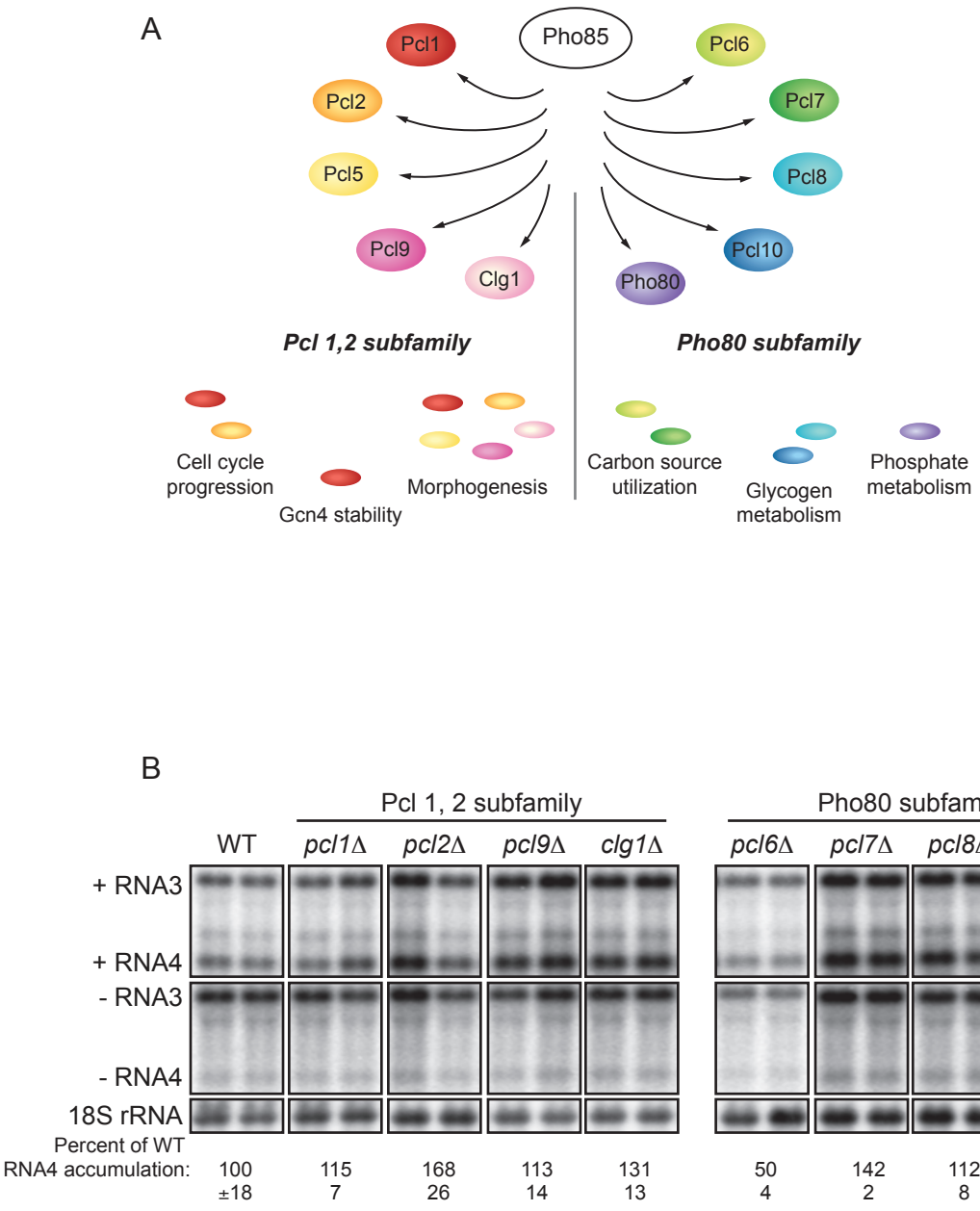

Figure 4.10. BMV RNA replication is inhibited in cells lacking Pho85 cyclins Pcl6 or Pho80. (A) The ten Pho85 cyclins (Pcls) and their functions. Cyclins belong to one of two subfamilies based on sequence homology. The lower graphics indicate cyclin-specific functions for members of the each subfamily. Adapted from Carroll, A.S. and O'Shea, E.K (32). (B) BMV RNA accumulation in WT yeast and Pcl yeast deletion mutants co-expressing BMV 1a, $2a^{Pol}$ and RNA3. Total RNA was extracted from cells and RNA was detected by Northern blotting using a BMV RNA4-specific probe. Equal loading of total RNA was verified by probing for 18S rRNA.

4.3 DISCUSSION

Accumulating evidence suggests protein phosphorylation controls multiple aspects of positive-strand RNA virus infection. However, the biological role of this post-translational modification remains unresolved for many viral nonstructural proteins (89). Here we investigate the role of phosphorylation in BMV RNA replication, with specific focus on the RNA-dependent RNA polymerase, $2a^{Pol}$. We combined phosphosite server predictions with biochemical and genetic approaches to demonstrate that BMV $2a^{Pol}$ is phosphorylated *in vivo* and reveal a critical role for T168 in viral RNA synthesis. Moreover, loss-of-function experiments identified novel interacting host factors required for BMV RNA replication, cyclin-dependent kinase Pho80-Pho85. Our data support a model in which the dynamic process of phosphorylation modulates $2a^{Pol}$ function(s). The possible mechanistic roles for this important signaling event in BMV RNA replication are discussed in detail below.

4.3.1 BMV $2a^{Pol}$ is a phosphoprotein

Multiple results, including ^{32}P-orthophosphate labeling (Fig. 4.2), Pro-Q Diamond phosphospecific staining (Fig. 4.5) and phosphatase treatment (Fig. 4.5) demonstrate that $2a^{Pol}$ is a phosphoprotein. Detection of $2a^{Pol}$ with a pThr-specific antibody (Fig. 4.6) was consistent with predictions that identified 19 putative phosphorylation sites in $2a^{Pol}$ and assigned the highest phosphorylation potential to T163, which is neighbored by T160 and T168 (Figs. 4.2-4.5 and Table 4.1). Triple alanine substitutions of T160, T163 and T168 decreased BMV $2a^{Pol}$ phosphorylation (Fig. 4.7B) and abolished BMV RNA replication (Fig. 4.8A), providing the first evidence that phosphorylation of $2a^{Pol}$ might be important for BMV RNA replication. The replication defect observed in the triple alanine mutant was mapped to a single critical residue, T168 (Fig. 4.8B). Although it is possible that the alanine substitution caused a conformational change within the viral polymerase that inhibited RNA replication, the observation that $2a^{Pol\ T160A}$ and $2a^{Pol\ T163A}$ were capable of RNA synthesis (Fig. 4.8B) suggest that the replication defect in

cells expressing $2a^{Pol\ T168A}$ is due to an inactive phosphosite. Collectively, our data are consistent with reports that phosphorylation of positive-strand RNA virus polymerase proteins, including cucumber mosaic virus 2a (111), Dengue virus NS5 (106) and hepatitis C virus NS5B (86, 112), among others, regulates the multiple coordinated events of viral RNA replication.

4.3.2 The Pho80-Pho85 complex is critical for BMV RNA replication

Protein phosphorylation is regulated by the catalytic action of kinases, which transfer the γ-phosphate from ATP to serine, threonine and tyrosine residues. Analysis of the amino acids surrounding $2a^{Pol}$ residue T168, which is required for RNA replication, revealed sequence similarity to the consensus motif of Pho85, a multifunctional cyclin-dependent kinase regulated by 10 cyclins, which determine the substrate specificity of Pho85 (Figs. 4.7A and 4.10A) (32, 81). A direct link between the Pho85 and BMV RNA replication was demonstrated by the ability of Pho85p to complement the 10-fold inhibition of RNA accumulation observed in *pho85Δ* cells (Fig. 4.9B). Moreover, deleting Pho85 cyclin partner Pho80 also exhibited a 10-fold defect in RNA replication (Fig. 4.10B). The dependence of BMV on the Pho80-Pho85 complex could be due to the catalytic action of Pho80-Pho85 on BMV components, or to the role of this specific cyclin-cdk complex in phosphate metabolism and/or calcium signaling (81) and the effects of these pathways on viral replication. The primary downstream effectors of Pho80-Pho85 in phosphate metabolism and calcium signaling are *PHO4* and *CRZ1*, respectively, and deleting either of these genes had no effect on BMV RNA replication (119). Collectively, these data suggest that the Pho80-Pho85 kinase activity is required for BMV RNA replication.

4.4.3 Possible role(s) of phosphorylation in BMV RNA replication

Although we currently lack direct proof that Pho80-Pho85 is the kinase that phosphorylates T168, the combination of genetic evidence and the near-exact Pho85 consensus sequence in this region strongly support this hypothesis. While awaiting confirmation

of a link between cdk Pho85 and the phosphorylation state of $2a^{Pol}$ T168, it is valuable to consider the possible role(s) of phosphorylation in BMV RNA replication. An initial step of RNA replication is the localization of replication proteins 1a and $2a^{Pol}$ to perinuclear ER membranes, which are sites of RNA replication complex formation and subsequent viral RNA synthesis (123, 189, 190, 196). 1a-dependent ER localization of $2a^{Pol}$ requires N-proximal sequences within the first 120 amino acids of the viral polymerase (36). Given the close proximity of T168 to these critical 1a-$2a^{Pol}$ binding domains, an attractive model is that phosphorylation at this residue acts as a temporal switch to modulate 1a-$2a^{Pol}$ interaction and subsequent recruitment of $2a^{Pol}$ to membrane-associated replication compartments, a scenario that is consistent with the role of phosphorylation in regulating the subcellular localization of proteins (24). Additionally, studies in cucumber mosaic virus (CMV), a close relative to BMV, revealed phosphorylation of the CMV 1a-interacting N-terminal 126 amino acid region of CMV 2a polymerase inhibited interaction between CMV 1a and 2a. Similarly, Dengue virus replication protein NS3 preferentially interacts with the *hypo*phosphorylated form of RdRp NS5 (106). These data indicate that regulation of viral protein interactions by phosphorylation might be a conserved regulatory mechanism employed by multiple positive-strand RNA viruses.

Alternatively, since T168 is adjacent to the polymerase-like core domain (~aa 200-689), phosphorylation of this residue may regulate catalytic activity of the viral polymerase, which is required for RNA synthesis. Since positive-strand RNA virus genomes are templates for both translation and replication, such a model would support the observation that coordinated switching between translation and the recruitment of viral genomes to the replication complex is essential for efficient RNA replication (161, 162).

Phosphorylation is a key reversible protein modification that regulates enzymatic activity, subcellular localization, complex formation and protein degradation. Positive-strand RNA virus replication is a complex, multi-step process requiring coordinated interactions between the viral genome, virus-encoded replication proteins and host factors (7, 159). As such, it is plausible

that $2a^{Pol}$ cycles through different phosphorylation states to regulate multiple steps of RNA replication. Not surprisingly, emerging results highlight crucial roles for phosphorylation in nearly every step of positive-strand RNA virus replication, including viral protein-protein and protein/RNA interaction (106, 111, 200), stability of replication proteins (77, 177) and catalytic activation of RdRps (90, 111, 112) among others. The conserved features of positive-strand RNA virus replication combined with the dependence of many viruses in this class on phosphorylation makes cellular kinases, the driving forces of this host signaling pathway, appealing targets for the development of antivirals.

4.4 MATERIALS AND METHODS

4.4.1 Yeast strains and cell growth

BY4743 (*MAT*a/α *his3*Δ*1/his3*Δ*1 leu2*Δ*0/leu2*Δ*0 LYS2/lys2*Δ*0 met15*Δ*0/MET15 ura3*Δ*0/ura3*Δ*0)* and its single-gene deletion derivatives were used for Pho85 and Pcl analysis. YPH500 (*MATα ura3–52 lys2–801 ade2–101 trp1-Δ63 his3-Δ200 leu2-Δ1*) was used for all other experiments. The lithium acetate-polyethylene glycol (PEG) method was used to transform plasmids into yeast strains (58). Yeast strains containing BMV expression plasmids were grown overnight at 30°C in synthetic medium containing 2% glucose as a carbon source, subcultured to a starting starting OD_{600}=0.08-0.2 in medium containing 2% galactose as a carbon source. Cells were grown for 2 passages (36 to 48 hr) and harvested when the OD_{600} was between 0.4-1.0. Depending on the assay, leucine, hisitidine, uracil or combinations thereof were omitted to maintain plasmid selection.

For ^{32}P-labeling experiments, cells were grown overnight at 30°C in synthetic medium containing 2% glucose as a carbon source, subcultured to a starting starting OD_{600}=0.2 in medium containing 2% galactose as a carbon source in the presence or absence of 10 μCi/ml

^{32}P-orthophosphate (NEX053001MC; Perkin Elmer, Waltham, MA) at 30°C with shaking. Cells were harvested after 6 or 12 hrs of growth in the presence or absence of ^{32}P-orthophosphate. Leucine was omitted to maintain plasmid selection.

4.4.2 Plasmids and plasmid construction

BMV 2a^{Pol} and GFP-2a^{Pol}, both under the control of a *GAL1* promoter, were expressed from pB2YT5 and pB2YT5-G2, respectively (36, 206). To express BMV 1a and 2a^{Pol} for assaying BMV RNA replication, pB12AON3 was used which expresses 1a and 2a^{Pol}, each under the control of an *ADH1* promoter. *CUP1* promoter-driven BMV RNA3 was launched from pB3VG128-H in medium lacking copper from. pB12VG128-H expresses a BMV RNA3 derivative in which the coat protein gene has a four-nucleotide insertion and a point substitution, abolishing expression of the coat protein (12), allowing analysis of RNA3 and RNA4 levels while avoiding any effects of possible variations in coat protein expression and RNA encapsidation (52, 226, 243). Alanine and aspartic acid substitutions of T160, T163 and/or T168 were introduced into the BMV 2a^{Pol} coding sequence by PCR-based site-directed mutagenesis (78). PCR fragments with each of these mutations were digested with NcoI and PacI and cloned into pB2YT5 to replace the corresponding wt fragments. After cloning, all of the fragments were sequenced to confirm the presence of intended substitutions and absence of unintended mutations.

4.4.3 Immunoprecipitation and Western blotting

Yeast cells were grown to an OD_{600} of 0.4-1.0 and 5 OD_{600} units of cells were harvested. Cells were lysed in RIPA buffer (1% NP-40, 0.1% SDS, 50 mM Tris pH 8.0, 150 mM NaCl, 0.5% Sodium deoxycholate, 5 mM EDTA, 10 mM NaF, 10 mM NaPPi, 2 mM phenylmethylsulfonyl, 5mM benzamidine, and 10 ug/ml each of chymostatin, pepstatin A, leupeptin, bestatin) using glass beads and a bead beater and the supernatant was collected after centrifugation. With the

exception of experiments evaluating CIP treatment, 3x HALT™ Phosphatase Inhibitor Cocktail (78420; Thermo Scientific, Rockford, IL) was added to RIPA buffer. For immunoprecipitation, yeast lysates were mixed with Protein A Sepharose beads (17-0780-01; GE Healthcare. Piscataway, NJ) and anti-$2a^{Pol}$ mouse monoclonal antibodies 13E2G6 and O5H5B2 (each at a 1:100 dilution) overnight at 4°C. Beads were pelleted and washed with RIPA buffer before boiling in 1x SDS gel loading buffer. Equal volumes of immunoprecipitates were separated on 4-15% Criterion™ TGX™ precast polyacrylamide gels (Bio-Rad, Hercules, CA). Proteins were transferred to PVDF membrane, which were blocked for 1 hr with non-fat dry milk (5% in TBS containing 0.1% Tween 20) prior to antibody incubation. Expression of target proteins was detected by incubating membranes with the following antibodies and dilutions: mouse anti-BMV $2a^{Pol}$ O5H5B2 at 1:3,000, mouse anti-phosphothreonine (13-9200; Life Technologies, Grand Island, NY) at 1:500 using HRP-conjugated secondary antibodies (Thermo Scientific, Rockford, IL) and Supersignal West Femto substrate (Thermo Scientific, Rockford, IL). Chemiluminescence was detected with a Bio-Rad ChemiDoc™ XRS (Bio-Rad, Hercules, CA).

4.4.4 ProQ-Diamond and SYPRO Ruby gel staining

Yeast cells were grown to an OD_{600} of 0.4-1.0 and 5 OD_{600} units of cells were harvested. Cells were lysed in RIPA buffer (1% NP-40, 0.1% SDS, 50 mM Tris pH 8.0, 150 mM NaCl, 0.5% Sodium deoxycholate, 5 mM EDTA, 10 mM NaF, 10 mM NaPPi, 2 mM phenylmethylsulfonyl, 5mM benzamidine, and 10 ug/ml each of chymostatin, pepstatin A, leupeptin, bestatin) containing 3x HALT™ Phosphatase Inhibitor Cocktail (78420; Thermo Scientific, Waltham MA) using glass beads and a bead beater and the supernatant was collected after centrifugation. Yeast lysates were mixed with Protein A Sepharose beads (17-0780-01; GE Healthcare. Piscataway, NJ) and anti-$2a^{Pol}$ mouse monoclonal antibodies 13E2G6 and O5H5B2 (each at a 1:100 dilution) overnight at 4°C. Beads were pelleted and washed with RIPA buffer before boiling in 1x SDS gel loading buffer. Equal volumes of immunoprecipitates were separated on 4-

15% Criterion™ TGX™ precast polyacrylamide gels (Bio-Rad, Hercules, CA). Pro-Q® Diamond phosphoprotein gel stain (P-33300; Life Technologies, Grand Island, NY) and SYPRO® Ruby total protein gel stain (S-12000; Life Technologies, Grand Island, NY) were used according to manufacturer's instructions. Briefly, following SDS-PAGE, gels were fixed with 50% methanol and 10% acetic acid (v/v) for 1 hour. The residual methanol and acetic acid was removed by washing with 50 ml ultra pure water for 10 min with gentle agitation. After repeating the wash a total of three times, gels were incubated with 50 ml of Pro-Q® Diamond phophoprotein gel stain for 1 hr in the dark, with gentle agitation. To reduce background and non-specific staining, the gel was incubated with destaining solution [20% acetonitrile (v/v), 50 mM NaOAc] for 30 min and this step was repeated two additional times for a total destaining time of 90 min. Destained gels were washed with 50 ml ultra pure water for 5 min and this step was repeated once for a total of two washes. Fluorescent phosphospecific staining was detected on a Bio-Rad FX scanner using the following scan settings: 532 nm excitation, 555 nm longpass, 532 band length. Immediately after scanning, the gel was incubated in 60 ml SYPRO® Ruby total protein gel stain overnight and washed for 30 min with 10% methanol and 7% acetic acid (v/v). Total protein fluorescence was imaged on Bio-Rad FX scanner using the following scan settings: 532 nm excitation, 555 nm longpass, 1064 band length).

4.4.5 RNA extraction and analysis

Total RNA was isolated from yeast cells using acidic hot phenol and ethanol precipitation as described elsewhere (125). Northern blotting was performed as previously described (131) except that 2 µg of RNA total per sample was separated in 1% (wt/vol) agarose-MOPS (morpholinepropanesulfonic acid)-formaldehyde gels. BMV RNAs were detected using ^{32}P-labeled probes specific for positive- or negative-strand BMV RNA3 and RNA4 as previously described (124). The 18S rRNA probe was derived from pTRI RNA 18S templates (Ambion, Austin, TX). Probes were synthesized using an Epicenter Riboscribe probe synthesis kit

(Madison, WI) with the appropriate enzyme, i.e., T7 or or SP6 polymerase. Northern blots were imaged on a Typhoon 9200 instrument (Amersham Biosciences, Piscataway, NJ) and band intensities were analyzed with ImageQuant software (Molecular Dynamics, Piscataway, NJ).

Chapter 5

CONCLUSIONS AND FUTURE DIRECTIONS

Among the six different virus classes, positive-strand RNA viruses encompass over one third of all virus genera and include important human pathogens such as the SARS coronavirus, West Nile virus and hepatitis C virus, which chronically infects an estimated 130-170 million people worldwide (http://www.who.int/en/). Despite the significance of this virus class and its impact on human health, few vaccine treatments exist and alternative antiviral treatments are limited. To understand how positive-strand RNA viruses cause disease, it is critical to identify the host factors and pathways exploited in virus replication and characterize the nature of their contributions and interactions with virus-encoded replication factors. Previously, our laboratory screened a single-gene deletion library of non-essential yeast genes and identified ~100 genes whose loss affected RNA replication of a positive-strand RNA virus, brome mosaic virus (BMV) (119). However, classical yeast genetics and other approaches have demonstrated that genes essential for cell growth also modulate BMV (123, 124, 162, 213). To this end, the work in this thesis focused on identifying additional essential host genes required for BMV RNA replication, combining our results with previous analyses of host genes important for BMV (119) to reveal cellular pathways that modulate virus infection and characterizing these critical cellular components to understand their mechanistic contributions to viral RNA synthesis.

In Chapter 2 we employed a systematic, genome-wide approach to identify 24 novel, essential host genes from diverse cellular pathways that alter BMV RNA replication (68). In Chapter 3 we used microscopy combined with genetic and biochemical approaches to reveal that the highly conserved ubiquitin-proteasome system contributes to BMV RNA replication in multiple, mechanistically distinct ways (manuscript in preparation) and validated the necessity of

the UPS in natural plant hosts. In Chapter 4 we used biochemical and genetic approaches to provide the first evidence that BMV $2a^{Pol}$ is a phosphoprotein and map a critical phosphosite in the viral polymerase. Additionally, through sequence analysis and software predictions, we identified a novel host gene required for BMV RNA replication, cyclin dependent kinase Pho85. Lastly, in Appendix A, through collaboration with Deborah Chasman and Mark Craven, we utilized bioinformatics to reveal the broader interaction networks for host genes utilized by BMV. The work presented here provides a strong foundation for future experiments, which are explored below.

5.1. REFINE THE MECHANISTIC CONTRIBUTIONS OF THE UPS TO BMV RNA REPLICATION

Our results in Chapter 2 combined with results from a previous study revealed that ~10% of the 123 genes that altered BMV RNA replication are members of the ubiquitin-proteasome system (UPS) (Tables 3.1 and 3.2) (68, 119). These UPS genes, whose loss inhibited BMV RNA replication ~6- to 100-fold, are components of the 20S core (*PRE1, PRE9*), 19S regulatory particle (*SEM1, RPT6*) and accessory proteins (*UBR1, UBP6, UMP1, UFD4, UFD5*). In Chapter 3, we performed a detailed analysis to dissect the mechanistic role(s) of the UPS genes implicated in BMV RNA replication. UPS-dependent activation of lipid synthesis is required for BMV RNA replication (123, 124, 226), but lipid feeding only restored BMV replication defects in mutant *PRE1*, revealing that the remaining mutants contribute to BMV RNA replication through lipid-*independent*, UPS-dependent mechanisms. In UPS mutants *UBP6, UBR1, PRE9, UFD4, and UFD5*, BMV RNA replication defects were complemented by exogenous expression of ubiquitin, demonstrating that processes highly sensitive to ubiquitin concentration are important for BMV RNA replication. For *SEM1* and *UMP1*, BMV RNA replication defects were not

complemented by lipids or ubiquitin, showing that these genes contribute to RNA replication in ways different from the prior two classes. Collectively, our studies revealed that the UPS contributes to viral RNA replication in at least three mechanistically distinct ways: (i) UPS-dependent activation of lipid synthesis genes; (ii) UPS-dependent processes complementable by ubiquitin; and (iii) UPS-dependent processes not complementable by lipids or ubiquitin (Table 3.3). Although our data provide mechanistic insights into the roles of the UPS in BMV RNA replication, additional studies are required to further refine these contributions.

5.1.1 UPS-2a^{Pol} interactions

An initial step of RNA replication is the 1a-dependent localization of 2a^{Pol} to perinuclear ER membranes, which are sites of RNA replication complex formation and subsequent viral RNA synthesis (123, 189, 190, 196). Disruption of multiple UPS genes dramatically affected the accumulation and/or localization of 2a^{Pol}, but had only minimal effects on the 1a protein. Thus, it is important to evaluate if the UPS components analyzed in this work modulate BMV RNA replication through direct interactions with the viral polymerase. Co-immunoprecipitation experiments and/or mass spectrometry would be useful approaches in assessing interactions between UPS gene products and 2a^{Pol}. These techniques can also be used to determine if 2a^{Pol} is ubiquitinated, a post-translational modification that can dictate the activity and/or localization of client proteins and thus may regulate 2a^{Pol} localization. To determine if 2a^{Pol} colocalizes with UPS components, UPS proteins could be tagged (e.g. GFP, FLAG, etc.), co-expressed with 2a^{Pol} and analyzed by confocal laser microscopy. Additionally, co-immunoprecipitation experiments would also reveal if 1a-2a^{Pol} interactions, which are necessary for ER localization of 2a^{Pol}, are disrupted in UPS mutants.

5.1.2. UPS effects on RNA3 stabilization

In wt cells, expressing 1a increases the half-life of BMV genomic RNA3 from ~5 min without 1a to > 3hr in the presence of 1a (91) and stimulates an 8- to 30-fold increase in RNA3 accumulation, depending on the level of 1a expression (196). This 1a-dependent increase in RNA3 accumulation *in vivo* is associated with 1a-mediated transfer of RNA3 to a membrane-associated state, which represents its localization to spherular RNA replication complexes formed on the perinuclear ER membrane (196). A striking observation in some UPS mutants was the stabilization of RNA3 in the *absence* of 1a. It is possible that 20S proteasome RNAase activity, which has specificity for viral RNAs (94, 178), may be disrupted, a model that seems most likely for mutant *PRE9*, which is a component of the 20S core proteasome. To evaluate this possibility, RNA3 decay assays can be performed. Assaying the stability of cellular mRNAs (e.g. actin, GAPDH, globin, etc.) will be critical controls for demonstrating that the 1a-independent RNA3 stabilization observed is virus-specific. Disrupting the UPS may also cause mislocalization of RNA3 in the absence of 1a. Cell fractionation assays would be useful to definitively determine the subcellular localization of the 1a-independently stabilized RNA3 in UPS mutants *UBR1*, *PRE9*, *UFD4* and *UFD5* compared to that in wt cells.

5.2. PHOSPHORYLATION AND BMV RNA REPLICATION

Viral RNA-dependent RNA polymerases, in concert with other viral and host factors, perform multiple roles in RNA replication including localizing to the sites of RNA replication, assembling the replication complex and initiating and maintaining RNA synthesis. Since phosphorylation of target proteins functions as a molecular switch to induce rapid changes in protein function, localization and/or stability (24, 107, 179, 216) we investigated if BMV RNA replication might be modulated through $2a^{Pol}$ phosphorylation. Indeed, in Chapter 4 we showed that BMV $2a^{Pol}$ is phosphorylated *in vivo* when expressed independently of 1a and RNA3,

suggesting that RNA replication may require a specific form of the viral polymerase. Additionally, we revealed that cyclin-dependent kinase Pho85 and its cyclin partner Pho80 are required for BMV RNA replication. Our results show that phosphorylation is critical for BMV and provide a foundation for future experiments to assess its functional importance during viral RNA replication, which are discussed below.

5.2.1 Map additional $2a^{Pol}$ phosphorylation sites

Although we demonstrated that T168 is a critical phosphosite in the RNA-dependent RNA polymerase, prediction software identified 19 putative phosphosites in $2a^{Pol}$ independent of T168, indicating additional phosphosites likely exist. Mass spectrometry (MS) has been extensively used to analyze the post-translation modifications of proteins (100, 144, 150, 179, 242) and is the most rigorous method that can be used to identify additional putative phosphosites in $2a^{Pol}$. In collaboration with Robert Pugh, a post-doc in our laboratory with extensive protein purification experience, $2a^{Pol}$ will be expressed, purified and analyzed by mass spectrometry. Careful consideration must be given to the type of mass spectrometry used since post-translational modifications such as phosphorylation are labile and preferentially lost during peptide backbone fragmentation. Mass spectrometry methods incorporating electron-transfer dissociation (ETD) or electron-capture dissociation (ECD), techniques that preserve labile post-translational modifications, are well-established approaches for analyzing phosphoproteins (144, 242). Once phosphorylated residues are identified, mutants containing single alanine or aspartic acid substitutions of phosphosite residues can be analyzed in the context of BMV RNA replication to identify residues important for modulating viral RNA synthesis.

5.2.2 Determine if Pho85 kinase activity is required for BMV RNA replication

Loss-of-function experiments showed that cyclin-dependent kinase and its cyclin partner Pho80 are required for BMV RNA replication. Analysis of the amino acids surrounding $2a^{Pol}$

residue T168, a phosphosite required for RNA replication, revealed sequence similarity to the consensus motif of Pho85, implying that the Pho80-Pho85 kinase directly acts on BMV components. To determine if the Pho80-Pho85 kinase activity is required for RNA replication, BMV RNA replication can be analyzed in *pho85Δ* cells co-expressing 1a, $2a^{Pol}$, RNA3 and a Pho85 kinase inactive mutant ($pPho85^{KI}$) or wt Pho85 ($pPho85^{WT}$). If Pho85 kinase activity is required for BMV RNA replication, *pho85Δ* cells expressing BMV components and $pPho85^{KI}$ will exhibit inhibited BMV RNA replication compared to *pho85Δ* cells expressing BMV components and $pPho85^{WT}$, as we showed $pPho85^{WT}$ was able to complement the BMV RNA replication defect observed in *pho85Δ* cells. Wt cells expressing 1a, $2a^{Pol}$, RNA3 and $pPho85^{KI}$ or $pPho85^{WT}$ can be analyzed as a control. Since endogenous Pho85 is present in wt cells, RNA replication accumulation should not be affected by the presence of $Pho85^{WT}$ (demonstrated in Chapter 4) or $pPho85^{KI}$.

5.2.3 Determine if Pho85 phosphorylates $2a^{Pol}$ T168

Although our genetic studies demonstrated that T168 is a critical residue for BMV RNA replication, we currently lack direct proof that T168 is phosphorylated or that Pho80-Pho85 is the kinase that phosphorylates this site. We can determine if Pho85 phosphorylates T168 using gain-of-function experiments. For this approach, GFP- $2a^{Pol\ WT}$ and GFP-$2a^{Pol\ T168A}$ fusions would be generated and the phosphorylation state of $2a^{Pol}$ in wt and *pho85Δ* cells expressing these constructs would be analyzed by immunoprecipitation and subsequent immunoblotting with anti-phosphothreonine or by phosphoprotein specific gel staining. If Pho85 is the kinase required for phosphorylation of T168, a decrease in phosphothreonine signal should be observed in lysates from *pho85Δ* cells expressing GFP-$2a^{Pol\ T168A}$. GFP, which is not phosphorylated, serves as a negative control for these experiments. A caveat to this approach is that additional threonine phosphosites in $2a^{Pol}$ may preclude a detectable reduction in the phosphorylation signal from the phosphothreonine antibody and/or the phosphospecific stain. In this case, the same

experiment could be performed using N-terminal fragments of $2a^{Pol\ WT}$ or $2a^{Pol\ T168A}$ to minimize interfering signals from other phosphothreonine residues. Alternatively, purified full-length $2a^{Pol}$/$2a^{Pol\ T168A}$ or $2a^{Pol}$/$2a^{Pol\ T168A}$ fragments can be tested for *in vitro* phosphorylation by Pho85.

5.2.4 Determine RNA replication steps modulated by Pho85

An initial step of RNA replication is the localization of replication proteins 1a and $2a^{Pol}$ to perinuclear ER membranes, which are sites of RNA replication complex formation and subsequent viral RNA synthesis (123, 189, 190, 196). 1a-dependent ER localization of $2a^{Pol}$ requires N-proximal 1a-interacting sequences within the first 120 amino acids of the viral polymerase (36). Northern blotting revealed that positive-strand and negative-strand RNA synthesis were substantially inhibited in cells expressing $2a^{Pol\ T168A}$, however we do not know if earlier replication steps are affected by this mutation. Given the close proximity of T168 to these critical 1a-$2a^{Pol}$ binding domains, an attractive model is that phosphorylation at this residue acts as a temporal switch to modulate 1a-$2a^{Pol}$ interaction and subsequent recruitment of $2a^{Pol}$ to membrane-associated replication compartments, a scenario that is consistent with the role of phosphorylation in regulating the subcellular localization of proteins (24). To test this, $2a^{Pol\ WT}$ or $2a^{Pol\ T168A}$ can be fused to a polypeptide protein tag (e.g. FLAG, HIS, etc) and co-immunoprecipitations of lysates from yeast co-expressing 1a and $2a^{Pol\ WT}$ or $2a^{Pol\ T168A}$ can be performed to analyze 1a-2a interactions. If phosphorylation of T168 is important for 1a-$2a^{Pol}$ interaction, a loss of this interaction would be observed in cells co-expressing 1a and $2a^{Pol\ T168A}$. To complement these studies, yeast cells co-expressing 1a and $2a^{Pol\ WT}$ or $2a^{Pol\ T168A}$ can be analyzed by confocal microscopy and, if $2a^{Pol}$ localization is disrupted in the $2a^{Pol\ T168A}$ mutant, cellular fractionation assays can be used to determine the altered subcellular localization of the viral polymerase.

5.2.5 Validate phosphorylation of 2a^{Pol} in natural plant hosts

The ability of BMV to duplicate nearly all major replication features of its natural plant hosts in yeast, combined with yeast genetics, has advanced our understanding of BMV replication and virus-host interactions (3, 7, 119). However, an important and appropriate question is whether our results extend to natural plant hosts. A simple way to test the phosphorylation state of 2a^{Pol} in plants would be to transfect barley protoplasts with infectious *in vitro* transcripts containing complete copies of wt RNA1, RNA2 and RNA3 or RNA2 only, immunoprecipitate 2a^{Pol} from cell lysates using anti-2a^{Pol} antibodies and immunoblot with anti-2a^{Pol} and anti-phosphothreonine antibodies. Alternatively, or in parallel, immunoprecipitates can be analyzed with Pro-Q Diamond phosphospecific stain.

5.3. FINAL CONCLUSIONS

Collectively, the work in this thesis significantly advances our understanding of host genes and pathways utilized by BMV to achieve efficient genome replication. This study defined three mechanistically distinct roles for the ubiquitin-proteasome system in BMV RNA replication and future studies will likely reveal multiple, additional functions of this highly conserved cellular pathway that are important for BMV. Additionally, we provided the first evidence that phosphorylation of BMV 2a^{Pol} is required for RNA replication and further studies will define the replication steps modulated by phosphorylation. The conserved features of positive-strand RNA virus polymerases (9, 74, 115) combined with the necessity to regulate polymerase expression during the multiple, coordinated steps of RNA replication suggests phosphorylation of RdRps may be a common mechanism employed by RNA viruses. Additional studies are required to determine if this is indeed the case. Continuing to dissect the role of these important regulatory pathways will undoubtedly aid our understanding of basic virus biology and virus-host interactions. Moreover, coupling our experimental data with the bioinformatic approaches

developed through collaborative efforts will allow us to visualize unassayed host genes in the context of their interaction networks, potentially revealing links to genes already known to be important for BMV. Our approaches and insights appear relevant to other positive-strand RNA viruses and could also be used for extending such studies to other virus groups, thus potentially identifying common cellular targets for the development of broad-spectrum antivirals.

REFERENCES

1. **Agetsuma, M., T. Furumoto, S. Yanagisawa, and K. Izui.** 2005. The ubiquitin-proteasome pathway is involved in rapid degradation of phosphoenolpyruvate carboxylase kinase for C4 photosynthesis. Plant Cell Physiol **46:**389-398.

2. **Ahlquist, P.** 1992. Bromovirus RNA replication and transcription. Curr Opin Genet Dev **2:**71-76.

3. **Ahlquist, P.** 2006. Parallels among positive-strand RNA viruses, reverse-transcribing viruses and double-stranded RNA viruses. Nature reviews. Microbiology **4:**371-382.

4. **Ahlquist, P.** 2002. RNA-dependent RNA polymerases, viruses, and RNA silencing. Science **296:**1270-1273.

5. **Ahlquist, P., R. French, M. Janda, and L. S. Loesch-Fries.** 1984. Multicomponent RNA plant virus infection derived from cloned viral cDNA. Proc Natl Acad Sci U S A **81:**7066-7070.

6. **Ahlquist, P., and M. Janda.** 1984. cDNA cloning and in vitro transcription of the complete brome mosaic virus genome. Mol Cell Biol **4:**2876-2882.

7. **Ahlquist, P., A. O. Noueiry, W. M. Lee, D. B. Kushner, and B. T. Dye.** 2003. Host factors in positive-strand RNA virus genome replication. J Virol **77:**8181-8186.

8. **Ahlquist, P., A. O. Noueiry, W. M. Lee, D. B. Kushner, and B. T. Dye.** 2003. Host factors in positive-strand RNA virus genome replication. J. Virol. **77:**8181-8186.

9. **Ahlquist, P., E. G. Strauss, C. M. Rice, J. H. Strauss, J. Haseloff, and D. Zimmern.** 1985. Sindbis virus proteins nsP1 and nsP2 contain homology to nonstructural proteins from several RNA plant viruses. J Virol **53:**536-542.

10. **Ahlquist, P. K. a. P.** 1992. Molecular Plant Pathology: a Practical Approach. RNA-based viruses. , p. 23-43. *In* M. J. M. S.J. Gurr, D.J. Bowles (ed.), vol. 1. Oxford University Press.

11. **Ahola, T., and P. Ahlquist.** 1999. Putative RNA capping activities encoded by brome mosaic virus: methylation and covalent binding of guanylate by replicase protein 1a. J Virol **73:**10061-10069.

12. **Ahola, T., J. A. den Boon, and P. Ahlquist.** 2000. Helicase and Capping Enzyme Active Site Mutations in Brome Mosaic Virus Protein 1a Cause Defects in Template Recruitment, Negative-Strand RNA Synthesis, and Viral RNA Capping. J. Virol. **74:**8803-8811.

13. **Allison, R., C. Thompson, and P. Ahlquist.** 1990. Regeneration of a functional RNA virus genome by recombination between deletion mutants and requirement for cowpea chlorotic mottle virus 3a and coat genes for systemic infection. Proc Natl Acad Sci U S A **87:**1820-1824.

14. **Amerik, A. Y., S. J. Li, and M. Hochstrasser.** 2000. Analysis of the deubiquitinating enzymes of the yeast Saccharomyces cerevisiae. Biol Chem **381:**981-992.

15. **Aviram, S., E. Simon, T. Gildor, F. Glaser, and D. Kornitzer.** 2008. Autophosphorylation-induced degradation of the Pho85 cyclin Pcl5 is essential for response to amino acid limitation. Mol Cell Biol **28:**6858-6869.

16. **Barajas, D., Y. Jiang, and P. D. Nagy.** 2009. A unique role for the host ESCRT proteins in replication of Tomato bushy stunt virus. PLoS Pathog. **5:**e1000705.

17. **Barajas, D., Z. Li, and P. D. Nagy.** 2009. The Nedd4-Type Rsp5p Ubiquitin Ligase Inhibits Tombusvirus Replication by Regulating Degradation of the p92 Replication Protein and Decreasing the Activity of the Tombusvirus Replicase. J. Virol. **83:**11751-11764.

18. **Barajas, D., and P. D. Nagy.** 2010. Ubiquitination of tombusvirus p33 replication protein plays a role in virus replication and binding to the host Vps23p ESCRT protein. Virology **397:**358-368.

19. **Baumstark, T., and P. Ahlquist.** 2001. The brome mosaic virus RNA3 intergenic replication enhancer folds to mimic a tRNA TpsiC-stem loop and is modified in vivo. Rna **7:**1652-1670.

20. **Beinert, H., R. H. Holm, and E. Münck.** 1997. Iron-Sulfur Clusters: Nature's Modular, Multipurpose Structures. Science **277:**653-659.

21. **Belov, G. A., N. Altan-Bonnet, G. Kovtunovych, C. L. Jackson, J. Lippincott-Schwartz, and E. Ehrenfeld.** 2007. Hijacking components of the cellular secretory pathway for replication of poliovirus RNA. J Virol **81:**558-567.

22. **Belov, G. A., and E. Ehrenfeld.** 2007. Involvement of cellular membrane traffic proteins in poliovirus replication. Cell Cycle **6:**36-38.

23. **Belov, G. A., C. Habbersett, D. Franco, and E. Ehrenfeld.** 2007. Activation of cellular Arf GTPases by poliovirus protein 3CD correlates with virus replication. J Virol **81:**9259-9267.

24. **Blenis, J., and M. D. Resh.** 1993. Subcellular localization specified by protein acylation and phosphorylation. Curr Opin Cell Biol **5:**984-989.

25. **Blom, N., S. Gammeltoft, and S. r. Brunak.** 1999. Sequence and structure-based prediction of eukaryotic protein phosphorylation sites. Journal of Molecular Biology **294:**1351-1362.

26. **Bochtler, M., L. Ditzel, M. Groll, C. Hartmann, and R. Huber.** 1999. THE PROTEASOME. Annual Review of Biophysics and Biomolecular Structure **28:**295-317.

27. **Bode, J. G., E. D. Brenndorfer, J. Karthe, and D. Haussinger.** 2009. Interplay between host cell and hepatitis C virus in regulating viral replication. Biol Chem **390:**1013-1032.

28. **Bose, R., M. A. Holbert, K. A. Pickin, and P. A. Cole.** 2006. Protein tyrosine kinase‚Äìsubstrate interactions. Current Opinion in Structural Biology **16:**668-675.

29. **Bruce, J. W., P. Ahlquist, and J. A. Young.** 2008. The host cell sulfonation pathway contributes to retroviral infection at a step coincident with provirus establishment. PLoS Pathog **4:**e1000207.

30. **Camborde, L., S. v. Planchais, V. Tournier, A. Jakubiec, G. l. Drugeon, E. Lacassagne, S. p. Pflieger, M. l. Chenon, and I. Jupin.** 2010. The Ubiquitin-Proteasome System Regulates the Accumulation of Turnip yellow mosaic virus RNA-Dependent RNA Polymerase during Viral Infection. The Plant Cell Online **22:**3142-3152.

31. **Carette, J. E., M. Stuiver, J. Van Lent, J. Wellink, and A. Van Kammen.** 2000. Cowpea mosaic virus infection induces a massive proliferation of endoplasmic reticulum but not Golgi membranes and is dependent on de novo membrane synthesis. J Virol **74:**6556-6563.

32. **Carroll, A. S., and E. K. O'Shea.** 2002. Pho85 and signaling environmental conditions. Trends Biochem Sci **27:**87-93.

33. **Chapman, M. R., and C. C. Kao.** 1999. A minimal RNA promoter for minus-strand RNA synthesis by the brome mosaic virus polymerase complex. J Mol Biol **286:**709-720.

34. **Chatterji, U., M. Bobardt, S. Selvarajah, F. Yang, H. Tang, N. Sakamoto, G. Vuagniaux, T. Parkinson, and P. Gallay.** 2009. The Isomerase Active Site of Cyclophilin A Is Critical for Hepatitis C Virus Replication. Journal of Biological Chemistry **284:**16998-17005.

35. **Chen, D. C., B. C. Yang, and T. T. Kuo.** 1992. One-step transformation of yeast in stationary phase. Curr Genet **21:**83-84.

36. **Chen, J., and P. Ahlquist.** 2000. Brome mosaic virus polymerase-like protein 2a is directed to the endoplasmic reticulum by helicase-like viral protein 1a. J Virol **74:**4310-4318.

37. **Chen, J., A. Noueiry, and P. Ahlquist.** 2001. Brome mosaic virus Protein 1a recruits viral RNA2 to RNA replication through a 5' proximal RNA2 signal. J Virol **75:**3207-3219.

38. **Chen, X., W. Zhang, B. Zhang, J. Zhou, Y. Wang, Q. Yang, Y. Ke, and H. He.** 2011. Phosphoproteins regulated by heat stress in rice leaves. Proteome Sci **9:**37.

39. **Cheng, C. P., E. Serviene, and P. D. Nagy.** 2006. Suppression of viral RNA recombination by a host exoribonuclease. J. Virol. **80:**2631-2640.

40. **Chenon, M., L. Camborde, S. Cheminant, and I. Jupin.** 2012. A viral deubiquitylating enzyme targets viral RNA-dependent RNA polymerase and affects viral infectivity. EMBO J **31:**741-753.

41. **Cherry, S.** 2006. COPI activity coupled with fatty acid biosynthesis is required for viral replication. PLoS Pathog. **2:**e102.

42. **Cherry, S.** 2005. Genome-wide RNAi screen reveals a specific sensitivity of IRES-containing RNA viruses to host translation inhibition. Genes Dev. **19:**445-452.

43. **Chitteti, B. R., and Z. Peng.** 2007. Proteome and phosphoproteome dynamic change during cell dedifferentiation in Arabidopsis. Proteomics **7:**1473-1500.

44. **de Graauw, M., P. Hensbergen, and B. van de Water.** 2006. Phospho-proteomic analysis of cellular signaling. Electrophoresis **27:**2676-2686.

45. **De, I., C. Fata-Hartley, S. G. Sawicki, and D. L. Sawicki.** 2003. Functional analysis of nsP3 phosphoprotein mutants of Sindbis virus. J Virol **77:**13106-13116.

46. **den Boon, J. A., and P. Ahlquist.** 2010. Organelle-like membrane compartmentalization of positive-strand RNA virus replication factories. Annual review of microbiology **64:**241-256.

47. **den Boon, J. A., J. Chen, and P. Ahlquist.** 2001. Identification of sequences in Brome mosaic virus replicase protein 1a that mediate association with endoplasmic reticulum membranes. J Virol **75:**12370-12381.

48. **den Boon, J. A., A. Diaz, and P. Ahlquist.** 2010. Cytoplasmic viral replication complexes. Cell host & microbe **8:**77-85.

49. **den Boon, J. A., A. Diaz, and P. Ahlquist.** 2010. Cytoplasmic viral replication complexes. Cell host & microbe **8:**77-85.

50. **Diaz, A., and P. Ahlquist.** Role of host reticulon proteins in rearranging membranes for positive-strand RNA virus replication. Current Opinion in Microbiology.

51. **Diaz, A., A. Gallei, and P. Ahlquist.** 2012. Bromovirus RNA replication compartment formation requires concerted action of 1a's self-interacting RNA capping and helicase domains. J Virol **86:**821-834.

52. **Diaz, A., X. Wang, and P. Ahlquist.** 2010. Membrane-shaping host reticulon proteins play crucial roles in viral RNA replication compartment formation and function. Proc Natl Acad Sci U S A **107:**16291-16296.

53. **Dielen, A. S., S. Badaoui, T. Candresse, and S. German-Retana.** 2010. The ubiquitin/26S proteasome system in plant-pathogen interactions: a never-ending hide-and-seek game. Molecular plant pathology **11:**293-308.

54. **Dielen, A. S., F. T. Sassaki, J. Walter, T. Michon, G. Menard, G. Pagny, R. Krause-Sakate, G. Maia Ide, S. Badaoui, O. Le Gall, T. Candresse, and S. German-Retana.** 2011. The 20S proteasome alpha5 subunit of Arabidopsis thaliana carries an RNase activity and interacts in planta with the lettuce mosaic potyvirus HcPro protein. Molecular plant pathology **12:**137-150.

55. **Diez, J., M. Ishikawa, M. Kaido, and P. Ahlquist.** 2000. Identification and characterization of a host protein required for efficient template selection in viral RNA replication. Proc Natl Acad Sci U S A **97:**3913-3918.

56. **Dreher, T. W., J. J. Bujarski, and T. C. Hall.** 1984. Mutant viral RNAs synthesized in vitro show altered aminoacylation and replicase template activities. Nature **311:**171-175.

57. **Dye, B. T., L. Hao, and P. Ahlquist.** 2005. High-throughput isolation of Saccharomyces cerevisiae RNA. Biotechniques **38:**868, 870.

58. **Elble, R.** 1992. A simple and efficient procedure for transformation of yeasts. Biotechniques **13:**18-20.

59. **Enenkel, C., A. Lehmann, and P.-M. Kloetzel.** 1998. Subcellular distribution of proteasomes implicates a major location of protein degradation in the nuclear envelope-ER network in yeast. EMBO J **17:**6144-6154.

60. **Felden, B., C. Florentz, R. Giege, and E. Westhof.** 1994. Solution structure of the 3'-end of brome mosaic virus genomic RNAs. Conformational mimicry with canonical tRNAs. J Mol Biol **235:**508-531.

61. **Finley, D.** 2009. Recognition and processing of ubiquitin-protein conjugates by the proteasome. Annu Rev Biochem **78:**477-513.

62. **Flint, J. S., Enquist, L.W., Racaniello, V.R., Skalka, A.M.** 2004. Principles of Virology. ASM Press, Washington D.C.

63. **French, R., and P. Ahlquist.** 1987. Intercistronic as well as terminal sequences are required for efficient amplification of brome mosaic virus RNA3. J Virol **61:**1457-1465.

64. **Funakoshi, M., X. Li, I. Velichutina, M. Hochstrasser, and H. Kobayashi.** 2004. Sem1, the yeast ortholog of a human BRCA2-binding protein, is a component of the proteasome regulatory particle that enhances proteasome stability. Journal of Cell Science **117:**6447-6454.

65. **Gaither, L. A., J. Borawski, L. J. Anderson, K. A. Balabanis, P. Devay, G. Joberty, C. Rau, M. Schirle, T. Bouwmeester, C. Mickanin, S. Zhao, C. Vickers, L. Lee, G. Deng, J. Baryza, R. A. Fujimoto, K. Lin, T. Compton, and B. Wiedmann.** 2010. Multiple cyclophilins involved in different cellular pathways mediate HCV replication. Virology **397:**43-55.

66. **Gamarnik, A. V., and R. Andino.** 2000. Interactions of viral protein 3CD and poly(rC) binding protein with the 5,Ä≤ untranslated region of the poliovirus genome. J. Virol. **74:**2219-2226.

67. **Gamarnik, A. V., and R. Andino.** 1998. Switch from translation to RNA replication in a positive-stranded RNA virus. Genes Dev. **12:**2293-2304.

68. **Gancarz, B. L., L. Hao, Q. He, M. A. Newton, and P. Ahlquist.** 2011. Systematic identification of novel, essential host genes affecting bromovirus RNA replication. PloS one **6:**e23988.

69. **Gilfoy, F., R. Fayzulin, and P. W. Mason.** 2009. West Nile virus genome amplification requires the functional activities of the proteasome. Virology **385:**74-84.

70. **Gorchakov, R., E. Frolova, and I. Frolov.** 2005. Inhibition of Transcription and Translation in Sindbis Virus-Infected Cells. J. Virol. **79:**9397-9409.

71. **Grdzelishvili, V. Z., H. Garcia-Ruiz, T. Watanabe, and P. Ahlquist.** 2005. Mutual Interference between Genomic RNA Replication and Subgenomic mRNA Transcription in Brome Mosaic Virus. J. Virol. **79:**1438-1451.

72. **Gu, Z., L. M. Steinmetz, X. Gu, C. Scharfe, R. W. Davis, and W.-H. Li.** 2003. Role of duplicate genes in genetic robustness against null mutations. Nature **421:**63-66.

73. **Guinea, R., and L. Carrasco.** 1990. Phospholipid biosynthesis and poliovirus genome replication, two coupled phenomena. EMBO J **9:**2011-2016.

74. **Haseloff, J., P. Goelet, D. Zimmern, P. Ahlquist, R. Dasgupta, and P. Kaesberg.** 1984. Striking similarities in amino acid sequence among nonstructural proteins encoded by RNA viruses that have dissimilar genomic organization. Proc Natl Acad Sci U S A **81:**4358-4362.

75. **Heaton, N. S.** 2010. Dengue virus nonstructural protein 3 redistributes fatty acid synthase to sites of viral replication and increases cellular fatty acid synthesis. Proc. Natl Acad. Sci. USA **107:**17345-17350.

76. **Heaton, N. S., and G. Randall.** 2011. Multifaceted roles for lipids in viral infection. Trends in microbiology **19:**368-375.

77. **Hericourt, F., S. Blanc, V. Redeker, and I. Jupin.** 2000. Evidence for phosphorylation and ubiquitinylation of the turnip yellow mosaic virus RNA-dependent RNA polymerase domain expressed in a baculovirus-insect cell system. Biochem J **349:**417-425.

78. **Ho, S. N., H. D. Hunt, R. M. Horton, J. K. Pullen, and L. R. Pease.** 1989. Site-directed mutagenesis by overlap extension using the polymerase chain reaction. Gene **77:**51-59.

79. **Hochstrasser, M., M. Deng, A. R. Kusmierczyk, X. Li, S. G. Kreft, T. Ravid, M. Funakoshi, M. Kunjappu, and Y. Xie.** 2008. Molecular genetics of the ubiquitin-proteasome system: lessons from yeast. Ernst Schering Foundation symposium proceedings**:**41-66.

80. **Hochstrasser, M., P. R. Johnson, C. S. Arendt, A. Amerik, S. Swaminathan, R. Swanson, S. J. Li, J. Laney, R. Pals-Rylaarsdam, J. Nowak, and P. L. Connerly.** 1999. The Saccharomyces cerevisiae ubiquitin-proteasome system. Philosophical transactions of the Royal Society of London. Series B, Biological sciences **354:**1513-1522.

81. **Huang, D., H. Friesen, and B. Andrews.** 2007. Pho85, a multifunctional cyclin-dependent protein kinase in budding yeast. Molecular microbiology **66:**303-314.

82. **Huang, D., G. Patrick, J. Moffat, L. H. Tsai, and B. Andrews.** 1999. Mammalian Cdk5 is a functional homologue of the budding yeast Pho85 cyclin-dependent protein kinase. Proc Natl Acad Sci U S A **96:**14445-14450.

83. **Hughes, T. R., M. J. Marton, A. R. Jones, C. J. Roberts, R. Stoughton, C. D. Armour, H. A. Bennett, E. Coffey, H. Dai, Y. D. He, M. J. Kidd, A. M. King, M. R. Meyer, D. Slade, P. Y. Lum, S. B. Stepaniants, D. D. Shoemaker, D. Gachotte, K. Chakraburtty, J. Simon, M. Bard, and S. H. Friend.** 2000. Functional discovery via a compendium of expression profiles. Cell **102:**109-126.

84. **Hwang, C. S., A. Shemorry, D. Auerbach, and A. Varshavsky.** 2010. The N-end rule pathway is mediated by a complex of the RING-type Ubr1 and HECT-type Ufd4 ubiquitin ligases. Nat Cell Biol **12:**1177-1185.

85. **Hwang, C. S., and A. Varshavsky.** 2008. Regulation of peptide import through phosphorylation of Ubr1, the ubiquitin ligase of the N-end rule pathway. Proc Natl Acad Sci U S A **105:**19188-19193.

86. **Hwang, S. B., K. J. Park, Y. S. Kim, Y. C. Sung, and M. M. Lai.** 1997. Hepatitis C virus NS5B protein is a membrane-associated phosphoprotein with a predominantly perinuclear localization. Virology **227:**439-446.

87. **Ingrell, C. R., M. L. Miller, O. N. Jensen, and N. Blom.** 2007. NetPhosYeast: prediction of protein phosphorylation sites in yeast. Bioinformatics **23:**895-897.

88. **Ishikawa, M., M. Janda, M. A. Krol, and P. Ahlquist.** 1997. In vivo DNA expression of functional brome mosaic virus RNA replicons in Saccharomyces cerevisiae. J Virol **71:**7781-7790.

89. **Jakubiec, A., and I. Jupin.** 2007. Regulation of positive-strand RNA virus replication: the emerging role of phosphorylation. Virus research **129:**73-79.

90. **Jakubiec, A., V. Tournier, G. Drugeon, S. Pflieger, L. Camborde, J. Vinh, F. Hericourt, V. Redeker, and I. Jupin.** 2006. Phosphorylation of viral RNA-dependent RNA polymerase and its role in replication of a plus-strand RNA virus. J Biol Chem **281:**21236-21249.

91. **Janda, M., and P. Ahlquist.** 1998. Brome mosaic virus RNA replication protein 1a dramatically increases in vivo stability but not translation of viral genomic RNA3. Proc Natl Acad Sci U S A **95:**2227-2232.

92. **Janda, M., and P. Ahlquist.** 1993. RNA-dependent replication, transcription, and persistence of brome mosaic virus RNA replicons in S. cerevisiae. Cell **72:**961-970.

93. **Janda, M., R. French, and P. Ahlquist.** 1987. High efficiency T7 polymerase synthesis of infectious RNA from cloned brome mosaic virus cdna and effects of 5' extensions on transcript infectivity. Virology **158:**259-262.

94. **Jarrousse, A. S., K. Gautier, S. Apcher, S. Badaoui, G. Boissonnet, M. H. Dadet, L. Henry, J. P. Bureau, H. P. Schmid, and F. Petit.** 1999. Relationships between proteasomes and viral gene products. Mol Biol Rep **26:**113-117.

95. **Jiang, Y., E. Serviene, J. Gal, T. Panavas, and P. D. Nagy.** 2006. Identification of essential host factors affecting tombusvirus RNA replication based on the yeast Tet promoters Hughes Collection. J. Virol. **80:**7394-7404.

96. **Jiang, Y., E. Serviene, J. Gal, T. Panavas, and P. D. Nagy.** 2006. Identification of essential host factors affecting tombusvirus RNA replication based on the yeast Tet promoters Hughes Collection. J Virol **80:**7394-7404.

97. **Johnson, E. S., P. C. Ma, I. M. Ota, and A. Varshavsky.** 1995. A proteolytic pathway that recognizes ubiquitin as a degradation signal. J Biol Chem **270:**17442-17456.

98. **Ju, D., and Y. Xie.** 2004. Proteasomal degradation of RPN4 via two distinct mechanisms, ubiquitin-dependent and -independent. J Biol Chem **279:**23851-23854.

99. **Jungkunz, I., K. Link, F. Vogel, L. M. Voll, S. Sonnewald, and U. Sonnewald.** 2011. AtHsp70-15-deficient Arabidopsis plants are characterized by reduced growth, a constitutive cytosolic protein response and enhanced resistance to TuMV. The Plant Journal **66:**983-995.

100. **Kalume, D. E., H. Molina, and A. Pandey.** 2003. Tackling the phosphoproteome: tools and strategies. Curr Opin Chem Biol **7:**64-69.

101. **Kampinga, H. H., and E. A. Craig.** 2010. The HSP70 chaperone machinery: J proteins as drivers of functional specificity. Nat Rev Mol Cell Biol **11:**579-592.

102. **Kao, C. C., and P. Ahlquist.** 1992. Identification of the domains required for direct interaction of the helicase-like and polymerase-like RNA replication proteins of brome mosaic virus. J Virol **66:**7293-7302.

103. **Kao, C. C., and K. Sivakumaran.** 2000. Brome mosaic virus, good for an RNA virologist's basic needs. Molecular plant pathology **1:**91-97.

104. **Kapadia, S. B., and F. V. Chisari.** 2005. Hepatitis C virus RNA replication is regulated by host geranylgeranylation and fatty acids. Proc Natl Acad Sci U S A **102:**2561-2566.

105. **Kapadia, S. B., and F. V. Chisari.** 2005. Hepatitis C virus RNA replication is regulated by host geranylgeranylation and fatty acids. Proc. Natl Acad. Sci. USA **102:**2561-2566.

106. **Kapoor, M., L. Zhang, M. Ramachandra, J. Kusukawa, K. E. Ebner, and R. Padmanabhan.** 1995. Association between NS3 and NS5 Proteins of Dengue Virus Type 2 in the Putative RNA Replicase Is Linked to Differential Phosphorylation of NS5. Journal of Biological Chemistry **270:**19100-19106.

107. **Karin, M., and T. Hunter.** 1995. Transcriptional control by protein phosphorylation: signal transmission from the cell surface to the nucleus. Current biology : CB **5:**747-757.

108. **Kash, J. C., A. G. Goodman, M. J. Korth, and M. G. Katze.** 2006. Hijacking of the host-cell response and translational control during influenza virus infection. Virus research **119:**111-120.

109. **Kaul, A., S. Stauffer, C. Berger, T. Pertel, J. Schmitt, S. Kallis, M. Zayas Lopez, V. Lohmann, J. Luban, and R. Bartenschlager.** 2009. Essential Role of Cyclophilin A for Hepatitis C Virus Replication and Virus Production and Possible Link to Polyprotein Cleavage Kinetics. PLoS Pathog **5:**e1000546.

110. **Kim, M. J., B.-K. Ham, and K.-H. Paek.** 2006. Novel protein kinase interacts with the Cucumber mosaic virus 1a methyltransferase domain. Biochemical and Biophysical Research Communications **340:**228-235.

111. **Kim, S. H., P. Palukaitis, and Y. I. Park.** 2002. Phosphorylation of cucumber mosaic virus RNA polymerase 2a protein inhibits formation of replicase complex. EMBO J **21:**2292-2300.

112. **Kim, S. J., J. H. Kim, Y. G. Kim, H. S. Lim, and J. W. Oh.** 2004. Protein kinase C-related kinase 2 regulates hepatitis C virus RNA polymerase function by phosphorylation. J Biol Chem **279:**50031-50041.

113. **Knipe, D. M. a. H., P.M. editors.** 2001. *Fields Virology*, 4th ed. Lippincott Williams and Wilkins, Philadelphia.

114. **Kong, F., K. Sivakumaran, and C. Kao.** 1999. The N-terminal half of the brome mosaic virus 1a protein has RNA capping-associated activities: specificity for GTP and S-adenosylmethionine. Virology **259:**200-210.

115. **Koonin, E. V.** 1991. The phylogeny of RNA-dependent RNA polymerases of positive-strand RNA viruses. Journal of General Virology **72:**2197-2206.

116. **Krol, M. A., N. H. Olson, J. Tate, J. E. Johnson, T. S. Baker, and P. Ahlquist.** 1999. RNA-controlled polymorphism in the in vivo assembly of 180-subunit and 120-subunit virions from a single capsid protein. Proc Natl Acad Sci U S A **96:**13650-13655.

117. **Kuroha, K., T. Tatematsu, and T. Inada.** 2009. Upf1 stimulates degradation of the product derived from aberrant messenger RNA containing a specific nonsense mutation by the proteasome. EMBO Rep **10:**1265-1271.

118. **Kushner, D. B.** 2003. Systematic, genome-wide identification of host genes affecting replication of a positive-strand RNA virus. Proc. Natl Acad. Sci. USA **100:**15764-15769.

119. **Kushner, D. B., B. D. Lindenbach, V. Z. Grdzelishvili, A. O. Noueiry, S. M. Paul, and P. Ahlquist.** 2003. Systematic, genome-wide identification of host genes affecting replication of a positive-strand RNA virus. Proc Natl Acad Sci U S A **100:**15764-15769.

120. **Lastarza, M. W., A. Grakoui, and C. M. Rice.** 1994. Deletion and Duplication Mutations in the C-Terminal Nonconserved Region of Sindbis Virus nsP3: Effects on Phosphorylation and on Virus Replication in Vertebrate and Invertebrate Cells. Virology **202:**224-232.

121. **Lee, D. H., and A. L. Goldberg.** 1998. Proteasome inhibitors: valuable new tools for cell biologists. Trends in Cell Biology **8:**397-403.

122. **Lee, W. M., and P. Ahlquist.** 2003. Membrane synthesis, specific lipid requirements, and localized lipid composition changes associated with a positive-strand RNA virus RNA replication protein. J. Virol. **77:**12819-12828.

123. **Lee, W. M., and P. Ahlquist.** 2003. Membrane synthesis, specific lipid requirements, and localized lipid composition changes associated with a positive-strand RNA virus RNA replication protein. J Virol **77:**12819-12828.

124. **Lee, W. M., M. Ishikawa, and P. Ahlquist.** 2001. Mutation of host delta9 fatty acid desaturase inhibits brome mosaic virus RNA replication between template recognition and RNA synthesis. J Virol **75:**2097-2106.

125. **Leeds, P., S. W. Peltz, A. Jacobson, and M. R. Culbertson.** 1991. The product of the yeast UPF1 gene is required for rapid turnover of mRNAs containing a premature translational termination codon. Genes & development **5:**2303-2314.

126. **Leggett, D. S., J. Hanna, A. Borodovsky, B. Crosas, M. Schmidt, R. T. Baker, T. Walz, H. Ploegh, and D. Finley.** 2002. Multiple associated proteins regulate proteasome structure and function. Mol Cell **10:**495-507.

127. **Li, G., M. W. La Starza, W. Reef Hardy, J. H. Strauss, and C. M. Rice.** 1990. Phosphorylation of sindbis virus nsP3 in vivo and in vitro. Virology **179:**416-427.

128. **Li, Q.** 2009. A genome-wide genetic screen for host factors required for hepatitis C virus propagation. Proc. Natl Acad. Sci. USA **106:**16410-16415.

129. **Lill, R.** 2009. Function and biogenesis of iron-sulphur proteins. Nature **460:**831-838.

130. **Lill, R., and U. Mühlenhoff.** 2008. Maturation of Iron-Sulfur Proteins in Eukaryotes: Mechanisms, Connected Processes, and Diseases. Annual Review of Biochemistry **77:**669-700.

131. **Lindenbach, B. D., J.-Y. Sgro, and P. Ahlquist.** 2002. Long-Distance Base Pairing in Flock House Virus RNA1 Regulates Subgenomic RNA3 Synthesis and RNA2 Replication. J. Virol. **76:**3905-3919.

132. **Liu, C., J. Apodaca, L. E. Davis, and H. Rao.** 2007. Proteasome inhibition in wild-type yeast Saccharomyces cerevisiae cells. Biotechniques **42:**158, 160, 162.

133. **Liu, L., W. M. Westler, J. A. den Boon, X. Wang, A. Diaz, H. A. Steinberg, and P. Ahlquist.** 2009. An amphipathic alpha-helix controls multiple roles of brome mosaic virus protein 1a in RNA replication complex assembly and function. PLoS Pathog **5:**e1000351.

134. **Liu, Y., X. Xu, and M. H. Kuo.** 2010. Snf1p regulates Gcn5p transcriptional activity by antagonizing Spt3p. Genetics **184:**91-105.

135. **Liu, Z., F. Yang, J. M. Robotham, and H. Tang.** 2009. Critical Role of Cyclophilin A and Its Prolyl-Peptidyl Isomerase Activity in the Structure and Function of the Hepatitis C Virus Replication Complex. J. Virol. **83:**6554-6565.

136. **Lopez, T., D. Silva-Ayala, S. Lopez, and C. F. Arias.** 2011. Replication of the rotavirus genome requires an active ubiquitin-proteasome system. J Virol **85:**11964-11971.

137. **Mackenzie, J.** 2005. Wrapping things up about virus RNA replication. Traffic **6:**967-977.

138. **Mas, A., I. Alves-Rodrigues, A. Noueiry, P. Ahlquist, and J. Diez.** 2006. Host deadenylation-dependent mRNA decapping factors are required for a key step in brome mosaic virus RNA replication. J Virol **80:**246-251.

139. **McHutchison, J. G.** 2004. Understanding hepatitis C. Am J Manag Care **10:**S21-29.

140. **Measday, V., L. Moore, R. Retnakaran, J. Lee, M. Donoviel, A. M. Neiman, and B. Andrews.** 1997. A family of cyclin-like proteins that interact with the Pho85 cyclin-dependent kinase. Mol Cell Biol **17:**1212-1223.

141. **Meimoun, P., F. Ambard-Bretteville, C. Colas-des Francs-Small, B. Valot, and J. Vidal.** 2007. Analysis of plant phosphoproteins. Analytical Biochemistry **371:**238-246.

142. **Mendu, V., M. Chiu, D. Barajas, Z. Li, and P. D. Nagy.** 2010. Cpr1 cyclophilin and Ess1 parvulin prolyl isomerases interact with the tombusvirus replication protein and inhibit viral replication in yeast model host. Virology **406:**342-351.

143. **Meng, L., G. Michaud, J. Merkel, F. Zhou, J. Huang, D. Mattoon, and B. Schweitzer.** 2008. Protein kinase substrate identification on functional protein arrays. BMC Biotechnology **8:**22.

144. **Mikesh, L. M., B. Ueberheide, A. Chi, J. J. Coon, J. E. P. Syka, J. Shabanowitz, and D. F. Hunt.** 2006. The utility of ETD mass spectrometry in proteomic analysis. Biochimica et Biophysica Acta (BBA) - Proteins & Proteomics **1764:**1811-1822.

145. **Miller, S., and J. Krijnse-Locker.** 2008. Modification of intracellular membrane structures for virus replication. Nature reviews. Microbiology **6:**363-374.

146. **Miller, S., and J. Krijnse-Locker.** 2008. Modification of intracellular membrane structures for virus replication. Nature Rev. Microbiol. **6:**363-374.

147. **Mise, K., and P. Ahlquist.** 1995. Host-specificity restriction by bromovirus cell-to-cell movement protein occurs after initial cell-to-cell spread of infection in nonhost plants. Virology **206:**276-286.

148. **Mise, K., R. F. Allison, M. Janda, and P. Ahlquist.** 1993. Bromovirus movement protein genes play a crucial role in host specificity. J Virol **67:**2815-2823.

149. **Mnaimneh, S., A. P. Davierwala, J. Haynes, J. Moffat, W. T. Peng, W. Zhang, X. Yang, J. Pootoolal, G. Chua, A. Lopez, M. Trochesset, D. Morse, N. J. Krogan, S. L. Hiley, Z. Li, Q. Morris, J. Grigull, N. Mitsakakis, C. J. Roberts, J. F. Greenblatt, C. Boone, C. A. Kaiser, B. J. Andrews, and T. R. Hughes.** 2004. Exploration of essential gene functions via titratable promoter alleles. Cell **118:**31-44.

150. **Monetti, M., N. Nagaraj, K. Sharma, and M. Mann.** 2011. Large-scale phosphosite quantification in tissues by a spike-in SILAC method. Nature methods **8:**655-658.

151. **Mongiovi, A. M., P. R. Romano, S. Panni, M. Mendoza, W. T. Wong, A. Musacchio, G. Cesareni, and P. Paolo Di Fiore.** 1999. A novel peptide-SH3 interaction. EMBO J **18:**5300-5309.

152. **Morozova, O. V., N. A. Tsekhanovskaya, T. G. Maksimova, V. N. Bachvalova, V. A. Matveeva, and Y. Kit.** 1997. Phosphorylation of tick-borne encephalitis virus NS5 protein. Virus research **49:**9-15.

153. **Mumberg, D., R. Muller, and M. Funk.** 1994. Regulatable promoters of Saccharomyces cerevisiae: comparison of transcriptional activity and their use for heterologous expression. Nucleic Acids Res **22:**5767-5768.

154. **Münk, C., S. M. Brandt, G. Lucero, and N. R. Landau.** 2002. A dominant block to HIV-1 replication at reverse transcription in simian cells. Proceedings of the National Academy of Sciences **99:**13843-13848.

155. **Myung, J., K. B. Kim, and C. M. Crews.** 2001. The ubiquitin-proteasome pathway and proteasome inhibitors. Medicinal Research Reviews **21:**245-273.

156. **Nag, D. K., and D. Finley.** 2012. A small-molecule inhibitor of deubiquitinating enzyme USP14 inhibits Dengue virus replication. Virus research **165:**103-106.

157. **Nagy, P. D., and J. Pogany.** 2012. The dependence of viral RNA replication on co-opted host factors. Nature reviews. Microbiology **10:**137-149.

158. **Ng, T. I.** 2007. Identification of host genes involved in hepatitis C virus replication by small interfering RNA technology. Hepatology **45:**1413-1421.

159. **Noueiry, A. O., and P. Ahlquist.** 2003. Brome mosaic virus RNA replication: revealing the role of the host in RNA virus replication. Annual review of phytopathology **41:**77-98.

160. **Noueiry, A. O., and P. Ahlquist.** 2003. Brome mosaic virus RNA replication: revealing the role of the host in RNA virus replication. Annu. Rev. Phytopathol. **41:**77-98.

161. **Noueiry, A. O., J. Chen, and P. Ahlquist.** 2000. A mutant allele of essential, general translation initiation factor DED1 selectively inhibits translation of a viral mRNA. Proc Natl Acad Sci U S A **97:**12985-12990.

162. **Noueiry, A. O., J. Diez, S. P. Falk, J. Chen, and P. Ahlquist.** 2003. Yeast Lsm1p-7p/Pat1p deadenylation-dependent mRNA-decapping factors are required for brome mosaic virus genomic RNA translation. Mol Cell Biol **23:**4094-4106.

163. **Novoa, R. R., G. Calderita, R. Arranz, J. Fontana, H. Granzow, and C. Risco.** 2005. Virus factories: associations of cell organelles for viral replication and morphogenesis. Biol Cell **97:**147-172.

164. **O'Reilly, E. K., J. D. Paul, and C. C. Kao.** 1997. Analysis of the interaction of viral RNA replication proteins by using the yeast two-hybrid assay. J Virol **71:**7526-7532.

165. **Obenauer, J. C., L. C. Cantley, and M. B. Yaffe.** 2003. Scansite 2.0: Proteome-wide prediction of cell signaling interactions using short sequence motifs. Nucleic Acids Res **31:**3635-3641.

166. **Orsatti, L., E. Forte, L. Tomei, M. Caterino, A. Pessi, and F. Talamo.** 2009. 2-D Difference in gel electrophoresis combined with Pro-Q Diamond staining: a successful approach for the identification of kinase/phosphatase targets. Electrophoresis **30:**2469-2476.

167. **Osman, T. A., and K. W. Buck.** 2003. Identification of a region of the tobacco mosaic virus 126- and 183-kilodalton replication proteins which binds specifically to the viral 3'-terminal tRNA-like structure. J. Virol. **77:**8669-8675.

168. **Panavas, T., and P. D. Nagy.** 2003. Yeast as a model host to study replication and recombination of defective interfering RNA of Tomato bushy stunt virus. Virology **314:**315-325.

169. **Panavas, T., E. Serviene, J. Brasher, and P. D. Nagy.** 2005. Yeast genome-wide screen reveals dissimilar sets of host genes affecting replication of RNA viruses. Proc. Natl Acad. Sci. USA **102:**7326-7331.

170. **Pannunzio, V. G., H. I. Burgos, M. Alonso, J. R. Mattoon, E. H. Ramos, and C. A. Stella.** 2004. A Simple Chemical Method for Rendering Wild-Type Yeast Permeable to Brefeldin A That Does Not Require the Presence of an erg6 Mutation. Journal of Biomedicine and Biotechnology **2004:**150-155.

171. **Pathak, K. B., Z. Sasvari, and P. D. Nagy.** 2008. The host Pex19p plays a role in peroxisomal localization of tombusvirus replication proteins. Virology **379:**294-305.

172. **Pathak, K. B., Z. Sasvari, and P. D. Nagy.** 2008. The host Pex19p plays a role in peroxisomal localization of tombusvirus replication proteins. Virology **379:**294-305.

173. **Perera, R., S. Daijogo, B. L. Walter, J. H. Nguyen, and B. L. Semler.** 2007. Cellular protein modification by poliovirus: the two faces of poly(rC)-binding protein. J. Virol. **81:**8919-8932.

174. **Perez, L., R. Guinea, and L. Carrasco.** 1991. Synthesis of Semliki Forest virus RNA requires continuous lipid synthesis. Virology **183:**74-82.

175. **Pickart, C. M.** 2001. Mechanisms underlying ubiquitination. Annu Rev Biochem **70:**503-533.

176. **Pickart, C. M., and D. Fushman.** 2004. Polyubiquitin chains: polymeric protein signals. Current Opinion in Chemical Biology **8:**610-616.

177. **Pietschmann, T., V. Lohmann, G. Rutter, K. Kurpanek, and R. Bartenschlager.** 2001. Characterization of Cell Lines Carrying Self-Replicating Hepatitis C Virus RNAs. Journal of Virology **75:**1252-1264.

178. **Pouch, M.-N. I., F. Petit, J. Buri, Y. Briand, and H.-P. Schmid.** 1995. Identification and Initial Characterization of a Specific Proteasome (Prosome) Associated RNase Activity. Journal of Biological Chemistry **270:**22023-22028.

179. **Ptacek, J., G. Devgan, G. Michaud, H. Zhu, X. Zhu, J. Fasolo, H. Guo, G. Jona, A. Breitkreutz, R. Sopko, R. R. McCartney, M. C. Schmidt, N. Rachidi, S.-J. Lee, A. S. Mah, L. Meng, M. J. R. Stark, D. F. Stern, C. De Virgilio, M. Tyers, B. Andrews, M. Gerstein, B. Schweitzer, P. F. Predki, and M. Snyder.** 2005. Global analysis of protein phosphorylation in yeast. Nature **438:**679-684.

180. **Pukszta, S., B. Schilke, R. Dutkiewicz, J. Kominek, K. Moczulska, B. Stepien, K. G. Reitenga, J. M. Bujnicki, B. Williams, E. A. Craig, and J. Marszalek.** 2010. Co-evolution-driven switch of J-protein specificity towards an Hsp70 partner. EMBO Rep **11:**360-365.

181. **Quadt, R., M. Ishikawa, M. Janda, and P. Ahlquist.** 1995. Formation of brome mosaic virus RNA-dependent RNA polymerase in yeast requires coexpression of viral proteins and viral RNA. Proc Natl Acad Sci U S A **92:**4892-4896.

182. **Raaben, M., C. C. Posthuma, M. H. Verheije, E. G. te Lintelo, M. Kikkert, J. W. Drijfhout, E. J. Snijder, P. J. M. Rottier, and C. A. M. de Haan.** 2010. The Ubiquitin-Proteasome System Plays an Important Role during Various Stages of the Coronavirus Infection Cycle. J. Virol. **84:**7869-7879.

183. **Rahman-Roblick, R., U. Hellman, S. Becker, F. G. Bader, G. Auer, K. G. Wiman, and U. J. Roblick.** 2008. Proteomic identification of p53-dependent protein phosphorylation. Oncogene **27:**4854-4859.

184. **Ramos, P. C., J. r. H√∂ckendorff, E. S. Johnson, A. Varshavsky, and R. J. r. Dohmen.** 1998. Ump1p Is Required for Proper Maturation of the 20S Proteasome and Becomes Its Substrate upon Completion of the Assembly. Cell **92:**489-499.

185. **Randall, G.** 2007. Cellular cofactors affecting hepatitis C virus infection and replication. Proc. Natl Acad. Sci. USA **104:**12884-12889.

186. **Rao, A. L. N.** 2005. Preparation and Inoculation of Mesophyll Protoplasts from Monocotyledenous and Dicotyledenous Hosts, Current Protocols in Microbiology. John Wiley & Sons, Inc.

187. **Reed, K. E., A. E. Gorbalenya, and C. M. Rice.** 1998. The NS5A/NS5 proteins of viruses from three genera of the family flaviviridae are phosphorylated by associated serine/threonine kinases. J Virol **72:**6199-6206.

188. **Reiss, S.** 2011. Recruitment and activation of a lipid kinase by hepatitis C virus NS5A is essential for integrity of the membranous replication compartment. Cell host & microbe **9:**32-45.

189. **Restrepo-Hartwig, M., and P. Ahlquist.** 1996. Brome mosaic virus helicase- and polymerase-like proteins colocalize on the endoplasmic reticulum at sites of viral RNA synthesis. J. Virol. **70:**8908-8916.

190. **Restrepo-Hartwig, M., and P. Ahlquist.** 1999. Brome mosaic virus RNA replication proteins 1a and 2a colocalize and 1a independently localizes on the yeast endoplasmic reticulum. J Virol **73:**10303-10309.

191. **Rietveld, K., C. W. Pleij, and L. Bosch.** 1983. Three-dimensional models of the tRNA-like 3' termini of some plant viral RNAs. EMBO J **2:**1079-1085.

192. **Rumpf, S., and S. Jentsch.** 2006. Functional division of substrate processing cofactors of the ubiquitin-selective Cdc48 chaperone. Mol Cell **21:**261-269.

193. **Salonen, A., T. Ahola, and L. Kaariainen.** 2005. Viral RNA replication in association with cellular membranes. Current topics in microbiology and immunology **285:**139-173.

194. **Santamaria, D., C. Barriere, A. Cerqueira, S. Hunt, C. Tardy, K. Newton, J. F. Caceres, P. Dubus, M. Malumbres, and M. Barbacid.** 2007. Cdk1 is sufficient to drive the mammalian cell cycle. Nature **448:**811-815.

195. **Scheller, N., L. B. Mina, R. P. Galao, A. Chari, M. Gimenez-Barcons, A. Noueiry, U. Fischer, A. Meyerhans, and J. Diez.** 2009. Translation and replication of hepatitis C virus genomic RNA depends on ancient cellular proteins that control mRNA fates. Proc Natl Acad Sci U S A **106:**13517-13522.

196. **Schwartz, M., J. Chen, M. Janda, M. Sullivan, J. den Boon, and P. Ahlquist.** 2002. A positive-strand RNA virus replication complex parallels form and function of retrovirus capsids. Mol Cell **9:**505-514.

197. **Schwartz, M., J. Chen, W. M. Lee, M. Janda, and P. Ahlquist.** 2004. Alternate, virus-induced membrane rearrangements support positive-strand RNA virus genome replication. Proceedings of the National Academy of Sciences of the United States of America **101:**11263-11268.

198. **Serviene, E.** 2005. Genome-wide screen identifies host genes affecting viral RNA recombination. Proc. Natl Acad. Sci. USA **102:**10545-10550.

199. **Serviene, E., Y. Jiang, C. P. Cheng, J. Baker, and P. D. Nagy.** 2006. Screening of the yeast yTHC collection identifies essential host factors affecting tombusvirus RNA recombination. J. Virol. **80:**1231-1241.

200. **Shapka, N., J. Stork, and P. D. Nagy.** 2005. Phosphorylation of the p33 replication protein of Cucumber necrosis tombusvirus adjacent to the RNA binding site affects viral RNA replication. Virology **343:**65-78.

201. **Shaw, P. E.** 2007. Peptidyl-prolyl cis/trans isomerases and transcription: is there a twist in the tail? EMBO Rep **8:**40-45.

202. **Si, X., G. Gao, J. Wong, Y. Wang, J. Zhang, and H. Luo.** 2008. Ubiquitination is required for effective replication of coxsackievirus B3. PloS one **3:**e2585.

203. **Spallek, T., S. Robatzek, and V. Gohre.** 2009. How microbes utilize host ubiquitination. Cellular microbiology **11:**1425-1434.

204. **Storey, J. D., and R. Tibshirani.** 2003. Statistical significance for genomewide studies. Proc Natl Acad Sci U S A **100:**9440-9445.

205. **Stukey, J. E., V. M. McDonough, and C. E. Martin.** 1989. Isolation and characterization of OLE1, a gene affecting fatty acid desaturation from Saccharomyces cerevisiae. J Biol Chem **264:**16537-16544.

206. **Sullivan, M. L., and P. Ahlquist.** 1999. A brome mosaic virus intergenic RNA3 replication signal functions with viral replication protein 1a to dramatically stabilize RNA in vivo. J Virol **73:**2622-2632.

207. **Supekova, L.** 2008. Identification of human kinases involved in hepatitis C virus replication by small interference RNA library screening. J. Biol. Chem. **283:**29-36.

208. **Swaminathan, S., A. Y. Amerik, and M. Hochstrasser.** 1999. The Doa4 deubiquitinating enzyme is required for ubiquitin homeostasis in yeast. Molecular biology of the cell **10:**2583-2594.

209. **Talbot, S. J., and D. H. Crawford.** 2004. Viruses and tumours--an update. Eur J Cancer **40:**1998-2005.

210. **Tarrant, M. K., and P. A. Cole.** 2009. The Chemical Biology of Protein Phosphorylation, p. 797-825, Annual Review of Biochemistry, vol. 78. Annual Reviews, Palo Alto.

211. **Taylor, M. P., and K. Kirkegaard.** 2008. Potential subversion of autophagosomal pathway by picornaviruses. Autophagy **4:**286-289.

212. **Toh-e, A., K. Tanaka, Y. Uesono, and R. B. Wickner.** 1988. PHO85, a negative regulator of the PHO system, is a homolog of the protein kinase gene, CDC28, of Saccharomyces cerevisiae. Mol Gen Genet **214:**162-164.

213. **Tomita, Y., T. Mizuno, J. Diez, S. Naito, P. Ahlquist, and M. Ishikawa.** 2003. Mutation of host DnaJ homolog inhibits brome mosaic virus negative-strand RNA synthesis. J Virol **77:**2990-2997.

214. **Tran, K., J. A. Mahr, and D. H. Spector.** 2010. Proteasome subunits relocalize during human cytomegalovirus infection, and proteasome activity is necessary for efficient viral gene transcription. J Virol **84:**3079-3093.

215. **Tu, H.** 1999. Hepatitis C virus RNA polymerase and NS5A complex with a SNARE-like protein. Virology **263:**30-41.

216. **Ubersax, J. A., and J. E. Ferrell Jr.** 2007. Mechanisms of specificity in protein phosphorylation. Nat Rev Mol Cell Biol **8:**530-541.

217. **van Regenmortel MHV, F. C., Bishop DHL, Carsten EB, Estes MK, et al. (ed.).** 2000. Virus Taxonomy. Seventh Report of the International Committee on Taxonomy of Viruses, 1st ed. Academic Press, San Diego.

218. **Van Wynsberghe, P. M., and P. Ahlquist.** 2009. 5' cis elements direct nodavirus RNA1 recruitment to mitochondrial sites of replication complex formation. J. Virol. **83:**2976-2988.

219. **Vierstra, R. D.** 2009. The ubiquitin-26S proteasome system at the nexus of plant biology. Nat Rev Mol Cell Biol **10:**385-397.

220. **Wagner, A.** 2000. Robustness against mutations in genetic networks of yeast. Nat Genet **24:**355-361.

221. **Walter, B. L., T. B. Parsley, E. Ehrenfeld, and B. L. Semler.** 2002. Distinct poly(rC) binding protein KH domain determinants for poliovirus translation initiation and viral RNA replication. J. Virol. **76:**12008-12022.

222. **Wang, C.** 2005. Identification of FBL2 as a geranylgeranylated cellular protein required for hepatitis C virus RNA replication. Mol. Cell **18:**425-434.

223. **Wang, R. Y., J. Stork, and P. D. Nagy.** 2009. A key role for heat shock protein 70 in the localization and insertion of tombusvirus replication proteins to intracellular membranes. J. Virol. **83:**3276-3287.

224. **Wang, R. Y.-L., J. Stork, and P. D. Nagy.** 2009. A Key Role for Heat Shock Protein 70 in the Localization and Insertion of Tombusvirus Replication Proteins to Intracellular Membranes. J. Virol. **83:**3276-3287.

225. **Wang, X.** 2005. Brome mosaic virus 1a nucleoside triphosphatase/helicase domain plays crucial roles in recruiting RNA replication templates. J. Virol. **79:**13747-13758.

226. **Wang, X., A. Diaz, L. Hao, B. Gancarz, J. A. den Boon, and P. Ahlquist.** 2011. Intersection of the Multivesicular Body Pathway and Lipid Homeostasis in RNA Replication by a Positive-Strand RNA Virus. J. Virol. **85:**5494-5503.

227. **Wang, X., W.-M. Lee, T. Watanabe, M. Schwartz, M. Janda, and P. Ahlquist.** 2005. Brome Mosaic Virus 1a Nucleoside Triphosphatase/Helicase Domain Plays Crucial Roles in Recruiting RNA Replication Templates. J. Virol. **79:**13747-13758.

228. **Wang, Z., J. Ni, J. Li, B. Shi, Y. Xu, and Z. Yuan.** 2011. Inhibition of Hepatitis B Virus Replication by cIAP2 Involves Accelerating the Ubiquitin-Proteasome-Mediated Destruction of Polymerase. Journal of Virology **85:**11457-11467.

229. **Wei, T.** 2010. Sequential recruitment of the endoplasmic reticulum and chloroplasts for plant potyvirus replication. J. Virol. **84:**799-809.

230. **Weiss, S. R., and S. Navas-Martin.** 2005. Coronavirus Pathogenesis and the Emerging Pathogen Severe Acute Respiratory Syndrome Coronavirus. Microbiology and Molecular Biology Reviews **69:**635-664.

231. **Weissman, A. M.** 2001. Themes and variations on ubiquitylation. Nature reviews. Molecular cell biology **2:**169-178.

232. **Welchman, R. L., C. Gordon, and R. J. Mayer.** 2005. Ubiquitin and ubiquitin-like proteins as multifunctional signals. Nat Rev Mol Cell Biol **6:**599-609.

233. **White, J. P., A. M. Cardenas, W. E. Marissen, and R. E. Lloyd.** 2007. Inhibition of Cytoplasmic mRNA Stress Granule Formation by a Viral Proteinase. Cell host & microbe **2:**295-305.

234. **Widjaja, I., E. de Vries, D. M. Tscherne, A. Garcia-Sastre, P. J. M. Rottier, and C. A. M. de Haan.** 2010. Inhibition of the Ubiquitin-Proteasome System Affects Influenza A Virus Infection at a Postfusion Step. J. Virol. **84:**9625-9631.

235. **Xia, Z., A. Webster, F. Du, K. Piatkov, M. Ghislain, and A. Varshavsky.** 2008. Substrate-binding sites of UBR1, the ubiquitin ligase of the N-end rule pathway. J Biol Chem **283:**24011-24028.

236. **Xie, Y., and A. Varshavsky.** 2000. Physical association of ubiquitin ligases and the 26S proteasome. Proc Natl Acad Sci U S A **97:**2497-2502.

237. **Xie, Y., and A. Varshavsky.** 2001. RPN4 is a ligand, substrate, and transcriptional regulator of the 26S proteasome: a negative feedback circuit. Proc Natl Acad Sci U S A **98:**3056-3061.

238. **Yamanaka, T.** 2002. Complete inhibition of tobamovirus multiplication by simultaneous mutations in two homologous host genes. J. Virol. **76:**2491-2497.

239. **Yamanaka, T.** 2000. TOM1, an Arabidopsis gene required for efficient multiplication of a tobamovirus, encodes a putative transmembrane protein. Proc. Natl Acad. Sci. USA **97:**10107-10112.

240. **Yang, F., J. M. Robotham, H. Grise, S. Frausto, V. Madan, M. Zayas, R. Bartenschlager, M. Robinson, A. E. Greenstein, A. Nag, T. M. Logan, E. Bienkiewicz, and H. Tang.** 2010. A Major Determinant of Cyclophilin Dependence and Cyclosporine Susceptibility of Hepatitis C Virus Identified by a Genetic Approach. PLoS Pathog **6:**e1001118.

241. **Ye, J., C. Wang, R. Sumpter, Jr., M. S. Brown, J. L. Goldstein, and M. Gale, Jr.** 2003. Disruption of hepatitis C virus RNA replication through inhibition of host protein geranylgeranylation. Proc Natl Acad Sci U S A **100:**15865-15870.

242. **Zhang, H., and Y. Ge.** 2011. Comprehensive Analysis of Protein Modifications by Top-Down Mass Spectrometry. Circulation: Cardiovascular Genetics **4:**711.

243. **Zhang, J., A. Diaz, L. Mao, P. Ahlquist, and X. Wang.** 2012. Host acyl coenzyme a binding protein regulates replication complex assembly and activity of a positive-strand RNA virus. J Virol **86:**5110-5121.

244. **Zhang, S., Y. Skalsky, and D. J. Garfinkel.** 1999. MGA2 or SPT23 is required for transcription of the delta9 fatty acid desaturase gene, OLE1, and nuclear membrane integrity in Saccharomyces cerevisiae. Genetics **151:**473-483.

Appendix A

INFERRING HOST SUBNETWORKS INVOLVED IN VIRAL REPLICATION

This section is in preparation for submission to PLoS Computational Biology, and represents work by the following authors:

Deborah Chasman[1,2], Brandi Gancarz[3], Linhui Hao[3,4], Michael Ferris[1], Paul Ahlquist[3,4,5], and Mark Craven[2,1]

[1]Department of Computer Sciences, [2]Department of Biostatistics and Medical Informatics, [3]Institute for Molecular Virology, [4]Howard Hughes Medical Institute, and [5]Morgridge Institute for Research, University of Wisconsin–Madison, USA.

Abstract

Motivation: Systematic, genome-wide loss-of-function experiments can be used to identify host factors that directly or indirectly facilitate or inhibit the replication of a virus in a host cell. We present an approach that uses an integer linear program to infer the pathways through which those host factors modulate viral replication. The input is a set of viral phenotypes observed in single-host-gene mutants and a background network consisting of a variety of host intracellular interactions. The output is an ensemble of subnetworks that provides a consistent explanation for the measured phenotypes, predicts which unassayed host factors modulate the virus, and predicts which host factors are the most direct interfaces with the virus.

Results: We analyze data from experiments screening the yeast genome for genes modulating the replication of two RNA viruses. We conduct a cross-validation experiment in which we predict whether held-aside test genes have an effect on viral replication. Our approach is able to make these predictions with accuracy greater than or equal to than several baseline methods that do not predict mechanistic pathways. Additionally, we use our approach to predict which unassayed host genes are likely to be involved in viral replication. Multiple predictions are supported by recent independent experimental data.

A.1 INTRODUCTION

A virus requires host cellular machinery to complete its life cycle. Understanding the interactions that occur between viruses and their hosts can contribute to the development of preventative and therapeutic methods to control their effects on human health. To this end, several recent studies have performed genome-wide loss-of-function experiments to identify host factors that modulate the virus life cycle in a host cell. These studies have used either yeast mutant libraries (12, 24, 36, 37) or RNA interference (4, 6, 15, 22, 23) to systematically suppress the production of host gene products. For each host gene that is manipulated, the effect on the virus is assessed by measuring the replicative yield of viral genetic material or viral proteins relative to a control. Typically, these genome-wide screens identify a large number of host genes, which we refer to as *hits*, whose loss has a significant effect on the virus. However, the screens themselves do not reveal how these hits are organized into the pathways that modulate the virus, nor do they indicate which host genes directly interface with a viral component, and which indirectly affect the virus. We consider the computational task of inferring subnetworks that hypothesize the pathways through which each hit modulates viral replication. The value of these inferred subnetworks is that they can be used to (i) predict which unassayed genes may be involved in viral replication, (ii) interpret the role of each hit in modulating the virus, and (iii) guide further experimentation that is aimed at uncovering and validating the mechanisms of host-virus interaction.

We present an approach that uses an integer linear program to infer the pathways that are involved in the life cycle of a virus in a host cell. Given phenotypes measured in a genome-wide loss-of-function assay, and a *background network* characterizing known interactions among host cellular components, our approach infers subnetworks of these interactions that provide consistent explanations for the measured phenotypes. Inferring such subnetworks entails predicting

which components of the network are the most direct *interfaces* to the virus, and determining at least one directed, consistent path from every hit to the virus. We evaluate our approach by conducting a cross-validation experiment in which we predict whether held-aside test genes are hits or not. Our computational experiments demonstrate that our approach is able to make these predictions with accuracy that is comparable to leading baseline methods that do not predict mechanistic pathways. Additionally, we use our approach to predict which unassayed genes are likely to be modulators of viral replication, and we discuss independent biological evidence supporting a selection of these predictions.

Figure A.1 provides an overview of our computational approach, with A.1(A) illustrating what is provided as input to the approach using a graph representation. Nodes in the graph represent genes, protein complexes and small molecules, and the color of a gene node specifies the observed phenotype when production of the gene's product is suppressed. The connecting edges in the graph provide a simplified representation of known interactions among genes, complexes and small molecules. Figure A.1(B) shows the various phenotype labels, and the types of interactions we employ and how they are distilled into a simplified representation in which each interaction is represented by an edge indicating the *direction* and *sign* (activating or inhibiting) of the interaction, when these properties are known. Figure A.1(C) shows the result of the inference process, which is a subnetwork that explains the phenotype of each hit. In the subnetwork shown, genes **K** and small molecule **M** are predicted to be interfaces to the virus, as indicated by the directed edges to the virus node. Some of the edges and nodes, shown in gray, are deemed to be not relevant to viral replication, and hence not useful for explaining the measured phenotypes. The other edges, which are considered part of the inferred subnetwork, are assigned directions and signs in cases where these properties are not specified by the background network. The signs and directions for the relevant edges are set such that there is at least one consistent pathway

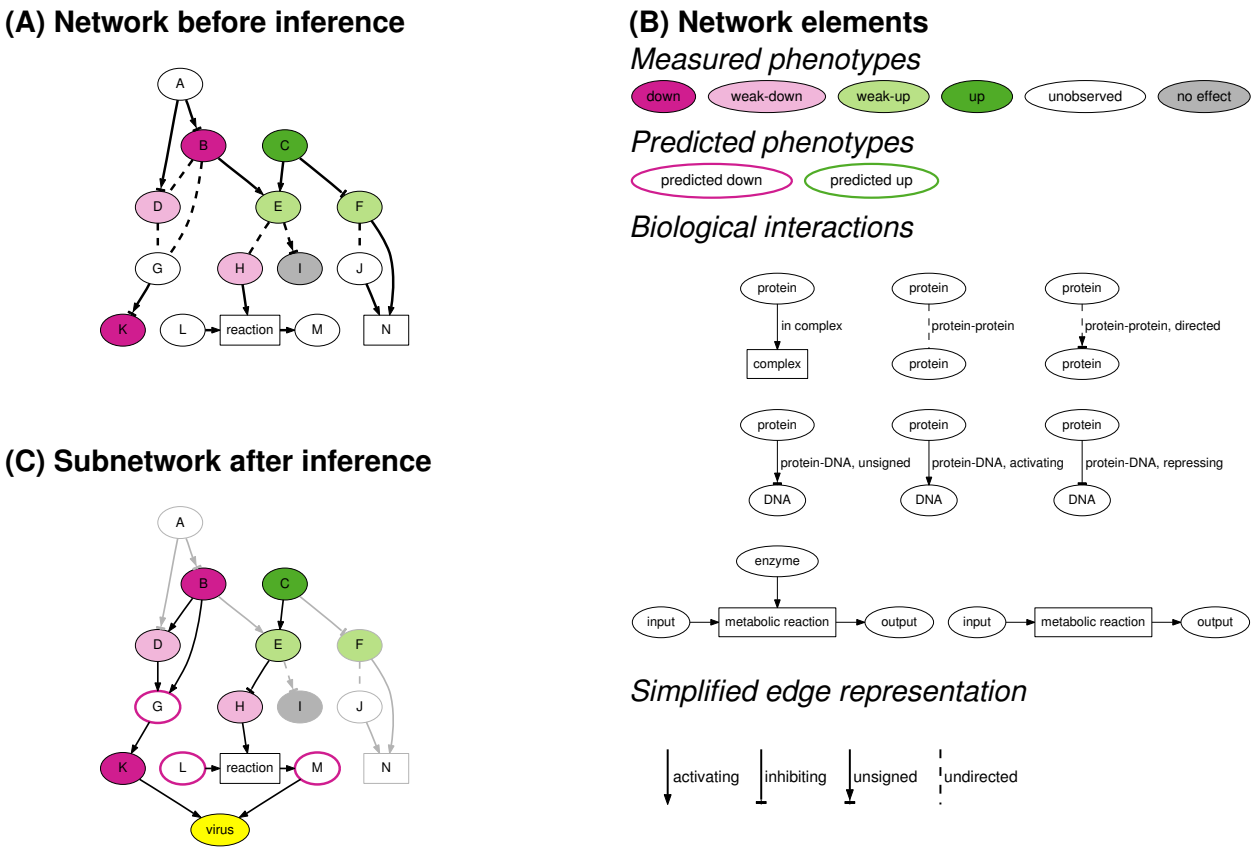

Figure A.1: **(A)** The inputs to our subnetwork inference approach: phenotypes measured in a loss-of-function assay, and a background network characterizing known interactions. **(B)** The network elements represented in panels **A**, **C**, and other figures. **(C)** An inferred subnetwork for the given inputs. The subnetwork includes a directed, consistent path linking each hit (gene with an **up** or **down** phenotype) to the virus. Edges shown in gray are not included in the subnetwork.

linking each hit to the virus. For example, gene **E** has a **weak-up** phenotype and modulates the virus by inhibiting **H** which catalyzes a reaction producing the interface molecule **M**. Additionally, the subnetwork predicts that several genes and small molecules (**G**, **L**, and **M**) whose phenotypes were unobserved are actually key host factors involved in viral replication.

Our work is related to methods that address several different categories of problems: finding mechanistic explanations for source-target pairs, subnetwork extraction, candidate gene discovery, and gene set enrichment.

One closely related task is to infer the physical interactions that mediate the observed direct or indirect relationships between a source gene and a target gene. The input to these methods is a set of source-target pairs and a background network consisting of unsigned protein-protein and/or protein-DNA interactions. The output is a subnetwork that provides a connection between each source and target. Most closely related to our work are the approaches that globally infer a subnetwork to account for all given pairs. The Markov network-based Physical Network Model (46) and the integer programming-based SPINE (32) both infer subnetworks in which each source must be connected to its targets by one or more acyclic pathways, and in which the sign of each edge is also inferred. The Physical Network Model also infers directions for edges. Other methods (13, 27, 39) infer edge directions, but not edge signs or node phenotypes. Yosef *et al.* (47) infer rooted trees that connect a set of sources with a set of targets. Additionally, some methods account for source-target pairs separately, rather than in a global inferred subnetwork (38, 42). Others employ genetic interactions or correlation of mRNA expression in addition to protein-protein interactions to infer indirect or direct relationships between genes (31, 44). Our work has similarities to these approaches, particularly the integer program approaches, but differs in some key respects. In our setting, the common target of all hits – the virus – is external to the background network, and the host factors that interact with it directly must be predicted.

Additionally, our background network encompasses a greater variety of biological interactions than the background networks used by these approaches. Unlike the methods that use mRNA expression profiles as the basis for determining direct or indirect relationships between genes, ours uses phenotypes derived from a genome-wide mutant assay.

Other methods apply graph kernels or flow algorithms to an interaction network to predict and prioritize additional hit genes (5, 29, 43). Notably, Murali *et al.* (29) predict which genes modulate HIV replication in human cell lines. Like these methods, our approach uses a gene ranking method to prioritize genes for inclusion in the inferred subnetwork. However, these methods themselves do not infer consistent, directed pathways, nor do they predict which host factors directly interact with the virus.

Other work has considered the task of extracting specific types of connecting structures from a background network when a biologically-motivated node- and/or edge-weighting function is available. The structures include rooted trees (34), Steiner trees (8, 35), random walks and short paths (10), parallel pathways (25), dense highly-connected subnetworks (3), and subnetworks that cover pairs of genes (48). Unlike our method, these approaches do not distinguish (or infer) phenotype signs and edge signs, nor do they apply global constraints to the extracted subnetwork, such as a small number of interfaces.

More distantly related to our work, gene set enrichment techniques are widely used to interpret hit sets identified by high-throughput experiments. These methods identify which pre-defined biological components and processes, such as Gene Ontology annotations or KEGG pathways (2, 21), are represented in a set of genes (17). In contrast, our method does not rely on predefined gene sets when predicting which interactions are relevant to host-virus interactions.

A.2 DATA

The input to our approach consists of a set of viral phenotypes observed in a loss-of-function experiment and a background network of intracellular interactions.

A.2.1 Experimental observations

We analyze data from experiments screening the yeast genome for genes modulating the replication of Brome Mosaic Virus (BMV) (12, 24) and Flock House Virus (FHV) (L.H. and P.A., unpublished). The experiments measure the replication of the virus in a yeast host when the expression of one gene is partially or completely depleted. Yeast mutant strains allow the majority of cell genes (of about 5,800 total genes in yeast) to be screened in parallel. For nonessential genes, the experiment was performed using the yeast deletion library (45). Essential genes were screened using a collection of yeast strains, each with a single essential gene promoter replaced by a doxycycline-repressible promoter, allowing repression of gene expression by adding doxycycline to the growth medium (28). The BMV and FHV data sets include at least two replicate assays for each mutant strain.

Each mutant strain was grown and transformed with two plasmids expressing viral components. The plasmid expressing viral RNA also contained a luciferase reporter gene, allowing the accumulation of viral RNA to be measured by the intensity of the light produced from luciferase gene expression. The output of the assay is the fold-change in accumulation of viral RNA between each mutant strain and the control. Let m be the virus expression level in the mutant strain, and c be the expression level in the control strain. Fold-change is computed as $-\frac{c}{m}$ if $m < c$, or $\frac{m}{c}$ if $m > c$.

We derive a discrete label for each assayed gene based on the sign, magnitude, and repro-

ducibility of the fold-change across replicate assays. If a mutant reproducibly yields a decrease in viral replication, the interpretation is that the missing gene product directly or indirectly facilitates virus replication. We label such mutants with a **down** or **weak-down** phenotype, depending on the magnitude of the fold-change. Conversely, the interpretation for a mutant that reproducibly results in an increase in viral replication is that, when expressed, the missing gene product directly or indirectly inhibits the replication of the virus. We label such mutants **up** or **weak-up**. The mutants with high-magnitude phenotypes, **down** and **up**, are considered *hits*. The threshold used to divide the hit and weak phenotypes was determined separately for each screen. If the sign of the fold-change is different across replicates, the gene is labelled **no-effect**. Finally, genes that were either not screened, or for which the yeast colony did not grow, are labelled **unobserved**. Table A.1 presents the distribution of phenotypes considered here for the BMV and FHV assays. While additional genes were assayed in the experiments, we limit our analysis to only those genes that are connected to some other host factor in the background network.

A.2.2 Background network

The interactions in the subnetworks inferred by our method are drawn from a background network that we have assembled from various publicly available data sets. The network consists of 5,709 entities and 13,633 interactions. The entities represent gene products, protein complexes, and small molecules. The interactions describe protein-protein and protein-DNA interactions, post-translational modifications of proteins, protein complex membership, transcriptional regulatory interactions, and metabolic reactions. High-confidence interactions were selected from each database using stringent filters; for example, protein-protein interactions were selected only if the interaction was observed by at least two different experimental methods. The details of the intracellular interaction network are described in Tables A.2 and A.3.

We represent the biological network as a graph in which the host factors are represented as nodes, and the interactions between the host factors are represented as edges. Since we are focused on inferring the direction and consistency of pathways, we do not need to represent all of the distinctions among the various types of interactions. Instead, we use a simple, general representation for all of the interactions. In this representation, each edge may have a direction and/or a sign. The direction determines which interactor is the source, and which is the target. For example, for a protein-DNA interaction, a transcription factor is the source, and the regulated gene is the target. The sign describes the effect, positive or negative, of the source on the synthesis, stability, or specific activity of the target. Edges with a positive sign are called *activating*, whereas edges with a negative sign are called *inhibiting*. For example, we represent the involvement of a protein in a complex as a directed, activating edge because the gene product (source) positively contributes to the activity of the complex (target). Not all edges in the background network have signs or directions: protein-protein interactions, for example, are undirected and unsigned.

While most of the edges represent binary interactions, the metabolic reactions are ternary interactions. In our representation, metabolic reactions are hyper-edges consisting of two possible sources (the input to the reaction, the enzyme that catalyzes the reaction) and one target (the output of the reaction). We consider the metabolic reactions to be activating, under the assumption that the enzyme and input are both required to produce the output.

A.3 METHODS

We have developed an integer-programming-based approach to infer a subnetwork of interactions that are relevant to virus replication in a host cell. The approach infers subnetworks that have the following properties:

- The subnetwork includes as many nodes as possible, subject to the following constraints.

Table A.1: Distribution of phenotypes for suppressed host genes.

Phenotype	BMV	FHV
up (hit)	48	49
weak-up	622	801
weak-down	1,072	652
down (hit)	55	7
no-effect	1,070	977

Table A.2: Node entities in the background network.

Node type	Count
Yeast ORFs	4,143
Small molecules	1,018
Protein complexes	504
Small RNAs	34
Mitochondrial ORFs	10

Table A.3: Interactions in the background network.

Interaction	Source	Sign.	Dir.	Count
Protein-protein	(41)	N	N	4,168
Post-translational modifications	(41)	N	Y	478
Protein-DNA	(26)	N	Y	4,097
Protein-DNA	(14)	Y	Y	924
Protein-DNA	(9)	Y	Y	389
Protein-complex	(16, 33)	Y	Y	1,920
Ternary metabolic reactions	(16)	Y	Y	1,088
Orphan metabolic reactions	(16)	Y	Y	569

(A) Step 1: Determine candidate interfaces

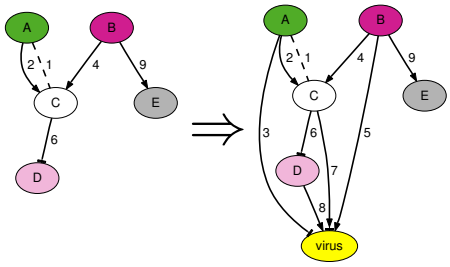

(B) Step 2: Determine candidate pathways

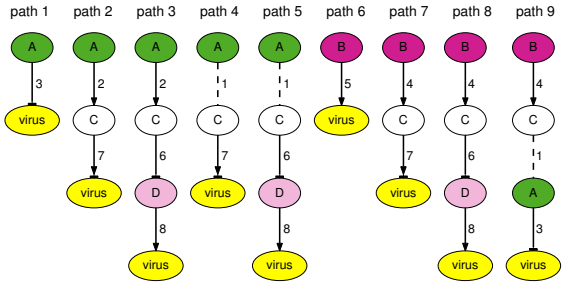

(C) Step 3: Infer an ensemble of consistent subnetworks

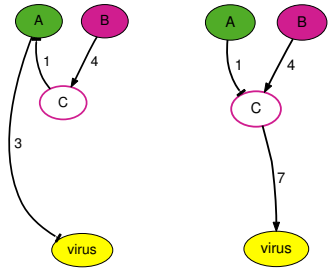

Figure A.2: The steps of our subnetwork inference approach. Each edge is shown with a numeric identifier for cross-reference.

- All hits are accounted for by at least one pathway to an interface.
- A small number of interfaces are predicted.
- The sign of each edge in the subnetwork is consistent with the phenotypes of the interacting host factors.

A.3.1 Overview of approach

In this section we present a high-level overview of the three steps of our approach. Figure A.2 illustrates each step applied to a small example network.

Step 1: Determine candidate interfaces. One aspect of the inference procedure is to predict which host factors most directly interact with a viral component. We refer to these as *interfaces*. To represent the possibility of any host component interacting with a viral component, we add a special “virus" node to the background network, and add a directed edge from each node in the background network, except those with a **no-effect** phenotype, to the virus node. We refer to the edges to the virus node as *external* edges, and edges between host factors as *internal* edges. Figure A.2(A) depicts the addition of the external edges to the five-node background network shown. Naturally, the set of external edges could be constrained if additional knowledge were available (*e.g.*, experimental evidence for specific interactions between host and viral proteins).

Step 2: Determine candidate pathways. An inferred subnetwork must account for each hit by either predicting it to be an interface itself, or by providing a directed, acyclic pathway to a predicted interface. We enumerate all possible pathways of a specified depth leading from each hit to the virus node. Nodes with a **no-effect** phenotype are not included in candidate pathways. Figure A.2(B) shows the candidate pathways for the given network.

Step 3: Infer an ensemble of consistent subnetworks. An inferred subnetwork comprises a union of pathways that consistently account for the hits and predict which host factors are interfaces. We refer to a selected pathway as a *relevant* pathway. Similarly, we refer to an edge (node) in a relevant pathway as a *relevant edge (node)*. If an external edge is predicted to be relevant, the source node (which is a host factor) is predicted to be an interface.

We infer the phenotypes of all relevant nodes and the signs of all relevant edges in cases

where they are not specified in the given data. (We do not infer these attributes for nodes and edges that are deemed irrelevant.) For an edge to be considered relevant, its sign must be consistent with the phenotypes of the interacting nodes. If a relevant edge has an activating sign, then the interactors should have the same phenotype. If a relevant edge is inhibiting, the signs of the phenotypes of the interactors should be opposite each other. We refer the network in Figure A.2(A) to illustrate this notion of consistency. In the background network, notice that both nodes **A** and **B** activate node **C**. If edge 2 is relevant, node **C** would have the phenotype **up**. However, if edge 4 is relevant, node **C** would have the phenotype **down**. Since a relevant node can have only one phenotype, we cannot predict that both edges 2 and 4 are relevant. Similarly, we can use the idea of consistency to infer the sign of unsigned edges. If both edges 4 and 1 are relevant, and the inferred phenotype for node **C** is **down**, then we infer that edge 1's sign is inhibiting.

The inference process also assigns a direction to all relevant, undirected edges. In the inferred subnetwork, each hit must be able to reach an interface by a directed pathway. Since a relevant edge can only take one direction, paths 4 and 9 in the example cannot both be predicted to be relevant because they require opposite directions for edge 1.

Inference is a matter of determining the optimal combinations of relevant pathways, node phenotypes, and edge signs and directions. Figure A.2(C) shows two inferred subnetworks that account for both hits **A** and **B** using one interface.

To infer subnetworks, we solve an integer program that encodes the properties listed as the beginning of this section in terms of constraints and an objective function. The program is described in detail in Section A.3.2. In our implementation, we use the GAMS modelling system (11) to build the integer program, and solve it using the CPLEX MIP solver (20).

Many of the interactions in the background network are unsigned and undirected. Conse-

quently the space of possible subnetworks that meet our requirements is very large. To represent this space, we infer an ensemble of subnetworks, where each subnetwork accounts for all of the hits. The CPLEX MIP solver uses a branch-and-cut approach to find a single optimal solution to the IP. Additional solutions can be found by revisiting branches that were pruned during the initial solution process. Each such solution represents a different subnetwork in the ensemble. We assess confidence in the relevance of a pathway (edge) as the fraction of subnetworks in the ensemble containing that pathway (edge). We measure confidence in the same way for inferred phenotypes, edge signs, and edge directions.

A.3.2 Integer program

Subnetwork inference is performed by solving a mixed integer linear program (IP). The IP consists of a set of linear constraints and an objective function, all of which are defined over a set of integer variables that characterize possible subnetworks. The values of some of the variables are determined by the input to the inference process (the phenotypes and background network), whereas others are inferred by the IP.

First, we describe the variables and notation. The predicted relevance of a pathway is represented with the variable σ, which takes the value 1 if the pathway is included in the inferred subnetwork, and 0 if it is not. As many as four variables describe each edge. The predicted relevance of an edge is represented with the variable x, which takes the value 1 if the edge is in at least one relevant pathway. The sign of an edge is represented by two mutually exclusive variables a and h. If $a = 1$ ($h = 1$), the edge is predicted to be relevant, and inferred to be activating (inhibiting). If an edge is not predicted to be relevant, $x = a = h = 0$. For activating edges given in the background network, h is fixed at 0; similarly, for inhibiting edges, a is fixed at 0. Each node has two variables: y, representing whether or not the node is present in any relevant pathways,

and v, representing its observed or inferred phenotype sign. For hits, we fix $y = 1$ to require that they are present. For **down** and **weak-down** genes, we fix $v = 0$; for **up** and **weak-up** genes, we fix $v = 1$. The variables are summarized in Table A.4. Figure A.3 shows the variables used to characterize one specific example pathway.

The interaction network is represented as a graph of nodes $\mathcal{N}$, edges $\mathcal{E}$, and pathways $\mathcal{P}$. $\mathcal{E}(p)$ and $\mathcal{N}(p)$ refer to the edges and nodes in a particular pathway p, and $\mathcal{N}(e)$ refers to the nodes in a particular edge. $\mathcal{H} \subseteq \mathcal{N}$ is the set of hits. Each pathway p specifies a direction for each of its undirected edges e, which is denoted as $dir(p, e)$. The set of edges $\mathcal{E} = (\mathcal{I} \cup \mathcal{X})$, where $\mathcal{I}$ is the set of internal edges, $\mathcal{X}$ is the set of external edges, and $\mathcal{I} \cap \mathcal{X} = \emptyset$. $\mathcal{U} \subseteq \mathcal{I}$ is the set of undirected internal edges. $\mathcal{M} \subseteq \mathcal{I}$ is the set of metabolic interaction edges. We denote an edge between nodes n_i and n_j as (n_i, n_j).

We encode the properties described at the beginning of this section in terms of an objective function and constraints in a integer program. Now we describe the details of this encoding.

As many nodes as possible are in the subnetwork. Because a hit may modulate the virus through several pathways, we want to include consistent nodes and edges generously. We use a graph kernel method to prioritize non-hit nodes for inclusion in the subnetwork. (All hits are already required to be included.) Specifically, we assign scores to nodes using a regularized Laplacian kernel (40). Intuitively, a node's score is a function of its proximity to each hit. Let A be the $|\mathcal{N}|$**x**$|\mathcal{N}|$ symmetric adjacency matrix, where $A_{ij} = 1$ if there is any edge between nodes n_i and n_j in the biological background network, and 0 otherwise. Let D be the diagonal degree matrix derived from A, where $D_{ii} = \sum_j^{|\mathcal{N}|} A_{ij}$. The normalized Laplacian L is then $D^{-1/2}AD^{-1/2}$, and the kernel $K(\lambda) = [I + \lambda L]^{-1}$. Let q be a vector of length $|\mathcal{N}|$ where $q_i = 1$ if $n_i \in \mathcal{H}$ and 0 otherwise. For each node n_i, the score $score(n_i)$ is calculated as $\sum_j^{|\mathcal{N}|} K(\lambda)_{ij}\ q_j$, with higher values indicating that the node's neighborhood is denser in hits. The objective function of our

Table A.4: Integer program variables.

Variable	Interpretation	Values
Pathways		
σ	Relevant	no=0, yes=1
Edges		
x	Relevant	no=0, yes=1
a	Relevant, activating	no=0, yes=1
h	Relevant, inhibiting	no=0, yes=1
d	Direction	back=0, forward=1
Nodes		
y	Relevant	no=0, yes=1
v	Phenotype	down=0, up=1

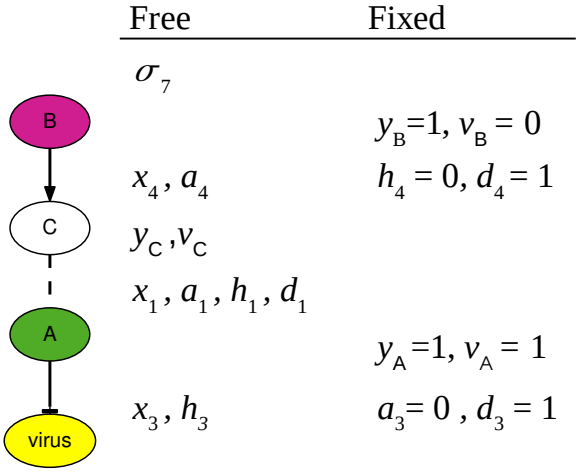

Figure A.3: Variables for pathway 7 from Figure A.2. The values of some variables are fixed by the data. The values of free variables are determined by the IP.

integer program maximizes the combined score of the non-hit relevant nodes.

$$max \left(\sum_{n \in \mathcal{N} - \mathcal{H}} score(n)\ y_n \right)$$

Our other subnetwork desiderata are represented as constraints that are used to select which edges and pathways are deemed relevant.

A small number of interfaces are inferred. The true number of interfaces is unknown. As a heuristic, we limit the number of interfaces in the inferred subnetwork to a specified integer γ. In Section A.4, we discuss experiments that vary this parameter.

$$\left(\sum_{e \in \mathcal{X}} x_e \right) \leq \gamma$$

Each hit is accounted for by the subnetwork. Each hit must participate in at least one relevant edge.

$$\forall n \in \mathcal{H} \quad \left(\sum_{e : n \in \mathcal{N}(e)} x_e \right) \geq 1$$

All edges in a relevant pathway are relevant. An edge must be in a relevant pathway to be relevant. A relevant pathway must contain all relevant edges.

$$\forall e \in \mathcal{E} \quad x_e \leq \sum_{p \in \mathcal{P}\ :\ e \in \mathcal{E}(p)} \sigma_p$$

$$\forall p \in \mathcal{P} \quad (\forall e \in \mathcal{E}(p) \quad \sigma_p \leq x_e)$$

All nodes in a relevant edge are relevant. A node is relevant if it is connected to a relevant edge,

and both nodes for a relevant edge must be relevant.

$$\forall n \in \mathcal{N} \quad y_n \leq \sum_{e \in \mathcal{E} \,:\, n \in \mathcal{N}(e)} x_e$$

$$\forall e \in \mathcal{E} \quad (\forall n \in \mathcal{N}(e) \quad x_e \leq y_n)$$

All relevant edges must be either activating or inhibiting. We must infer a single sign for every relevant edge.

$$\forall e \in \mathcal{E} \quad a_e + h_e \leq 1$$

$$x_e = a_e + h_e$$

The sign of a relevant edge is consistent with the phenotypes of the participating nodes. The following set of constraints guide the inference of phenotypes and edge signs for relevant nodes and edges. If a relevant internal edge $e = (n_i, n_j)$ is activating, the interacting nodes must have the same phenotype.

$$\forall e = (n_i, n_j) \in \mathcal{I} \quad v_{n_i} + a_e \leq 1 + v_{n_j}$$

$$v_{n_j} + a_e \leq 1 + v_{n_i}$$

If a relevant internal edge $e = (n_i, n_j)$ is inhibiting, the interacting nodes must have opposite phenotypes.

$$\forall e = (n_i, n_j) \in \mathcal{I} \quad h_e + v_{n_1} + v_{n_2} \leq 2$$

$$h_e \leq v_{n_1} + v_{n_2}$$

In a relevant ternary edge, all three nodes have the same phenotype. For an edge $e = (n_i, n_z, n_o) \in \mathcal{M}$, n_i, n_z and n_o represent the input, enzyme, output of the reaction.

$$\forall e = (n_i, n_z, n_o) \in \mathcal{M} \quad v_{n_i} + a_e \leq 1 + v_{n_o}$$
$$v_{n_o} + a_e \leq 1 + v_{n_i}$$
$$v_{n_z} + a_e \leq 1 + v_{n_o}$$
$$v_{n_o} + a_e \leq 1 + v_{n_z}$$

In a relevant pathway, all edges are directed toward the interface. Relevant undirected edges must be oriented toward the virus node at the end of the pathway. This direction is determined in Step 2, and is given by $dir(p, e)$. $I()$, the indicator function, returns 1 if the edge's inferred direction corresponds to the direction that the pathway requires for it.

$$\forall p \in \mathcal{P} \quad (\forall e \in \mathcal{E}(p) \;\; \sigma_p \leq I\left(d_e = dir(p, e)\right))$$

A.3.3 Heuristic Refinements

Here we present two additional heuristics that are based on other sources of background knowledge.

Screening the candidate pathways. We use a heuristic to screen the initial pool of candidate pathways. Hughes *et al.* (18) and Mnaimneh *et al.* (28) provide source-target pairs in which each pair describes the direct or indirect effect of a single-gene mutant (the source) on the mRNA expression of another yeast gene (the target). We posit that the directions of these pairs are likely to be relevant to host-virus interactions. We use the following heuristic to filter the candidate pathways before proceeding with inference: If two genes are a source-target pair, the source

must be an ancestor of the target in any relevant pathway in which they both occur. Pathways that use source-target pairs out of order are discarded.

Constraining the proportions of edge signs. In the BMV and FHV screens, the sign of a hit's phenotype is highly correlated with the phenotype signs of its neighbors in the background network. Therefore, we require that the proportion of activating internal edges in the inferred network is close to a proportion estimated from data. Considering all pairs of hits that interact (under any interaction) in the background network, we record the proportion of pairs with the same phenotype. For the BMV dataset, this is about 95%; for FHV, it is 100%. The following constraint gives a lower bound, α on the proportion of activating internal edges. By default, we set this $\alpha = 0.9$ to allow a small deviation from the proportion estimated from the data set.

$$\sum_{e \in \mathcal{I}} a_e \geq \quad \alpha \sum_{e \in \mathcal{I}} x_e$$

A.4 RESULTS

Although it is not practicable to fully evaluate our inferred subnetworks, we can assess their validity, in part, by determining how accurately they predict phenotypes that are not provided as input to the inference process.

A.4.1 Cross-validated phenotype prediction

We first describe an experiment in which we assess the accuracy of our approach in predicting whether test genes with held-aside phenotypes are hits or not. We refer to this as the *hit-prediction* task. Using a cross-validation methodology, we hold aside the measured phenotype for one gene at a time. The set of genes that are held-aside as test cases for the BMV

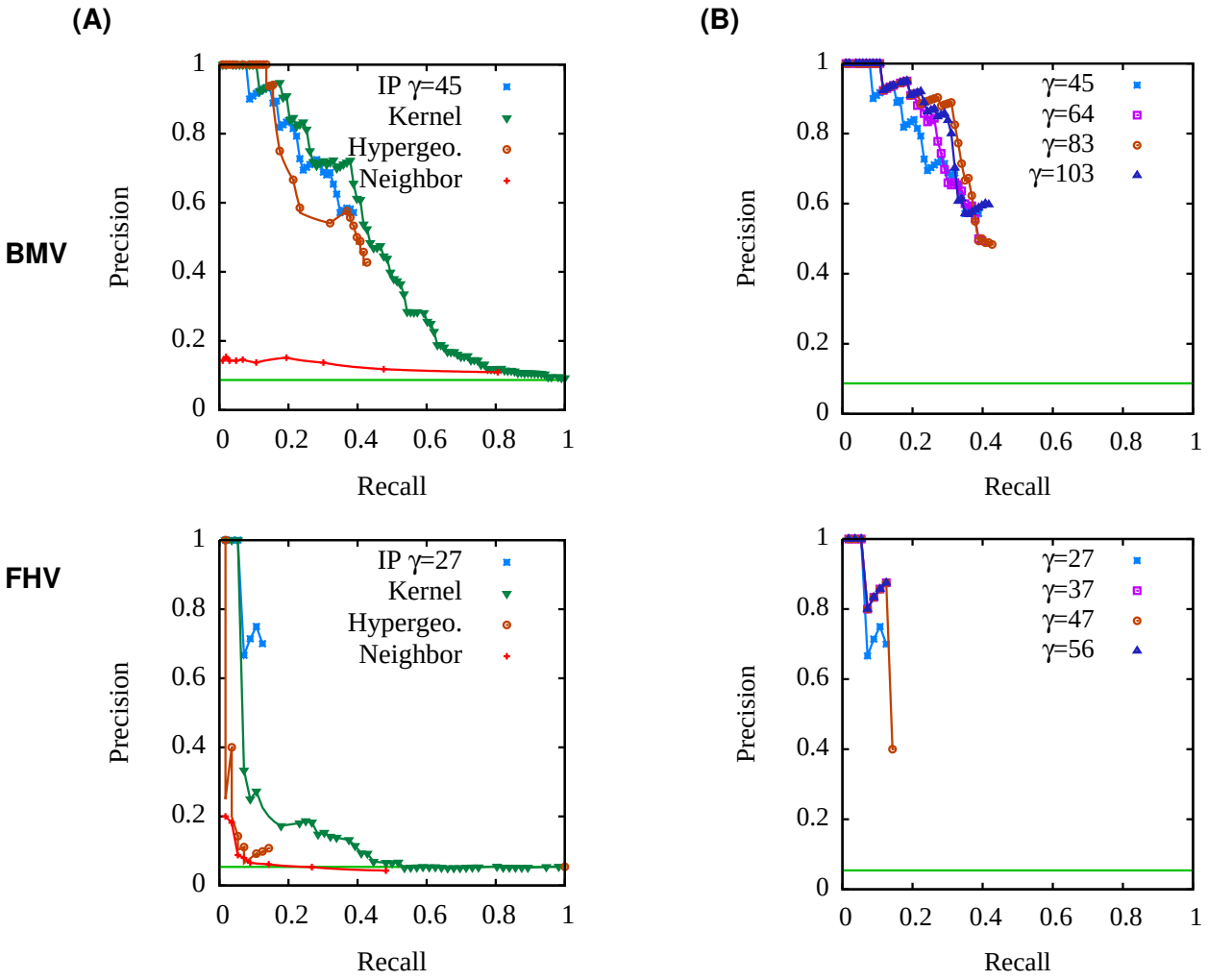

Figure A.4: Precision-recall curves for the hit-prediction task (BMV top, FHV bottom). **(A)** Comparison of our IP approach to the baselines. **(B)** The effect of varying γ, the number of interfaces.

dataset includes 103 hits (48 **up** and 55 **down**) and 1070 **no-effect** genes. The test set for the FHV dataset comprises 56 hits (49 **up** and 7 **down**) and 977 **no-effect** genes.

When a given gene is held aside, it is treated as if its phenotype has the **unobserved** label during the inference process. We use our integer programming approach to infer an ensemble of subnetworks for each held-aside test case. An individual subnetwork may include the held-aside gene and provide a predicted **up** or **down** phenotype for it, or it may exclude the gene. We assess our confidence in whether the gene is a hit or not by determining the fraction of subnetworks in which it is predicted to have an **up** or **down** phenotype. By varying a threshold on these confidence values, we can plot a precision-recall curve characterizing the predictive accuracy of our method. When a sequence of predictions has an equal confidence value, those predictions are ordered according to the score determined by the kernel. *Recall* is defined as the fraction of true hits in the test set that are predicted to be hits, and *precision* is defined as the fraction of predicted hits that are truly hits.

For all experiments, candidate pathways are limited to a depth of 3 interactions, and 100 subnetworks are inferred for the ensemble. The default setting for α, the fraction of inferred activating edges, is 0.9. We initially set γ, the maximum number of interfaces, to the minimum feasible number that can be used to consistently explain all hits. We determine this number for each data set by running a slightly modified version of our IP in which the objective is to minimize the number of interfaces.

We compare the predictive performance of our approach to three baselines. In the first baseline, the scores from the kernel method are used to produce a ranking of the hits and **no-effect** genes, from which we generate a precision-recall curve. The second baseline is a statistical significance test on the number of hits to which a query gene is directly connected in the background network. We use the hypergeometric distribution to assign a p-value to each query node based

on the likelihood of the node being randomly connected to as many or more hits, considering the total number of hits in the background network, and the number of neighbors adjacent to the query node. A third baseline is a naïve nearest-neighbor approach. A prediction is made for a held-aside gene based on the observed phenotypes, strong or weak, of its neighbors in the background network. Each neighbor with an observed phenotype contributes one vote to the prediction for the held-aside gene.

Precision-recall curves for the hit-prediction task are presented in Figure A.4(A). Also shown is the level of precision that would be achieved by predicting that all held-aside genes are hits. For both the BMV and the FHV datasets, the nearest neighbor and hypergeometric test baselines perform poorly in comparison to the kernel method and our method. These results indicates that the local neighborhood of a gene is insufficient for prediction. Using the minimal number of interfaces, our method is able to achieve slightly lower precision than the kernel method alone for BMV, and higher precision for FHV. We note, however, that our method is not able to achieve the same recall as the kernel method or nearest neighbor baseline. The recall of our approach is limited by whether the held-aside gene is included in an inferred subnetwork or not. To some extent, we can increase recall by allowing more interfaces in the subnetworks, and by enlarging the number of subnetworks generated in the ensembles. Moreover, precision is the more important consideration since high recall can always be achieved by combining the predictions of the various approaches.

To assess the robustness of the method with respect to the number of interfaces allowed, we vary γ (the maximum number of interfaces) over four values that range from the minimum feasible number to the number of hits present in the background network. Figure A.4(B) presents precision-recall curves for this experiment. For BMV, the precision of the method increases with the number of interfaces with this range, and recall increases slightly as more interfaces are

allowed. For the FHV dataset, precision also increases slightly as γ increases. Using more generous numbers of interfaces for both datasets, our method's precision also surpasses the kernel method alone.

We also performed additional experiments measuring the predictive accuracy of our heuristic refinements. Space limitations preclude us from showing the results. We tested our method under three different values of the parameter α, the proportion of activating edges: 0.90, 0.80, and 0.70. The results suggest that our approach is fairly insensitive to the value of this parameter. We also empirically assessed the value of the candidate-pathway screening heuristic presented in Section A.3.3. We found that using this heuristic provides a small increase in predictive accuracy.

As a secondary evaluation, we assess the accuracy of the methods in predicting the correct *sign* of the phenotype (**up, down**) for held-aside hits. We refer to this as the *sign-prediction* task. The methodology for this experiment is largely the same as for the previous one. We hold aside a given hit's phenotype, treating the gene as being **unobserved**, infer an ensemble of 100 subnetworks, and then predict the phenotype sign that is inferred by a plurality of subnetworks. The confidence in a predicted sign is given by the fraction of subnetworks in which the gene is predicted to take that sign. We compare the predictive accuracy of our approach to the neighbor voting baselines considered in the previous experiment. We also tested variants of these voting baselines in which neighbors vote using the notion of consistency described in Section A.3. That is, neighbors connected to the held-aside gene by unsigned and activating edges vote with their own phenotype, but neighbors connected by inhibiting edges vote with the phenotype of opposite sign. These consistency-based baselines performed no better than the simple neighbor voting methods, and thus we report the results only for the original baselines here.

We construct accuracy-coverage plots for our IP-based approach and both baselines. Accuracy is measured as the fraction of phenotype signs correctly predicted, and coverage is the

number of hits (with either **up** and **down** phenotype) for which predictions are made. The hits are sorted by the algorithm's confidence in the predicted phenotype, and accuracy is plotted as coverage increases. The results of this experiment are presented in Figure A.5.

For both datasets, the kernel method baseline achieves the strongest accuracy over the entire set of hits. Our IP approach achieves perfect accuracy for the early range of coverage, but loses accuracy faster than the baselines, with the exception of the neighbor baseline on the BMV data. We also evaluated our method's sign prediction accuracy for different values of α. Accuracy decreases with α, a result that supports our use of this heuristic to restrict edge signs.

A.4.2 Phenotype prediction for unobserved host factors

Key motives for our subnetwork-inference approach are to make predictions about which unobserved host factors may be involved in viral replication, and to guide further experimentation aimed at uncovering the mechanisms through which these factors modulate the virus. Toward this end, we apply our inference method the host factors that were not assayed in the genome-wide BMV screens (12, 24), and predict which of them are involved in modulating virus replication (i.e. are hits). To do this, we collect an ensemble of 100 inferred subnetworks using all available phenotype data. Out of 2,875 unobserved host factors in the background network, 117 are predicted to be relevant by all of the 100 inferred subnetworks in the ensemble. Here we discuss independent evidence supporting a selection of these predictions.

In numerous cases, the predicted hits include members of known pathways or protein complexes. In these cases, the inferred subnetworks correctly expanded the relevant complexes with other known components or functional partners that were absent from the given hit sets for technical reasons, such as non-viability of the relevant mutant strain. One example is the inclusion in the inferred subnetworks of LSM2, 3, 5 and 7, which are components of a protein complex that is

represented in the given hits by LSM1, LSM6, PAT1 and DHH1, and is involved in BMV RNA replication and translation (7, 30). Another example is the inferred inclusion of additional members of mediator, a protein complex involved in cellular mRNA synthesis that facilitates BMV replication in the yeast cells used in the genomic assays (24), potentially by facilitating expression of BMV RNA replication factors and templates from DNA plasmids, expression of critical host factors, or both.

Even more important biological validation of our results emerged from additional experimental studies. For example, one subnetwork component from our analysis, as shown in Figure A.6, predicts the involvement of SNF7 and VPS4. SNF7 and VPS4 are genes in the ESCRT pathway, which is involved in membrane bending and scission events in cell division, cell surface receptor down-regulation and other processes (19). Recent studies initiated independently of the work reported here have confirmed the predicted role of ESCRT pathway, and of SNF7 and VPS4 in particular, in facilitating BMV RNA replication (A. Diaz, X. Wang and P. Ahlquist, manuscript in preparation).

Similarly, our analysis predicted the involvement in BMV replication of multiple previously unimplicated components of the cellular ubiquitin-proteasome system, such as the 20S proteasome and components of the 19S regulator complex. Recent additional experiments, including inhibitor studies and other approaches, have confirmed the involvement of the 20S proteasome, the 19S regulator and other factors in this system in multiple aspects of BMV RNA replication (B.G. and P.A., unpublished results). A further example is provided by the inferred involvement of XRN1, a gene involved in RNA degradation. An independent study confirmed the strong impact of XRN1 on BMV replication by showing that a BMV mutant defective in modifying BMV RNAs by the addition of a 5' m^7G cap could not accumulate RNA in wild type yeast but did so in an XRN1 deletion strain (1).

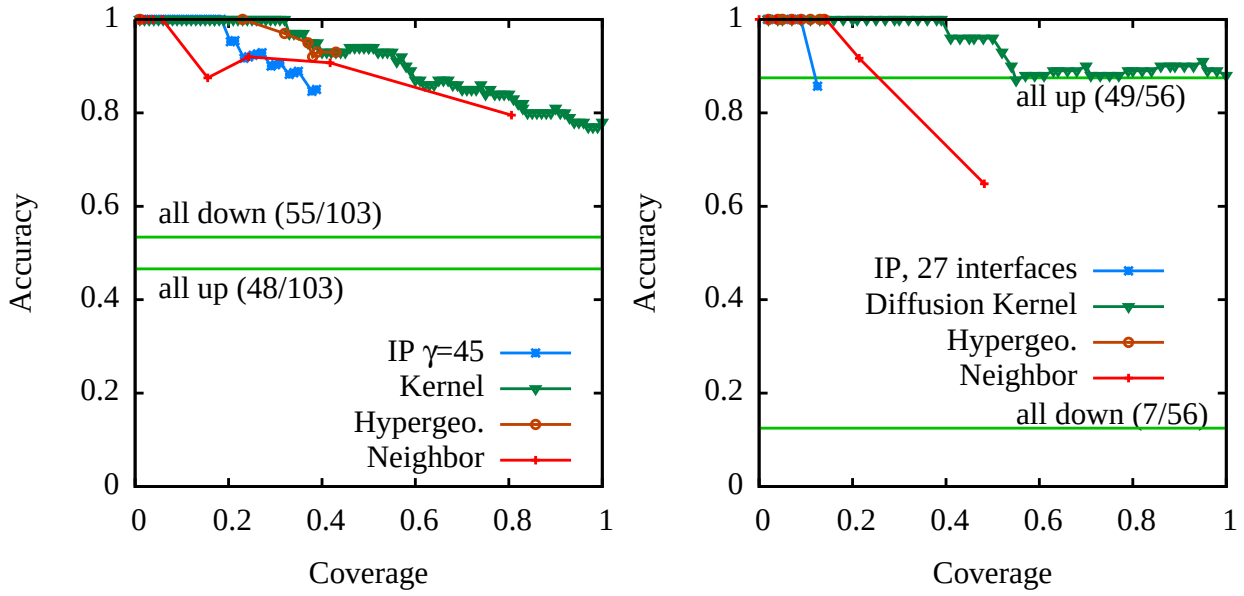

Figure A.5: Accuracy-coverage curves for the sign-prediction task (BMV on the left, FHV on the right).

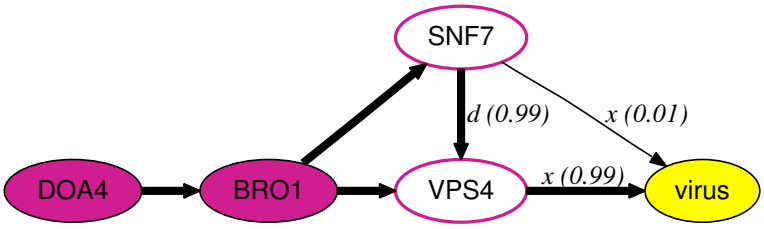

Figure A.6: A component from the inferred subnetwork ensemble showing the predicted involvement of SNF7 and VPS4 in viral replication. For predictions made about edge relevance, sign, and direction, confidence values < 1 are indicated. All other predictions were made by all 100 subnetworks in the ensemble.

A.5 Discussion

We have presented an approach that aims to elucidate how viruses exploit their host cells. Our approach uses known host intracellular interactions to infer subnetworks which provide consistent explanations for phenotypes measured in genome-wide loss-of-function assays. The value of these inferred subnetworks is that they can be used to (i) predict which unassayed genes may be involved in viral replication, (ii) interpret the role of each hit in modulating the virus, and (iii) guide further experimentation. Our empirical evaluation demonstrates that, using a gene-prioritization method as a sub-component, our method is able to predict phenotypes for unassayed genes with accuracy that is comparable to the gene-prioritization method alone.

There are a number of promising directions in which we plan to extend this work. Among them are (i) applying the method to RNAi studies in more complex host networks, (ii) using non-discretized phenotype magnitudes in the analysis, and (iii) incorporating literature-extracted interactions into the background network.

Acknowledgments

This work is supported by NIH/NLM training grant T15-LM007359, NIH grants R01-LM07050 and R01-GM35072, NSF grant CMMI-0928023, and Air Force Grant FA9550-10-1-0101.

REFERENCES

1. **Ahola, T., J. A. den Boon, and P. Ahlquist**. 2000. Helicase and capping enzyme active site mutations in Brome Mosaic Virus protein 1a cause defects in template recruitment, negative-strand RNA synthesis, and viral RNA capping. Journal of Virology. **74**:8803–8811.
2. **Ashburner, M., C. A. Ball, J. A. Blake, D. Botstein, H. Butler, J. M. Cherry, A. P. Davis, K. Dolinski, S. S. Dwight, J. T. Eppig, M. A. Harris, D. P. Hill, L. Issel-Tarver, A. Kasarskis, S. Lewis, J. C. Matese, J. E. Richardson, M. Ringwald, G. M. Rubin, and G. Sherlock**. 2000. Gene Ontology: tool for the unification of biology. Nature Genetics. **25**:25–29.

3. **Bader, G. and C. Hogue**. 2003. An automated method for finding molecular complexes in large protein interaction networks. BMC Bioinformatics. **4**:2. ISSN 1471-2105.

4. **Brass, A., D. Dykxhoorn, Y. Benita, N. Yan, A. Engelman, R. Xavier, J. Lieberman, and S. Elledge**. 2008. Identification of host proteins required for HIV infection through a functional genomic screen. Science. **319**:921–926.

5. **Chen, Y., T. Jiang, and R. Jiang**. 2011. Uncover disease genes by maximizing information flow in the phenome-interactome network. Bioinformatics. **27**:i167–i176.

6. **Cherry, S., T. Doukas, S. Armknecht, S. Whelan, H. Wang, P. Sarnow, and N. Perrimon**. 2005. Genome-wide RNAi screen reveals a specific sensitivity of IRES-containing RNA viruses to host translation inhibition. Genes and Development. **19**:445–452.

7. **Díez, J., M. Ishikawa, M. Kaido, and P. Ahlquist**. 2000. Identification and characterization of a host protein required for efficient template selection in viral RNA replication. Proceedings of the National Academy of Science U S A. **97**:3913–3918.

8. **Dittrich, M. T., G. W. Klau, A. Rosenwald, T. Dandekar, and T. MÃijller**. 2008. Identifying functional modules in protein-protein interaction networks: an integrated exact approach. Bioinformatics. **24**:i223–i231.

9. **Everett, L., A. Vo, and S. Hannenhalli**. 2009. PTM-Switchboard–a database of posttranslational modifications of transcription factors, the mediating enzymes and target genes. Nucleic Acids Research. **37**.

10. **Faust, K., P. Dupont, J. Callut, and J. van Helden**. 2010. Pathway discovery in metabolic networks by subgraph extraction. Bioinformatics. **26**:1211–1218.

11. **GAMS Development Corporation**. 2010. General Algebraic Modeling System Version 23.6.5.

12. **Gancarz, B. L., L. Hao, Q. He, M. A. Newton, and P. Ahlquist**. 2011. Systematic identification of novel, essential host genes affecting bromovirus RNA replication. PLoS ONE. **6**:e23988.

13. **Gitter, A., J. Klein-Seetharaman, A. Gupta, and Z. Bar-Joseph**. 2011. Discovering pathways by orienting edges in protein interaction networks. Nucleic Acids Research. **39**:e22.

14. **Guelzim, N., S. Bottani, P. Bourgine, and F. KÃľpÃĺs**. 2002. Topological and causal structure of the yeast transcriptional regulatory network. Nature Genetics. **31**:60–63.

15. **Hao, L., A. Sakurai, T. Watanabe, E. Sorensen, C. Nidom, M. Newton, and P. Ahlquist**. 2008. Drosophila RNAi screen identifies host genes important for influenza virus replication. Nature. **454**:890–893.

16. **Herrgård, M. J., N. Swainston, P. Dobson, W. B. Dunn, K. Y. Arga, M. Arvas, N. Buthgen, S. Borger, R. Costenoble, M. Heinemann, M. Hucka, N. Le Novere, P. Li, W. Liebermeister, M. L. Mo, A. P. Oliveira, D. Petranovic, S. Pettifer, E. Simeonidis, K. Smallbone, I. Spasie, D. Weichart, R. Brent, D. S. Broomhead, H. V. Westerhoff, B. Kurdar, M. Penttila, E. Klipp, B. O. Palsson, U. Sauer, S. G. Oliver, P. Mendes, J. Nielsen, and D. B. Kell**. 2008. A consensus yeast metabolic network reconstruction obtained from a community approach to systems biology. Nature Biotechnology. **26**:1155–1160.

17. **Huang, D. W., B. T. Sherman, and R. A. Lempicki**. 2009. Bioinformatics enrichment tools: paths toward the comprehensive functional analysis of large gene lists. Nucleic Acids Research. **37**.

18. **Hughes, T. R., M. J. Marton, A. R. Jones, C. J. Roberts, R. Stoughton, C. D. Armour, H. A. Bennett, E. Coffey, H. Dai, Y. D. He, M. J. Kidd, A. M. King, M. R. Meyer, D. Slade, P. Y. Lum, S. B. Stepaniants, D. D. Shoemaker, D. Gachotte, K. Chakraburtty, J. Simon, M. Bard, and S. H. Friend**. 2000. Functional discovery via a compendium of expression profiles. Cell. **102**:109–126.

19. **Hurley, J. H. and P. I. Hanson**. 2010. Membrane budding and scission by the ESCRT machinery: it's all in the neck. Nature Reviews Molecular Cell Biology. **11**:556–566.

20. **IBM**. 2010. IBM ILOG CPLEX Optimization Studio, Version 12.0.2.

21. **Kanehisa, M., S. Goto, Y. Sato, M. Furumichi, and M. Tanabe**. 2012. KEGG for integration and interpretation of large-scale molecular data sets. Nucleic Acids Research. **40**:D109–D114.

22. **Konig, R. and et al.** 2008. Global analysis of host-pathogen interactions that regulate early-stage HIV-1 replication. Cell. **135**:49–60.

23. **Krishnan, M. and et al.** 2008. RNA interference screen for human genes associated with West Nile virus infection. Nature. **455**:242–245.

24. **Kushner, D. B., B. D. Lindenbach, V. Z. Grdzelishvili, A. O. Noueiry, S. M. Paul, and P. Ahlquist**. 2003. Systematic, genome-wide identification of host genes affecting replication of a positive-strand RNA virus. Proceedings of the National Academy of Sciences of the United States of America. **100**:15764–15769.

25. **Lu, S., F. Zhang, J. Chen, and S.-H. Sze**. 2007. Finding pathway structures in protein interaction networks. Algorithmica. **48**:363–374.

26. **MacIsaac, K., T. Wang, D. B. Gordon, D. Gifford, G. Stormo, and E. Fraenkel**. 2006. An improved map of conserved regulatory sites for *Saccharomyces cerevisiae*. BMC Bioinformatics. **7**:113+.

27. **Medvedovsky, A., V. Bafna, U. Zwick, and R. Sharan**. 2008. An algorithm for orienting graphs based on cause-effect pairs and its applications to orienting protein networks. In *Proceedings of the 8th International Workshop on Algorithms in Bioinformatics*, WABI '08, pages 222–232. Springer-Verlag, Berlin, Heidelberg. ISBN 978-3-540-87360-0.

28. **Mnaimneh, S., A. P. Davierwala, J. Haynes, J. Moffat, W. T. Peng, W. Zhang, X. Yang, J. Pootoolal, G. Chua, A. Lopez, M. Trochesset, D. Morse, N. J. Krogan, S. L. Hiley, Z. Li, Q. Morris, J. Grigull, N. Mitsakakis, C. J. Roberts, J. F. Greenblatt, C. Boone, C. A. Kaiser, B. J. Andrews, and T. R. Hughes**. 2004. Exploration of essential gene functions via titratable promoter alleles. Cell. **118**:31–44.

29. **Murali, T. M., M. D. Dyer, D. Badger, B. M. Tyler, and M. G. Katze**. 2011. Network-based prediction and analysis of HIV dependency factors. PLoS Computational Biology. **7**:e1002164.

30. **Noueiry, A. O., J. Diez, S. P. Falk, J. Chen, and P. Ahlquist**. 2003. Yeast Lsm1p-7p/Pat1p deadenylation-dependent mRNA-decapping factors are required for Brome Mosaic Virus genomic RNA translation. Molecular & Cellular Biology. **23**:4094–4106.

31. **Novershtern, N., A. Regev, and N. Friedman**. 2011. Physical Module Networks: an integrative approach for reconstructing transcription regulation. Bioinformatics. **27**:i177–i185.

32. **Ourfali, O., T. Shlomi, T. Ideker, E. Ruppin, and R. Sharan**. 2007. SPINE: a framework for signaling-regulatory pathway inference from cause-effect experiments. Bioinformatics. **23**:i359–i366.

33. **Pu, S., J. Wong, B. Turner, E. Cho, and S. J. Wodak**. 2009. Up-to-date catalogues of yeast protein complexes. Nucleic Acids Research. **37**:825–831.

34. **Scott, J., T. Ideker, R. M. Karp, and R. Sharan**. 2006. Efficient algorithms for detecting signaling pathways in protein interaction networks. Journal of Computational Biology. **13**:133–144.

35. **Scott, M. S., T. Perkins, S. Bunnell, F. Pepin, D. Y. Thomas, and M. Hallett**. 2005. Identifying regulatory subnetworks for a set of genes. Molecular & Cellular Proteomics. **4**:683–692.

36. **Serviene, E., Y. Jiang, C. Cheng, J. Baker, and P. Nagy**. 2006. Screening of the yeast yTHC collection identifies essential host factors affecting tombusvirus RNA recombination. Proceedings of the National Academy of Science (USA). **80**:1231–1241.

37. **Serviene, E., N. Shapka, C. Cheng, T. Panavas, B. Phuangrat, J. Baker, and P. Nagy**. 2005. Genome-wide screen identifies host genes affecting viral RNA recombination. Proceedings of the National Academy of Science (USA). **102**:10545–10550.

38. **Shachar, R., L. Ungar, M. Kupiec, E. Ruppin, and R. Sharan**. 2008. A systems-level approach to mapping the telomere length maintenance gene circuitry. Molecular Systems Biology. **4**:172.

39. **Silverbush, D., M. Elberfeld, and R. Sharan**. 2011. Optimally orienting physical networks. In *Proceedings of the 15th Annual International Conference on Research in Computational Molecular Biology*, RECOMB'11, pages 424–436. Springer-Verlag, Berlin, Heidelberg. ISBN 978-3-642-20035-9.

40. **Smola, A. and R. Kondor**. 2003. Kernels and regularization on graphs. In B. Schölkopf and M. Warmuth, eds., *Proceedings of the Annual Conference on Computational Learning Theory and Kernel Workshop*, Lecture Notes in Computer Science. Springer.

41. **Stark, C., B.-J. J. Breitkreutz, T. Reguly, L. Boucher, A. Breitkreutz, and M. Tyers**. 2006. BioGRID: a general repository for interaction datasets. Nucleic Acids Research. **34**.

42. **Suthram, S., A. Beyer, R. M. Karp, Y. Eldar, and T. Ideker**. 2008. eQED: an efficient method for interpreting eQTL associations using protein networks. Molecular Systems Biology. **4**:162.

43. **Vanunu, O., O. Magger, E. Ruppin, T. Shlomi, and R. Sharan**. 2010. Associating genes and protein complexes with disease via network propagation. PLoS Computational Biology. **6**:e1000641.

44. **Vaske, C. J., C. House, T. Luu, B. Frank, C.-H. H. Yeang, N. H. Lee, and J. M. Stuart**. 2009. A factor graph nested effects model to identify networks from genetic perturbations. PLoS Computational Biology. **5**.

45. **Winzeler, E. A., D. D. Shoemaker, A. Astromoff, H. Liang, K. Anderson, B. Andre, R. Bangham, R. Benito, J. D. Boeke, H. Bussey, A. M. Chu, C. Connelly, K. Davis, F. Dietrich, S. W. Dow, M. E. Bakkoury, F. Foury, S. H. Friend, E. Gentalen, G. Giaever, J. H. Hegemann, T. Jones, M. Laub, H. Liao, N. Liebundguth, D. J. Lockhart, A. Lucau-Danila, M. Lussier, N. M'Rabet, P. Menard, M. Mittmann, C. Pai, C. Rebischung, J. L. Revuelta, L. Riles, C. J. Roberts, P. Ross-MacDonald, B. Scherens, M. Snyder, S. Sookhai-Mahadeo, R. K. Storms, S. VÃľronneau, M. Voet, G. Volckaert, T. R. Ward, R. Wysocki, G. S. Yen, K. Yu, K. Zimmermann, P. Philippsen, M. Johnston, and R. W. Davis**. 1999. Functional characterization of the *S. cerevisiae* genome by gene deletion and parallel analysis. Science. **285**:901–906.

46. **Yeang, C.-H., T. Ideker, and T. Jaakkola**. 2004. Physical network models. Journal of Computational Biology. **11**:243–262.

47. **Yosef, N., L. Ungar, E. Zalckvar, A. Kimchi, M. Kupiec, E. Ruppin, and R. Sharan**. 2009. Toward accurate reconstruction of functional protein networks. Molecular Systems Biology. **5**:248.

48. **Zhao, X.-M., R.-S. Wang, L. Chen, and K. Aihara**. 2008. Uncovering signal transduction networks from high-throughput data by integer linear programming. Nucleic Acids Research. **36**:e48.